Revision to Chapter 6.0, "Criticality Safety Evaluation", in its entirety

All pages are identified as Revision 2 and dated 9/2002.

A vertical line has been added in the right hand column to indicate where changes were made from Revision 1.

6.0 CRITICALITY SAFETY EVALUATION

6.1 GENERAL DESCRIPTION

This criticality safety analysis is performed to demonstrate safety of the New Powder Container (NPC). This transport package meets applicable IAEA and 10 CFR 71 requirements for a Type A fissile material-shipping container for homogeneous and heterogeneous uranium compounds enriched to a maximum of 5.00 wt. percent U-235.

The NPC transport package design features include an internal 3x3 array of stainless steel Inner Containment Canister Assemblies (ICCAs) enclosed in a near cubic stainless steel reinforced Outer Confinement Assembly (OCA) as described in Section 1.2, *Package Description.*

The uranium contents are contained within 8.515" (21.63-cm) maximum ID stainless steel canisters internally spaced on nominal 12.0" (30.48-cm) center-to-center positions within the OCA. Manufacturing tolerance effects on package models are addressed in Section 6.3.1, *General Model.*

Water exclusion from the ICCAs is not required for this package design. Each cylindrical inner container within the package is analyzed in both undamaged and damaged container arrays under optimal moderation conditions and is demonstrated to be a favorable geometry.

This analysis is performed at a maximum enrichment of 5.00 wt. percent U-235 for both homogeneous UO_2 powder and heterogeneous UO_2 in the form of pellets, and cylindrical elements to represent unrestricted particle size (e.g., outer diameter, OD, is varied through optimum). The most reactive condition is therefore modeled for each authorized payload to demonstrate safety. The following Table 6.1 summarizes the uranium mass limits per ICCA and per package for the NPC container. Other uranium compounds complying with the requirements stated in Table 6.1 are acceptable for shipment provided that the equivalent uranium payloads are not exceeded.

Table 6.1 - UO_2 and Uranium Equivalent Mass Limits* per NPC Package

Material Form (≤ 5.00 wt.% U-235)	Particle Size Restriction: Minimum OD (Inches)	Maximum Loading per ICCA (kgs)		Maximum Loading per NPC (kgs)	
		UO_2	Uranium	UO_2	Uranium
Homogeneous Uranium Oxides/Compounds	N/A	60.0	52.89	540.0	476.1
Heterogeneous UO_2 Pellets (BWR)	0.342	55.0	48.48	495.0	436.3
Heterogeneous UO_2 Pellets (PWR)	0.300	53.0	46.71	477.0	420.4
Heterogeneous Uranium Compounds	Unrestricted particle size	46.0	40.54	414.0	364.8

*For U-235 enrichments ≤ 5.00 wt. %.

The "Material Form" column in Table 6.1 includes both homogeneous and heterogeneous uranium compounds in the form of solids, or solidified or dried materials. All homogeneous and heterogeneous compounds are restricted to material forms having a bulk density ≤ 10.96 g/cc (theoretical UO2), with a percent uranium content ≤ 0.88144.

This specifically includes homogneous uranium oxides (UO_2, U_3O_8, or $UO_{x,\ x>2}$). Other homogeneos uranium compounds specifically authorized include dried (calcium containing) sludges, nitrates, uranyl nitrate hexahydrate (UNH, chemical formula $UO_2(NO_3)_2 \cdot 6H_2O$, with a theoretical density of 2.807 gm/cm^3), and uranium oxide bearing ash from combustible waste incineration.

A reactivity comparison between 5% enriched theoretical UO_2, U_3O_8, UNH, and $CaU_6O_{19} \cdot 11H_2O$ compounds with water is provided in Figure 6.0 demonstrating that the theoretical mixture of UO2 and water is conservative relative to other homogeneous uranium compounds. For k-infinite reactivity comparisons, refer Appendix 6.11 for a more complete material specification listing of uranium compounds evaluated.

Figure 6.0 K-infinite Comparison of U-compounds

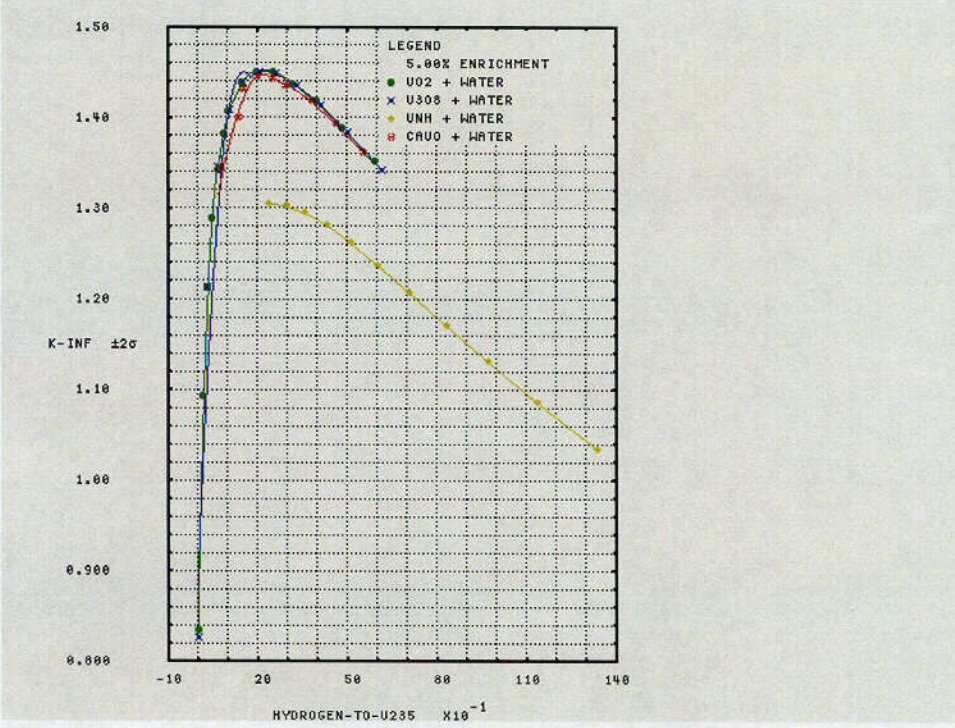

This also specifically includes heterogeneous uranium oxides (UO_2, U_3O_8, or $UO_{x,\ x>2}$) and UO2 pellets present in standard BWR and PWR reactor fuel assembly lattices designs (e.g., PWR: 17X17; BWR: 10X10, 9X9, 8X8 nuclear fuel assemblies). This analysis demonstrates safety for uranium compounds through optimal heterogeneity (unrestricted or unlimited particle size). As such, the specified pellets having diameters greater than or equal to the "Minimum" value specified in the table may be safely transported in the NPC package provided the tabulated UO_2 (or equivalent uranium) material contents per ICCA and package are met.

C01

Uranium-bearing contents may be moderated by water or carbon to any degree and may be mixed with other non-fissile materials with the exception of deuterium, tritium and beryllium. Materials such as uranium metal and uranium metal alloys are not covered by this analysis.

For this package, undamaged packages have been analyzed in infinite arrays and hence pursuant to 10 CFR §71.59(a)(2) the more restrictive value of "N" is derived from the damaged array calculations. The Transport Index for criticality control is then derived from this value of "N" per 10 CFR §71.59(b).

This analysis demonstrates safety for 2N=150 packages. The corresponding Transport Index (TI) for criticality control of non-exclusive vehicles is given by TI = 50/N. Since 2N = 150, it follows that N = 75, and TI = 50/75 = 0.6667 ≈ 0.7 [rounded to nearest tenth]. Using the rounded Transport Index result, the maximum allowable number of packages per non-exclusive use vehicle is 50/0.7 = 71.

6.2 PACKAGE DESCRIPTION

6.2.1 CONTENTS

The package shall be used to transport homogeneous or heterogeneous uranium compounds conforming to the requirements stated in Section 6.1 and with uranium enrichments of not greater than than 5.0 weight percent U-235. The uranium isotopic distribution considered in the models used in this criticality safety demonstration is shown in Table 6.2

Table 6.2 - Uranium Isotopic Distribution

Isotope	Modeled wt. %
^{235}U	5.0000
^{238}U	95.0000

This analysis conservatively demonstrates safety for homogeneous UO_2 powder, pellets, and heterogeneous forms of uranium oxides (unlimited particle size) over the entire range of UO_2 densities and degree of moderation by H_2O. The maximum UO_2 equivalent payload demonstrated safe in the NPC is specified in Table 6.1.

Any mass distribution including authorized non-uranium packaging materials such as plastic or metal in the form of bags, bottles, cans etc. within the 3 × 3 array of ICCAs is also acceptable, provided the total uranium content in any one ICCA does not exceed the applicable limit in Table 6.1 and provided that the entire contents meets the applicable total package weight limit.

6.2.2 PACKAGING

A general discussion of the NPC packaging design is provided in Section 1.2.1, *Packaging*. A detailed set of drawings of the NPC packaging is provided in the Appendix 1.3.1, *Packaging General Arrangement Drawings*. The NPC packaging is comprised of two primary components: 1) an Outer Confinement Assembly (OCA) consisting of the body and lid sections, and 2) nine Inner Containment Canister Assemblies (ICCAs). These major components are described below.

Product containment occurs inside an 18 gauge (0.048" wall thickness) Type 304L stainless steel Inner Containment Canister Assembly (ICCA). This ICCA is sequentially wrapped in a 0.020" (minimum) thick cadmium sheath, followed by a 0.570- inch thick polyethylene wrap (minimum), followed by a 24-gauge (.024" wall thickness) outer Type 304L stainless steel containment sheath welded closed to effectively contain the cadmium and polyethylene.

The bottom of an ICCA consists of a 9.72" OD, 7-gauge (0.188" thick) Type 304L stainless steel plate. The top of an ICCA includes 7-gauge (0.188" thick) Type 304L stainless steel upper ring (8.620" ID x 9.72" OD) to facilitate the poly wrap and welding of the 24 gauge outer sheath. The ICCA lid is a 16-gauge (0.0595" thick) Type 304L stainless steel cylinder and contains a molded silicon rubber gasket. The closure of the ICCAs is provided by a stainless steel band clamp assembly that utilizes a 5/16-24 T-bolt and nut.

Each ICCA is placed inside a 22-gauge Type 304L stainless steel cylindrical shield (silo), which is "foamed" in place on 12-inch X,Y centers within the OCA body. The OCA body assembly includes a 10-gauge (0.135" wall thickness) Type 304L stainless steel 42.81x42.81x37.66 inch outer-dimension cubic box. The nominal 37.66-inch height includes the height of eight 6x3x3/16x8.4" Type 304 stainless steel rectangular channels located on each corner of the package to facilitate fork lifting of the package from four sides. The Type 304L stainless steel structures associated with the eight (8) tube channels and the connecting 6" × 1.5" × 3/16" × 19.6" cross member ties are conservatively ignored at the bottom of the body assembly.

The central region of the NPC housing the 3 × 3 array of ICCAs is polyurethane foam with a density of 7 lb/ft^3 (nominal). A 4-inch (X,Y,Z) periphery surrounds the inner 3 × 3 array of ICCAs housed within the stainless steel silos. On the bottom and sides, a 3-inch periphery polyurethane foam with a density of 11 lb/ft^3 (nominal) surrounds the 7 lb/ft^3 region. The upper-most region of the OCA body that mates to the lid includes a rigid 1-3/8" layer of 40 lb/ft^3 polyurethane foam. The final 1-inch periphery of the body assembly contains 1-inch layer of ceramic fiberboard. This material is utilized for its thermal performance (heat resistance) properties.

The modeled OCA lid includes 10 gauge, 43.21" × 43.21" × 5.9" outer dimension Type 304L stainless steel box that is mated to the lower body assembly via 16 guide pins, which ensure proper lid seal alignment during closure. The outermost periphery again includes a modeled 1-inch ceramic fiberboard. The foam layer beneath the ceramic fiberboard includes a 3.5" layer of 15-lb/ft^3 (nominal) density polyurethane foam insulation. The lower 1-3/8" layer is rigid 40-lb/ft^3 (nominal) density polyurethane foam to protect the interface between the OCA body assembly and OCA lid assembly mating surfaces. This higher density 40 lb/ft^3 foam section in the lid includes cutouts to accommodate the upper lock ring closure of the ICCA.

The OCA lid dimensions include additional corner support structures, flanged edges, and ~2.3-inch overlap of 10-gauge stainless steel protecting the OCA body/lid interface (which are ignored in the final model construct). Closure of the OCA is provided by (16) 1/2-13UNC socket head cap screws. The closure is further secured by the OCA closure strips and (24) 7/16-14UNC hex head bolts. The NPC packaging is illustrated in Figure 1.1-1. Full details of the NPC packaging design are provided on the drawings in Appendix 1.3.1, Packaging General Arrangement Drawings. The OCA body containing up to nine loaded ICCAs, coupled with the OCA lid constitutes the entire NPC package assembly.

6.2.2.1 MATERIAL SPECIFICATIONS

One of the important aspects of the criticality safety demonstration for this package is the hydrogen content in the foam and polyethylene regions. Hydrogen is important due to its moderating and neutron capture characteristics.

The minimum specified hydrogen content in the foam is 6.4 weight percent. Likewise, the polyethylene region surrounding the cadmium is based on stoichiometric CH_2, with nominal hydrogen content of 14.3%.

To account for the potential high-temperature off-gassing of hydrogen in the polyurethane foam and polyethylene regions, and to assure the hydrogen content in the modeled regions is no greater than the package after physical testing, sample analysis of both regions were conducted as described in Section 2.10.1, Certification Tests, of this application:

- Polyurethane Foam: The average measured hydrogen content of the foam regions used to fabricate the test units was 6.48%. The average of 12 replicate samples taken from residual foam in the certification test units resulted in measured hydrogen content of 6.40% with the lowest observed value at 6.07% hydrogen. The 6.07% hydrogen value corresponded to a sample taken from what appeared to be one of the hottest areas observed. This criticality safety demonstration is performed using 6.00% hydrogen content in the foam material regions for all undamaged and damaged models and is conservative relative to the observed physical package post HAC testing (refer to Section 2.10.1.2, Summary, regarding the significant results of the hydrogen stability in the foam).

- Polyethylene: The average measured value of the hydrogen content in the polyethylene material use to fabricate the certification test units was 14.23%. The average measured value from four post-test replicate samples strategically withdrawn from what was believed to be the hottest regions observed was 14.09% with the lowest observed value of 14.01%. The average of eight additional replicate samples taken from various locations showing some indications of heating in the moderator averaged 14.20% with the lowest observed value of 14.09%. The measured values show little change in the hydrogen content in the polyethylene region before and after the test even in the hottest regions. This criticality safety demonstration is performed using 14.00% hydrogen content in the polyethylene wrap region surrounding each ICCA for all undamaged and damaged models and is conservative relative to the observed physical package post HAC testing (refer to Section 2.10.1.2, Summary, regarding the significant results of the hydrogen stability in the polyethylene).

Table 6.3 provides a listing of the applicable material specifications used in the NPC model construct. The table conservatively applies the minimum measured hydrogen content of the NPC polyurethane foam (6.00%) and polyethylene wrap (14.00%) in the applicable packaging regions for all normal and damaged model constructs.

The minimum composition values for C, O, N, H shown in Section 8.1.4.1.1.1, Polyurethane Foam Chemical Composition, are applied. Other trace foam constituents (P, Si, Cl, and other) are ignored. Additional package material conservatism is later described in Section 6.3.1.5, Models – Actual Package Differences.

Table 6.3 - Material Specifications for the NPC Shipping Package

Material	Density (g/cm^3)	Constituent	Atomic density (atoms/b-cm)
$U(5.00)O_2$ Fuel[1]	≤10.96	U-235 (max.)	1.2378E-03
		U-238 (max.)	2.3220E-02
		O (max.)	4.8916E-02
304L Stainless Steel	7.9	C	3.1691E-04
		Si	1.6940E-03
		Cr	1.6471E-02
		Fe	6.0360E-02
		Ni	6.4834E-03
		Mn	1.7321E-03
Cadmium	8.2175*	Cd	4.4000E-02
Polyethylene	0.92	H	7.6965E-02
		C	3.9504E-02
Polyurethane Foam	0.1122	C	2.8100E-03
(7 lb/ft^3)		O	5.9000E-04
		N	1.9000E-04
		H	4.0200E-03
Polyurethane Foam	0.1762	C	4.4200E-03
(11 lb/ft^3)		O	9.3000E-04
		N	3.0000E-04
		H	6.3200E-03
Polyurethane Foam	0.2404	C	6.0300E-03
(15 lb/ft^3)		O	1.2700E-03
		N	4.1000E-04
		H	8.6100E-03
Polyurethane Foam	0.6407	C	1.6080E-02
(40 lb/ft^3)		O	3.3800E-03
		N	1.1000E-03
		H	2.2970E-02
Full Density Water	1.00	H	6.68660E-02
		O	3.34330E-02

- 95% of theoretical density
- [1] Maximum values assumed for heterogeneous contents

6.3 CRITICALITY SAFETY ANALYSIS MODELS

6.3.1 GENERAL MODEL

6.3.1.1 Material Tolerance(s)

Table 6.4 provides sheet metal thickness dimensional tolerance from ASTM A240 and ASTM A480 (the former refers to the latter for specific tolerances). The maximum tolerance reductions in gauge sheet thickness are uniformly applied in all normal and damaged NPC model constructs.

The foam density distribution throughout the body assembly and lid assembly is varied as described in Section 6.2.2, *Packaging*. The manufacturers quality assurance program ensures the tolerance on the actual foam density is +15%/-10% at all times. For conservatism, the maximum 10% reduction in foam density is uniformly applied in all normal and damaged NPC model constructs.

Table 6.4 - Dimensional Tolerances

Type 304L Stainless Steel Sheet Gauge	Nominal Thickness (in.)	Permissible Variations* (in.)	Model Thickness Used (in.) [cm] (description)
7 ga	0.188	± 0 014	0.1740 [0 4420 cm] (ICCA ring)
10 ga	0.135	± 0 012	0.1230 [0.3124 cm] (OCA skin)
16 ga	0 0595	± 0 006	0 0535 [0.1359] (ICCA lid)
18 ga	0 048	± 0 005	0 0430 [0 1092] (ICCA inner skin)
22 ga.	0 029	± 0 004	0 0250 [0 0635] (ICCA silo)
24 ga.	0.0235	± 0.003	0 0205 [0 0521] (ICCA outer skin)

* ASTM-A240/A240M- 95a, Table A1 2, *Standard Specification for Heat Resisting Chromium and Chromium-Nickel Stainless Steel Plate, Sheet, and Strip for Pressure Vessels*, August 1995

6.3.1.2 Inner Containment Canister Assembly (ICCA)

Figure 6.1 shows the material constituent radial dimensions from center of the ICCA ID (δ1) through outer radius of the contamination shield (δ7). Figure 6.2 depicts the axial version of the ICCA and contamination shield. The ICCA model construct consists of a stackup of 11 separate axial pieces. This is performed to explicitly include the 1/8" (0.3175 cm) gaps of the high denisty polyethylene wrap on each end, the maximum axial seam gap tolerance between the three separate 10-1/8" (25.7175 cm) nominal wide cadmium wraps, the axial foam distribution density changes, and the fact that the ICCA silo is installed only in the lower body assembly. The upper section of the ICCA also penetrates the lid assembly to accommodate the vertical ICCA height, lock ring and bolt closure.

The 8.515-inch (21.63 cm) ID of the 18-gauge ICCA includes the maximum manufacturing tolerance. Modeled sheet gauge dimensions incorporate the maximum manufacturing tolerance specified in ASTM–A240 specified in Table 6.3 above. Since iron, chrome, and nickel constituents of stainless steel exhibit thermal and resonance absorption, the use of minimum sheet thickness values is also conservative.

For cadmium, a 25% reduction is applied to the actual 20-mil (minimum) thickness, for a modeled thickness of 15-mils (0.0381 cm)[1] and section width of 10.025" (25.4635 cm). The as-built stackup of the axial cadmium wraps allow for a maximum seam gap of 0.1" (0.254 cm). This gap is conservatively modeled as 0.15" (0.381 cm).

The high density polyethylene (HDP) is 30.3-inch in height and uniformly surrounds the cadmium, with no gaps, and its thickness ensured to be a minimum 0.570" thickness (1.4478 cm) by continuous wrapping of 15-mil (nominal) sheets and a quality control weight confirmation. To account for the small density reduction in the layered polyethylene wrap, the HDP (0.94-0.98 g/cc density) sheet material is conservatively modeled as a uniform low density polyethylene (0.92 g/cc) over the 0.570" thick (1.4478 cm) wrap (min. hydrogen areal density = 0.199 g/cm^2). The minimum required thickness, height, and quality weight measurement confirm this effective poly thickness and density is achieved.

Figure 6.1 Inner Containment Canister Assembly – Radial Dimensions

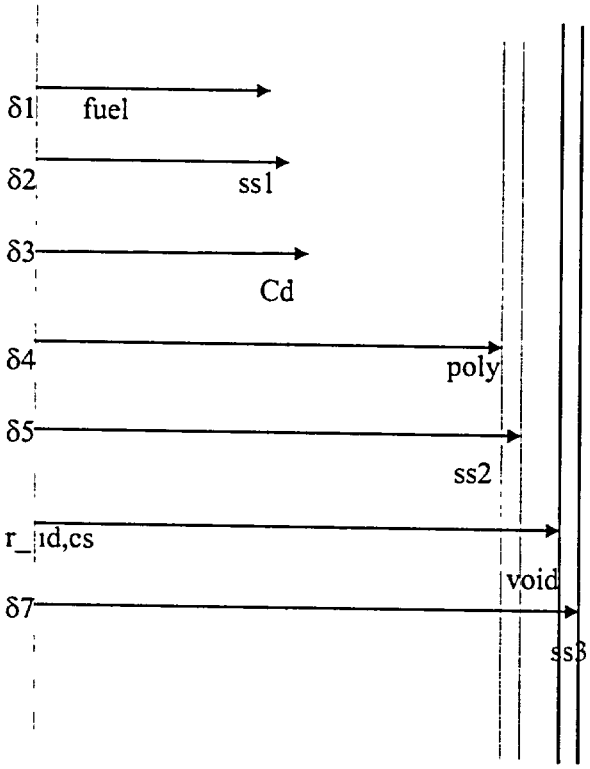

radial/material assignments:

δ1 = fuel region (e.g., UO_2+H_2O)
δ1 = 10.8141 cm (4.2575")
δ2 = δ1 + δss1 δss1 = 0.1092 cm
δ3 = δ2 + δcadmium δcad = 0.0381 cm
δ4 = δ3 + δpoly δpoly = 1.4478 cm
δ5 = δ4 + δss2, δss2 = 0.0521 cm
r_id = (10 x 2.54) / 2 = 12.7000 cm
δ7 = r_id, cs + δss3 δss3 = 0.0635 cm
beyond δ7 is polyurethane foam....

[1] Note: Limiting added absorber material credit to 75% without comprehensive tests is based on concerns for potential "streaming" of neutrons due to non-uniformities. The 75% value demonstrated by this work is conservative for several reasons: (1) cadmium is elemental and therefore homogeneous and is not distributed in granular fashion, and (2) the experimental work is based on the use of a monodirectional beam of neutrons, while in this package design, an isotropic neutron source exists, reducing intragranular transmission effects (if any)

Figure 6.2 ICCA Modeled Axial Dimensions

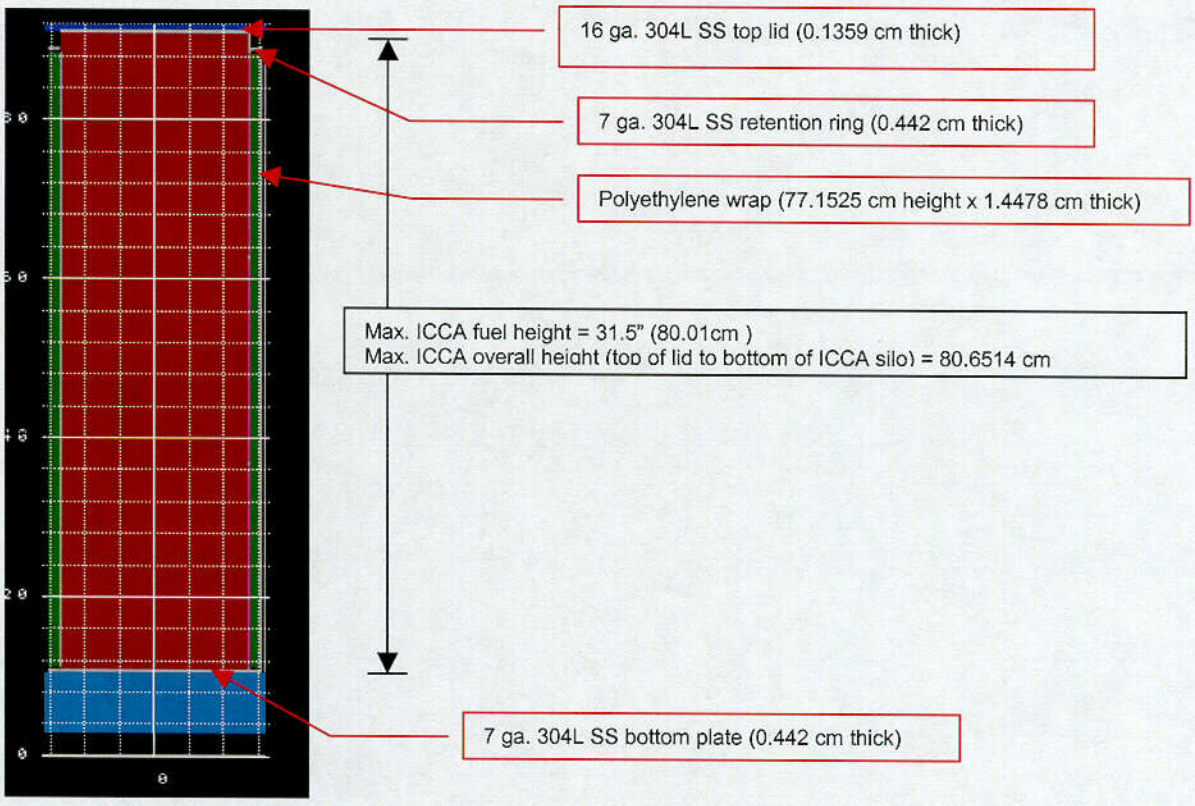

6.3.1.3 Body and Lid Assembly

For the basic model construct, the unit outer dimensions are modeled as a 42.81x42.81 inch square box. The inner height is computed based on the stack-up dimensions of the OCA body 34.573" (87.8154 cm) and lid 5.998" (15.2349 cm) for a total modeled package height of 40.571" (103.0503 cm). These outside dimensions of the near cubic package are conservative for the following reasons:

- the external corner support structure is ignored (x-y, x-z)
- the OCA locating buttons, and 16 ½-13UNC socket head cap screws are ignored (x-z)
- the lid flange overlap, OCA closure strip, and 24 7/16-14UNC hex head bolts are ignored (x-y)
- the heavy duty 6×3×3/16×8.4 rectangular fork-lift channel pocket structure is ignored (x-z)
- the affect of body/lid bowing due to HAC tests is ignored (x-y, x-z)

By ignoring the above effects, the NPC undamaged and damaged package array are modeled as close fitting and in contact, when in fact the aforementioned structure and OCA structure deformation and bowing would provide additional (x-y) and axial (x-z) spacing between individual package units.

The lighter 7-lb/ft^3 internal foam is modeled to encase the 3x3 Inner Containment Canister Assembly (ICCA) array. Important dimensions of the basic body + lid assembly, and foam density assignments are shown in the x-y and x-z cross-sectional slices of Figures 6.3a and 6.3b, respectively.

C02

Figure 6.3a Body Assembly (x,y) Dimensions and Foam Distribution

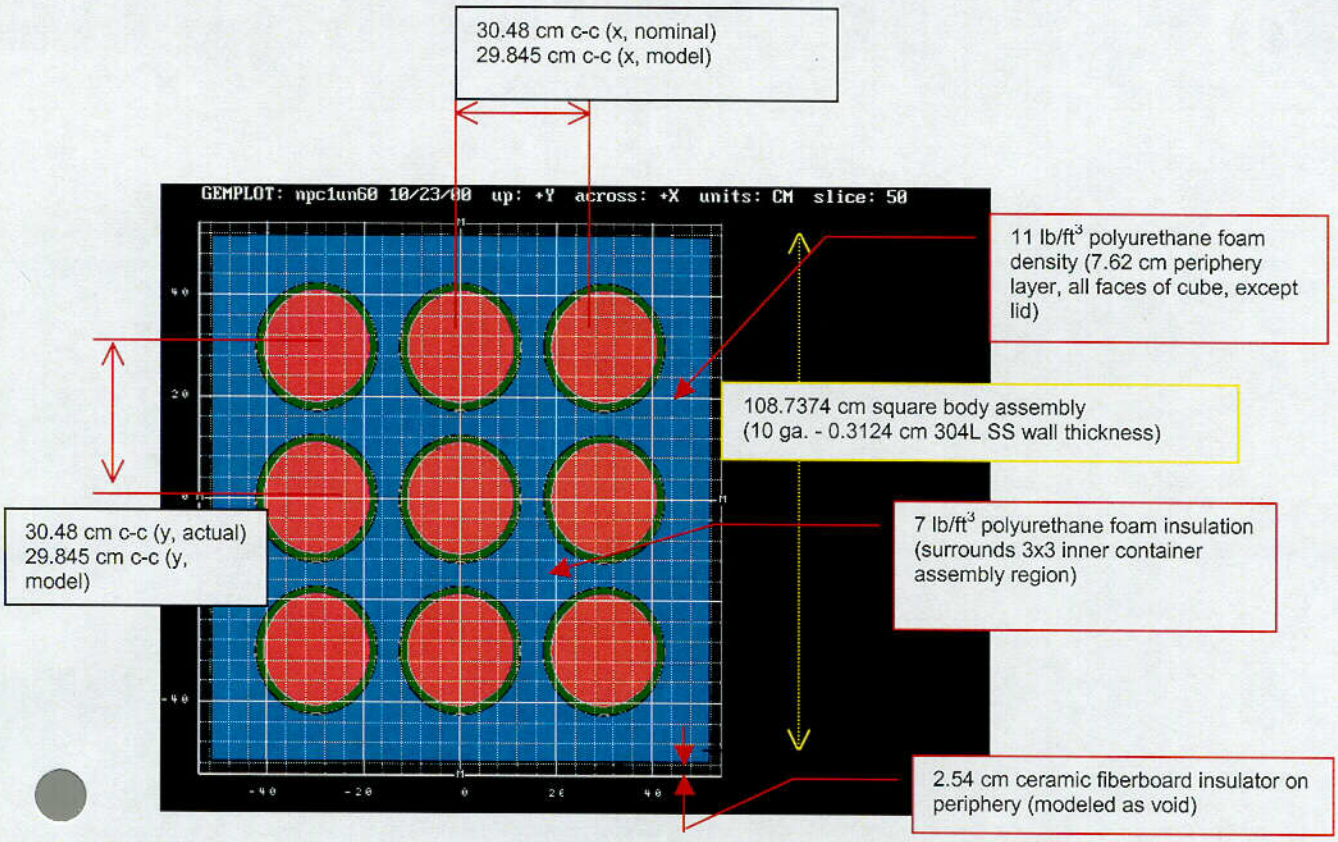

Figure 6.3b Body Assembly (x,z) Dimensions and Foam Distribution

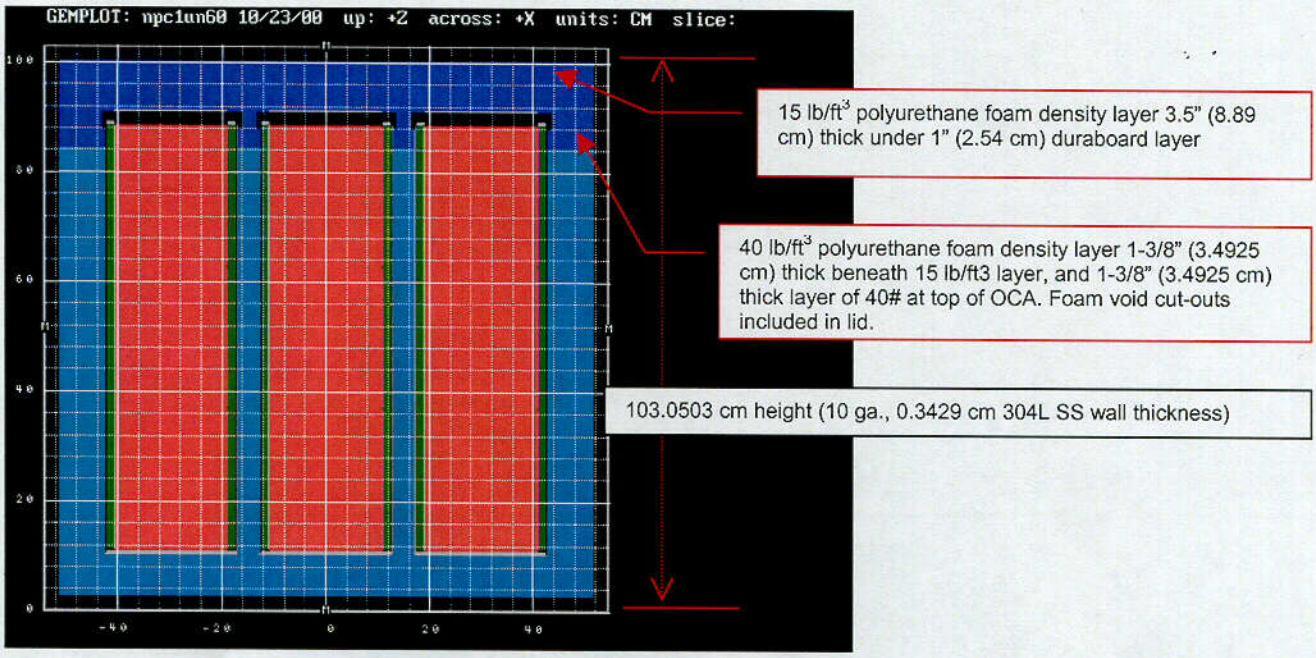

C03

6.3.1.4 Materials

Figure 6.4 shows blown up cross-section material assignment(s) of the ICCA within stainless steel silo. These mixture assignments are shown in color for illustration purposes, and used throughout this report (unless otherwise noted).

Figure 6.4 Inner Containment Canister Assembly (ICCA) within Silo - Mixture Assignments

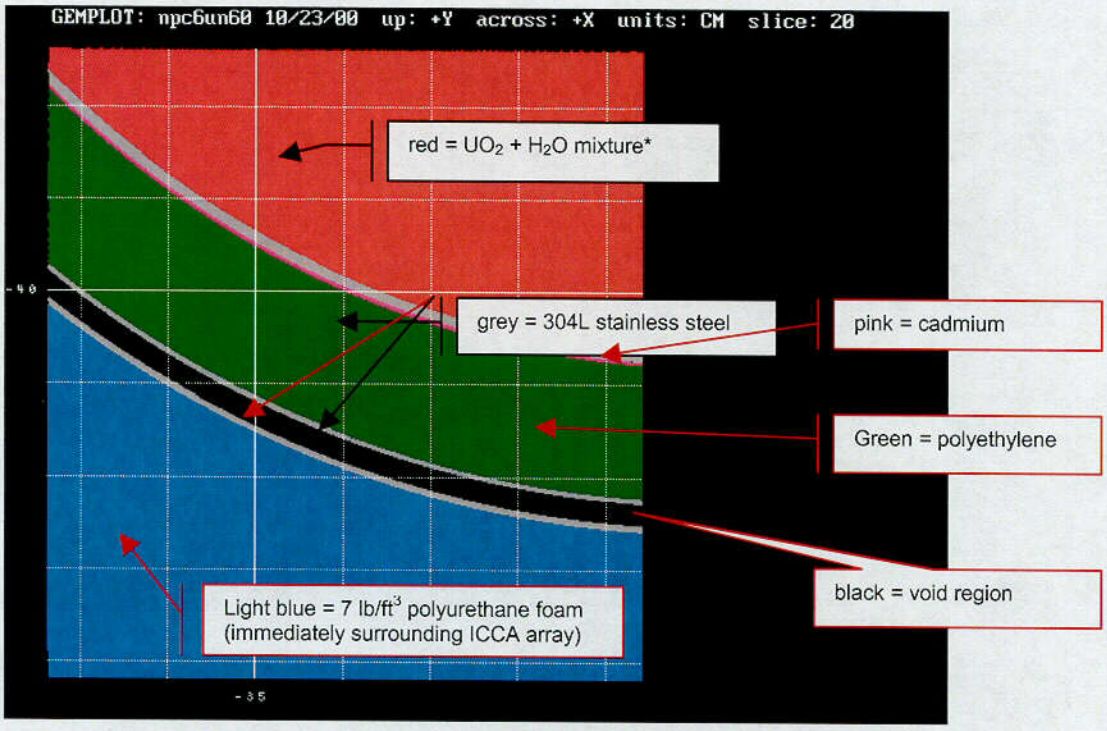

* For a further description of the fuel regions with homogeneous mixtures and heterogeneous lattices see Section 6.4.3

The UO_2 mixture (fuel) material specifications used in the NPC criticality safety demonstrations are dependent upon the case being modeled. The cases considered in the current analysis are (1) damaged single packages, (2) infinite arrays of undamaged packages and (3) 5X5X6 arrays of damaged packages. Contents include the applicable homogeneous and heterogeneous theoretical density $U(5.00)O_2$ and water mixtures, optimally moderated, and with the specified mass limits given in Table 6.1. Heterogeneous cases have been modeled as lattices of full density $U(5.00)O_2$ vertical fuel rods (with no cladding) in full density H_2O with the specified minimum diameters in column 2 of Table 6.1 and with lattice heights as determined by the lattice water to fuel (W/F) volume ratios, the Table 6.1 mass limits, and the assumed lattice boundary conditions (i.e. either overlap of the rods in the lattice with the ICCA wall, or no overlap).

Table 6.5 provides the resulting mixture data summary derived from an internal utility code called UFACT. For the cases in the table except the first (which is applicable to heterogeneous pellets and rods), a theoretical treatment of the fuel region is used, and the mixture height is not computed as the ICCA volume is modeled full (height fixed at 80.01 cm). Please also note that for theoretical UO_2, all voids are filled at approximately 11.5% water content – thus no density correction is required (e.g., DFACT = 1.0).

C04

The columns in the table with the corresponding compound identification (COM), weight fraction water (WF-W), U-235 fractional enrichment (ENR), density correction factor (DFACT), mixture density (RHOMIX), compound density (RHOC), and uranium density (RHOU), uranium fraction in the compound (UFACT), H/5 (H/U-235) and H/U atom ratios, and HEIGHT are defined as follows (and are equally valid for Table 6.6):

- **DFACT** = density correction factor = [MINIMUM (1.0, $RHOC_{max\text{-}credible}$)]/RHOC
- **RHOMIX** = mixture density = RHO_MIX=DFACT/[(1-WTFR_H_2O)/RHO_FUEL+WTFR_H_2O]
  where, RHO_FUEL = RHOC = RHO_UO_2 = compound density in mixture, and
  WTFR_H_2O = WF-W = weight fraction water in mixture
- **RHOC** = uranium compound density in mixture = (1 – WTFR_H_2O) * RHOMIX
- **$RHOC_{max\text{-}credible}$**= maximum credible density of uranium compound
- **RHOU** = uranium density in mixture = UFACT * RHOC = 0 88144 * RHOC
- **UFACT** = uranium fraction of compound = M_U / [M_U + (2*M_O)] = 0 88144 for 5 00% enriched UO_2
  where, Mi is the atomic mass of constituent i
- **H/5=H/U-235** = Atom ratio of hydrogen to U-235 = H_TO_U-235
  H_TO_U-235=W_TO_F*2*235 043928/(18 01534*RHO_FUEL*UFACT*ENR)
  where, W_TO_F=water-to-fuel ratio - WTFR_H2O*RHO_FUEL)/(1-WTFR_H2O)
  ENR=[N_U-235*235.043928]/(#+N_U-238*238 050788)
- **H/U** = Atom ratio of hydrogen to uranium = H_TO_U=WTFR_H_2O*ATM_U/[UFACT*.5*18.0153*(1-WTFR_H_2O)]
- **HEIGHT** = height of mixture in cylinder of specified radius and mixture mass [e g, HEIGHT= MASS/(PI*RAD**2*RHO_MIX)] or compound mass (e g, HEIGHT= MASS/(PI*RAD**2*RHOC)]

Table 6.5 Fuel Material Specifications – Damaged Single Package (theoretical UO_2 + H_2O mixture)

COM	WF-W	FR.ENR	DFACT	RHOMIX gm/cc	RHOC gm/cc	RHOU gm/cc	UFACT	H/5	H/U x10	HEIGHT cm
UO2	.000	.05000	1.0000	10.9600	10.9600	9.6606	.88144	104	0	n/a
UO2	.150	.05000	1.0000	4.3945	3.7354	3.2925	.88144	104	53	n/a
UO2	.200	.05000	1.0000	3.6631	2.9305	2.5830	.88144	148	75	n/a
UO2	.250	.05000	1.0000	3.1404	2.3553	2.0761	.88144	197	100	n/a
UO2	.300	.05000	1.0000	2.7482	1.9238	1.6957	.88144	254	128	n/a
UO2	.350	.05000	1.0000	2.4432	1.5881	1.3998	.88144	319	161	n/a
UO2	.400	.05000	1.0000	2.1990	1.3194	1.1630	.88144	395	200	n/a
UO2	.450	.05000	1.0000	1.9993	1.0996	0.9692	.88144	484	245	n/a

In the undamaged and damaged package array cases, homogeneous UO_2 + H_2O mixtures are modeled as mass and geometry limited systems. The UO_2 compound density is treated as theoretical (10.96 g/cc). The weight fraction water is computed such that the UO_2 + water mixture completely fills a volume up to the maximum of the Inner Containment Canister Assembly (ICCA). For the NPC package, these mass and geometry limited conditions are demonstrated to be the most reactive.

Table 6.6 provides the corresponding mixture, compound, and uranium densities for this treatment of the fuel region. The weight fraction of water for each UO_2 fuel mass limit is computed to just fill the ICCA volume. The UO_2 compound mass in the UO_2 + H_2O mixture is varied to determine the maximum acceptable payload of the package under hypothetical accident conditions. In the case of 60 kgs UO_2, additional cases at lower weight fraction water were run to confirm the most reactive condition. Higher weight fraction water conditions resulting in lower UO_2 mass are included in this table.

Table 6.6 Fuel Material Specifications – Undamaged and Damage Package Arrays (UO_2 + H_2O , optimal moderation, variable UO_2 mass)

COM	WF-W	FR.ENR	DFACT	RHOMIX gm/cc	RHOC gm/cc	RHOU gm/cc	UFACT	H/5	H/U x10	HEIGHT cm
undamaged package array cases:										
	RADIUS = 10.8141 CM				FUEL MASS = 60.000 KG					
UO2	.150	.05000	1.0000	4.3945	3.7354	3.2925	.88144	104	53	43 721
UO2	.200	.05000	1.0000	3 6631	2.9305	2.5830	.88144	148	75	55 729
UO2	.250	.05000	1.0000	3 1404	2.3553	2.0761	88144	197	100	69.339
UO2	.260	.05000	1.0000	3 0533	2.2594	1.9915	.88144	208	105	72.281
UO2	.270	.05000	1.0000	2 9708	2.1687	1.9116	88144	219	111	75.304
UO2	.285	.05000	1.0000	2.8549	2.0411	1.7992	.88144	236	119	80.010(*)
damaged package array cases:										
	RADIUS = 10.8141 CM				FUEL MASS = 40.000 KG					
UO2	.392	.05000	1.0000	2.2366	1.3608	1.1995	.88144	381	193	80.010
	RADIUS = 10.8141 CM				FUEL MASS = 45.000 KG					
UO2	360	.05000	1.0000	2.3912	1.5309	1 3494	.88144	333	168	80.010
	RADIUS = 10.8141 CM				FUEL MASS = 50.000 KG					
UO2	332	.05000	1.0000	2.5457	1 7009	1 4993	.88144	294	149	80.010
	RADIUS = 10.8141 CM				FUEL MASS = 55.000 KG					
UO2	.307	05000	1.0000	2.7004	1.8711	1 6492	.88144	262	133	80 010
	RADIUS = 10.8141 CM				FUEL MASS = 60.000 KG					
UO2	285	05000	1 0000	2.8549	2.0411	1.7992	.88144	236	119	80.010 (*)
	RADIUS = 10.8141 CM				FUEL MASS = 65.000 KG					
UO2	265	05000	1.0000	3.0095	2.2113	1.9491	88144	214	108	80.010
(*) ICCA full condition, wf-w = 0 28504										

6.3.1.5 Models - Actual Package Differences

The criticality safety analysis model of the loaded NPC differs from the actual package in 1) the allowance for water intrusion into the ICCA containment, 2) center-to-center canister spacing, 3) insulating foam distribution, 4) the modeled stainless steel structure, 5) the modeled cadmium thickness, and 6) the modeled poly density.

1) For homogeneous UO_2, the ICCA fuel region is modeled with variable UO_2 compound mass and variable H_2O content as described in the fuel material specifications above. In the limiting (damaged package array) models, the UO_2 compound mass is varied from 40-65 kgs UO_2 per ICCA. The water content is also varied to optimally moderate the ICCA for the mass limited damaged package array. This optimal internal moderation treatment is a known conservatism.

2) For heterogeneous materials, the ICCA fuel region is modeled as a lattice of variably spaced UO_2 fuel in the form of right circular cylindrical elements (rods) having a fixed total (UO_2) mass with full density H_2O in the ICCA region outside of the cylindrical elements. The fixed mass, either 55 kgs, 53 kgs or 46 kgs, is based on the minimum diameter of the pellets or particles size specified in Table 6.1. Similar to the homogeneous case, the degree of moderation in the individual fuel rod lattices is varied through optimum, which is done as a function of the lattice water-to-fuel volume ratios by varying the spacing between the rods. As in the homogeneous case, the modeling of accumulations of pellets or other random oriented high-density clumps or particles as uniform lattices of UO_2 cylindrical elements (rods) is a known conservatism.

3) The center-to-center spacing of the ICCAs is also different from the as-built package. The nominal spacing (X,Y) between the individual ICCA units in the 3 × 3 array is 12-inches (30.48 cm). All models use a nominal conservative ICCA center-to-center spacing of 11.75" (29.845 cm). For the limiting damaged package array models, sensitivity of the canister center-to-center spacing is quantified, by modeling the ICCAs from 11.75" (29.845 cm) to 11.25" (28.575 cm) spacing for a specified foam burn condition. Effects on system reactivity are assessed.

4) The insulating foam distribution within the package also differs from the actual package contents. In all cases, the minimum chemical composition in the foam is assumed. In addition, the density of the polyurethane foam is reduced by the maximum 10% manufacturing tolerance. Thus, the 7, 11, 15, and 40 lb/ft^3 foam densities are actually modeled as 6.3, 9.9, 13.5, and 36 lb/ft^3, respectively. This 10% foam density reduction results in a corresponding reduction in the hydrogen atom density. This is a known conservatism, as sensitivity studies demonstrate the more hydrogen between the ICCAs, the lower the overall system reactivity (due to hydrogen moderating and capture characteristics).

The foam distribution also differs in the mass of foam included. In the damaged single package and arrays, the effects of non-uniform foam burn are based on measured CTU-1 and CTU-2 test results. The limiting condition damaged array reactivity is based on the maximum burn observed in either certification test unit. The maximum burn treatment results in zero residual foam thickness on all 6-faces of the cube, as measured radially and axially from the ICCA centerline (refer to Sections 2.10.1.7.1.6 and 2.10.1.7.2.6).

The maximum burn condition, coupled with the minimum hydrogen content, uniform application of maximum foam density tolerance, and 2% reduction in poly density effectively results in conservative treatment of damaged package physical condition post HAC testing. The maximum foam burn results in minimum interstitial hydrogen between packages – which is shown to increase package reactivity.

The 1-inch periphery ceramic fiberboard is modeled as a void in all models. This material consists of approximately 44% Al_2O_3, and the balance as SiO_2 –both compounds are neutronically insignificant.

4) The amount of stainless steel structure used in the model also differs from the actual package. Since the maximum sheet gauge tolerance reductions were applied (refer to Table 6.4), and significant external structure ignored, the mass of stainless steel in the model is significantly lower than actual. Reducing amount of stainless steel in the model is conservative because there is less material to compete with the uranium for neutron absorption reactions (refer also to Section 6.6.2.7, Sensitivity Study – Damaged Package Array Structure).

5) The nuclear poison cadmium thickness is modeled at 0.015" (0.0381 cm) thick, which represents only 75% of the minimum absorber thickness of 0.020" (0.0508 cm).

6) In all damaged package array models, a 2% reduction in polyethylene density (0.92 * 0.98) is uniformly applied. This reduction in density effectively covers the observed 0.6% weight loss post HAC testing and 0.25% mass allowance for minimum specified poly height of 30.3" verses the modeled 30.375" height (refer also Section 6.6.2.8, Sensitivity Study – Damaged Package Array Poly Gap).

6.3.2 CONTENTS MODEL

A general discussion of the NPC package in the normal (undamaged) transport and hypothetical (damaged) accident condition case is given in Section 6.3.1.4, *Materials*, Tables 6.5 and 6.6. The following sections presents a discussion of the fissile material contents under these conditions of transport, along with an assessment of the foam burn distribution effects in the damaged single and array packages.

6.3.3 DAMAGED SINGLE-PACKAGE MODELS

A model of the single package damaged condition considers unlimited moderator intrusion into the ICCA containing UO_2 product. The single package was subjected to hypothetical accident condition tests per IAEA and 10 CFR §71.73 as specified in Section 2.7, *Hypothetical Accident Conditions*. The UO_2 contents of the single package were analyzed in accord with the Section 6.3.1.4, *Materials*, Table 6.5. The ICCAs within the package were modeled in the homogeneous case containing theoretical UO_2 and water mixtures, and in the heterogeneous case as water moderated lattices of UO_2 cylindrical elements (rods), with the corresponding weight fraction H_2O and water to fuel ratios varied through optimal moderation. In all damaged single package models, the unit is surrounded by a ≥ 30.48-cm thick water reflector.

6.3.3.1 Damaged Single Package with Theoretical UO_2 + H_2O Mixtures

For homogeneous UO_2 and H_2O fuel mixtures, four sets of damaged single package model constructs are considered. Two damage single package models are run using the limiting CTU-1 and CTU-2 observed foam burn conditions in which the average residual foam is modeled on each face of the cube. The third case conservatively applies a maximum observed burn on each face of the cube. The fourth damaged single package model applies a tight water reflector to the package for the limiting condition derived from the first three case sets.

The first three cases replace observed foam burn region with void. The fourth and final case replaces the burned foam region with water to assess the impacts of a fully flooded damaged package (applied to limiting burn condition). Figures 6.5a – 6.5d show vertical slices of the CTU-1, CTU-2, maximum observed burn, and the flooded damaged single package models.

Figure 6.5a – Fully reflected damaged single package, theoretical UO_2 + H_2O mixture, CTU-1 observed burn

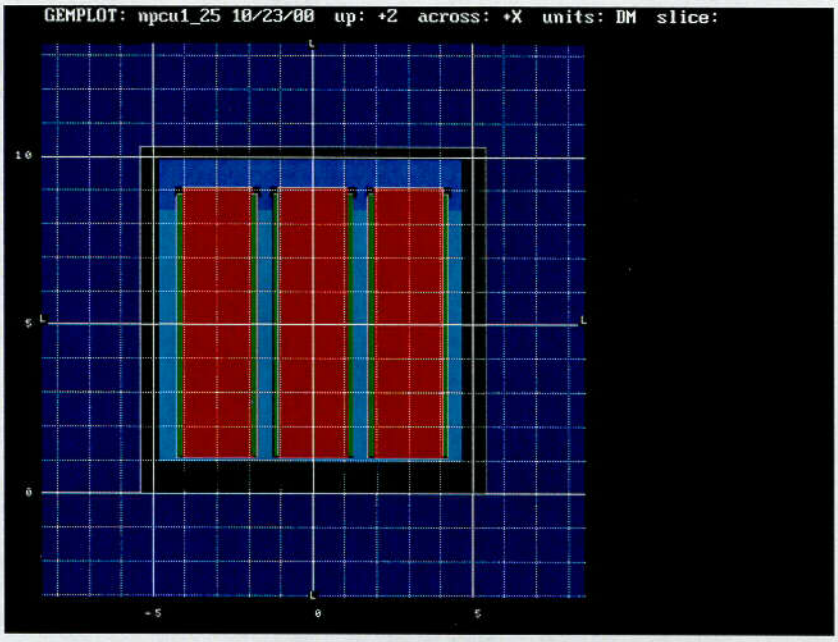

Figure 6.5b – Fully reflected damaged single package, theoretical UO_2 + H_2O mixture, CTU-2 observed burn

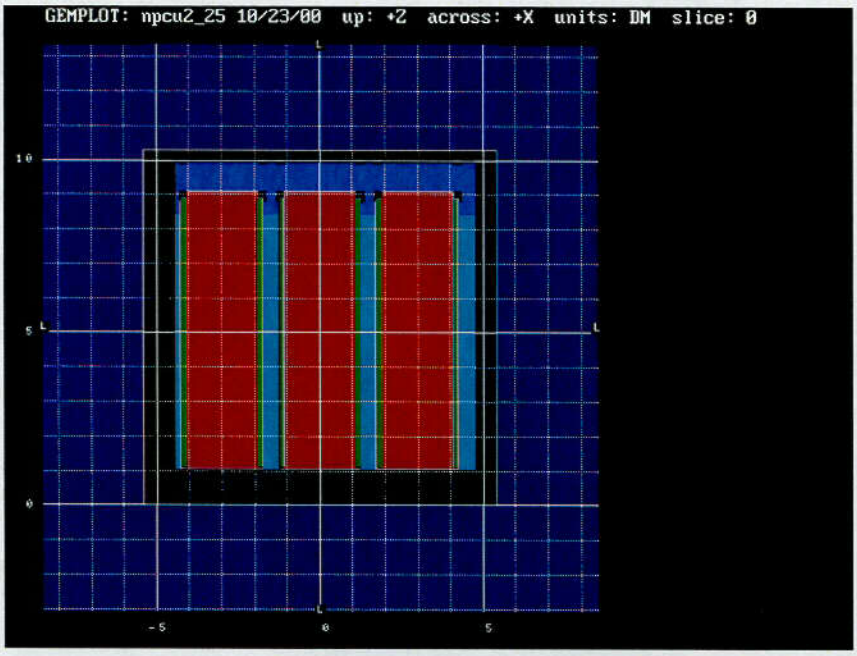

C05

Figure 6.5c – Fully reflected damaged single package, theoretical UO_2 + H_2O mixture, maximum burn

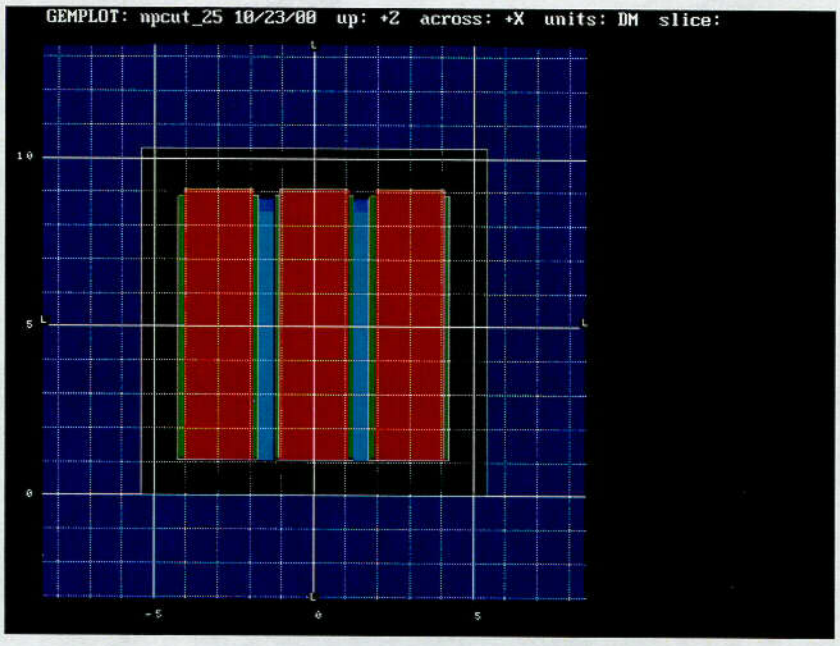

Figure 6.5d – Fully reflected damaged single package, theoretical UO_2 + H_2O mixture, maximum burn, flooded package

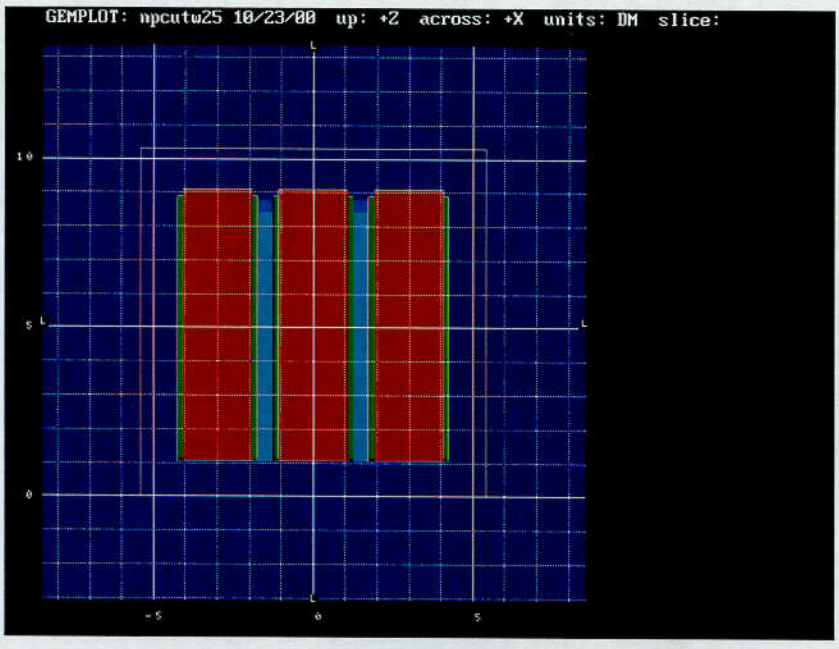

C06

6.3.3.2 Damaged Single Package with Heterogeneous UO_2 in H_2O

The package models for damaged single packages with heterogeneous UO_2 cylindrical elements (rods) in H_2O are the same as the worse case configuration as determined in the analyses for homogeneous mixtures, but with the fuel region less than or equal to the maximum ICCA inner height based upon the specified cylindrical rod lattice and UO_2 mass limit. This model is the one shown in Figure 6.5c, the "Fully reflected damaged single package ... maximum burn" construct, except for the potentially smaller fuel element lattice height. For less than maximum height lattices, the regions in the ICCAs above the lattice are modeled as voids.

In the evaluation of the NPC package with heterogeneous UO_2 fuel, three different types of model constructs have been used to represent the heterogeneous material contained in the ICCA fuel regions. Each type of model is then evaluated using both square and triangular lattice treatments, covering 26 different W/F ratios (from 0.58 to 8.00) and 4 different pellet outer diameters (ODs).

The first type of model consists of lattices of right circular cylinder elements (rods) in which the rods are permitted to overlap the ICCA boundary, with the parts of the rods internal to the ICCA kept in the model. Figure 6.6a shows XY depictions of the ICCA fuel regions for "17X17" cyclindrical lattices as the W/F ratios of the lattices are increased. Figure 6.6b shows the XZ layout (at Y = 0.0) of the same fuel regions with the decrease in the UO_2 mass in the ICCA noted when the maximum container height is reached. In this exact treatment with overlap, a total of 4 pellet ODs are considered. These include the "17x17", "10X10", "9X9" and "8X8" pellet sizes, each of which has progressively larger pellet diameters. The minimum diameter for the 17X17 PWR pellets is 0.300 inches; that for the BWR 10X10, 9X9 and 8X8 is 0.342 inches, 0.373 inches and 0.408 inches, respectively. In this analysis, pellet diameters which are larger than the 17x17 lattices are shown to be progressively less reactive.

The second type of model is similar to the first type except that right circular cylinder elements (rods) are not permitted to overlap the ICCA boundary and are deleted from the lattice if any part intersects with the ICCA wall. A comparison of the Overlap and Without Overlap models is given in Figure 6.6c. Except for the absence of the overlapping rods (which for the same UO_2 mass and W/F ratio results in a slightly higher lattice height), the Without Overlap models are entirely similar to the Overlap ones and the variation with W/F is the same as illustrated in Figures 6.6a and 6.6b.

The third type of model is one in which the right circular cylinder elements (rod) lattices are modeled in the ICCA using the Virtual Fill Option (VFO - see Section 6.4.3). Using this option, each individual neutron that is tracked in the ICCA fuel region is presented with the virtual equivalent of a rod lattice with overlap (as in the first type of model discussed above), but the rod lattice has its central point randomly displaced from the one seen by all other neutrons tracked in the region. Because of this random effect, the geometry plotting routines do not show the actual lattice geometry but assure that the neutron enters the Big Region at the center of a fuel region. Examples of this are shown in Figure 6.6d, in which the XY plots actually shows a type of pattern resulting from the way the plot routine (GEMPLOT) steps through the XY plane. The same pattern is not seen in the XZ plots because the Fill Region plotting is treated differently when parallel to right circular cylinders in the z-direction.

Figure 6.6a – NPC Container Square and Triangular 17X17 Fuel Rod Lattice XY Models With Overlap

W/F	Square		Triangular
1.00	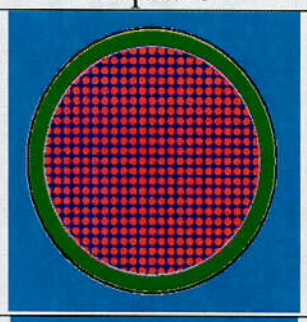		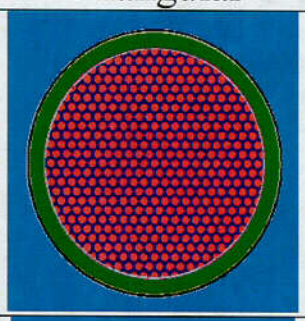
2.00	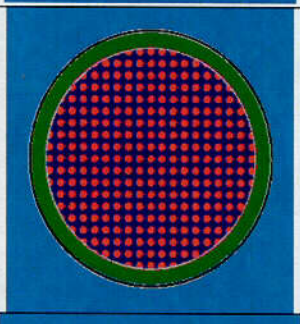		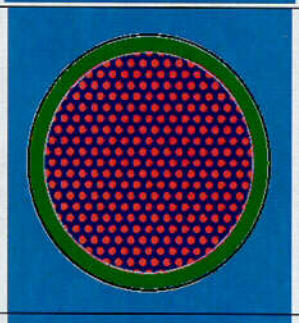
3.00	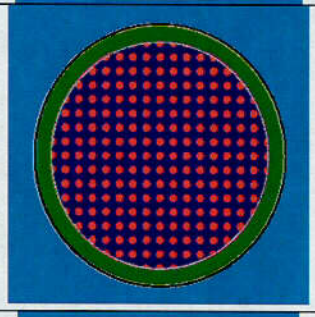		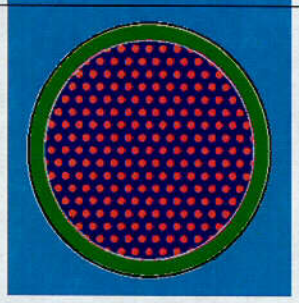
4.00	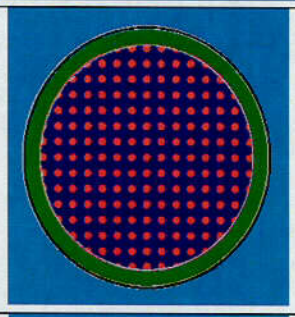		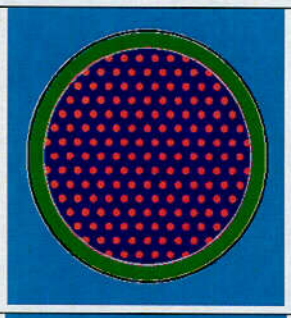
4.50	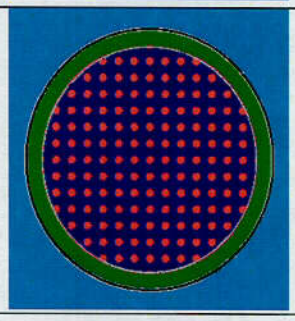		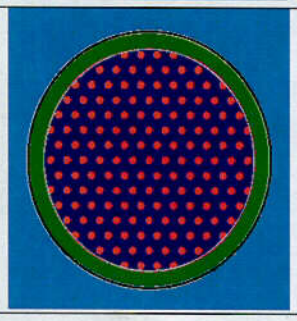

C07

Figure 6.6a – NPC Container Square and Triangular 17X17 Fuel Rod Lattice XY Models With Overlap - Continued

W/F	Square		Triangular
5.00	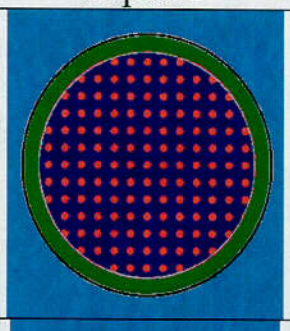		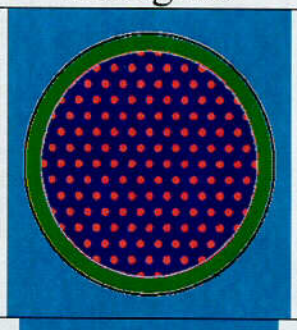
6.00	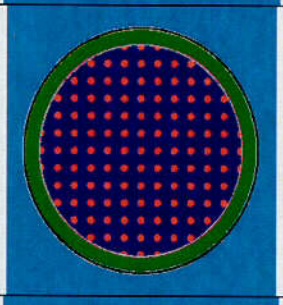		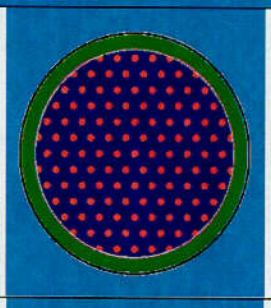
7.00	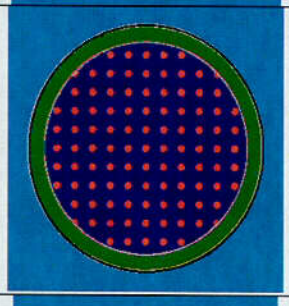		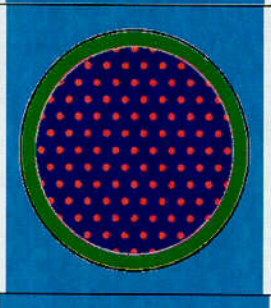
8.00	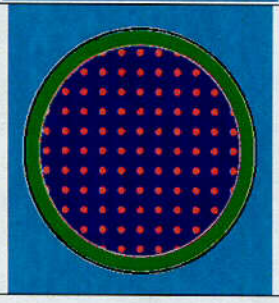		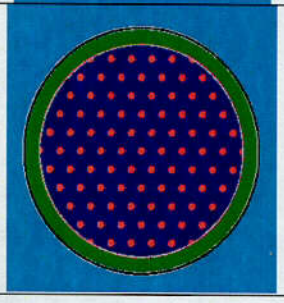

C08

Figure 6.6b – NPC Container Square and Triangular 17X17 Fuel Rod Lattice XZ Overlap Models With 55 KG UO_2

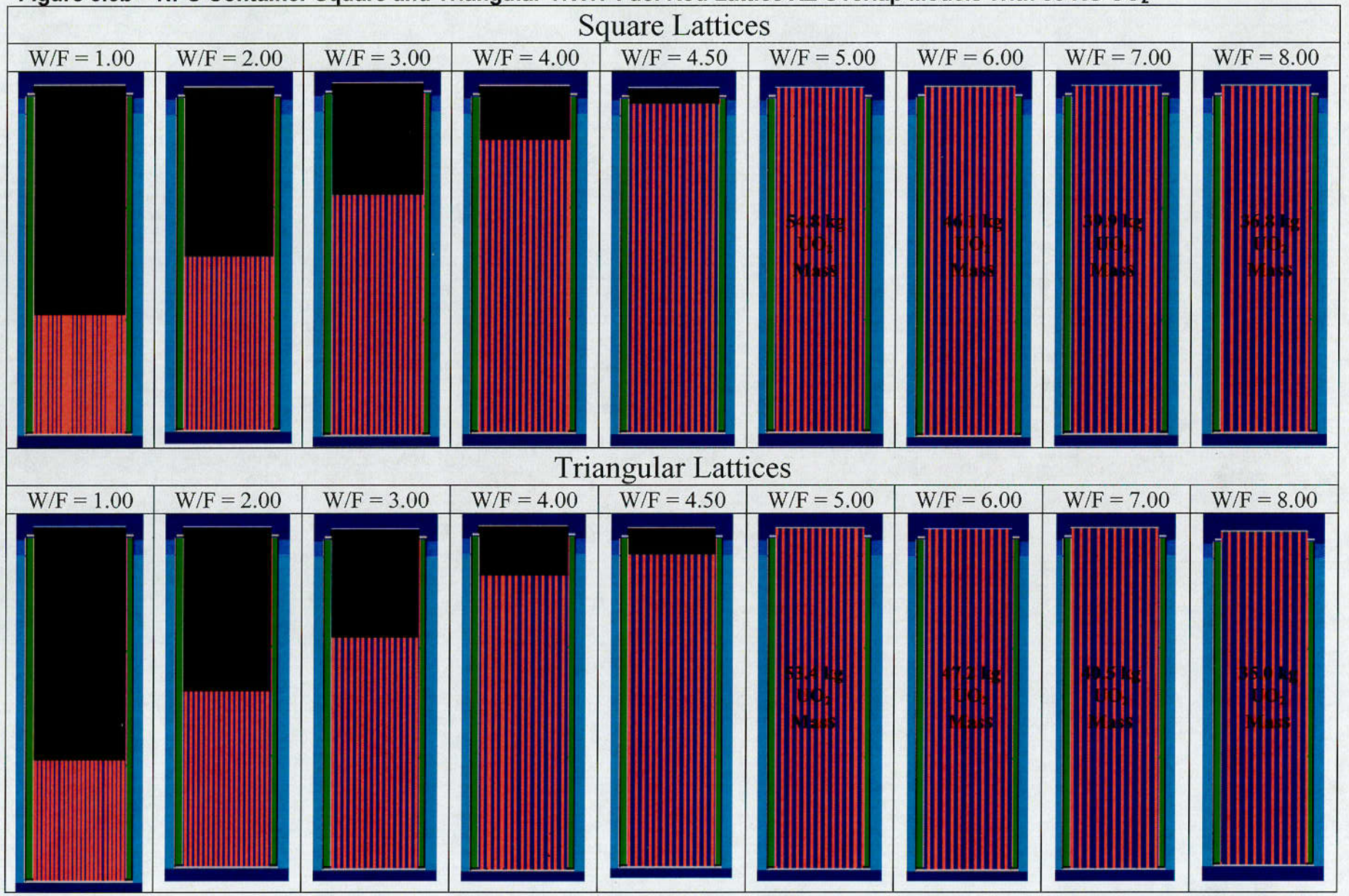

Figure 6.6c – Comparison of NPC Container Square and Triangular 17X17 Fuel Rod Lattice* Models With and Without Overlap

Model	With Overlap	Without Overlap
Square Lattice XY	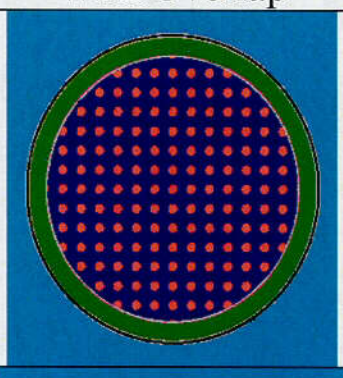	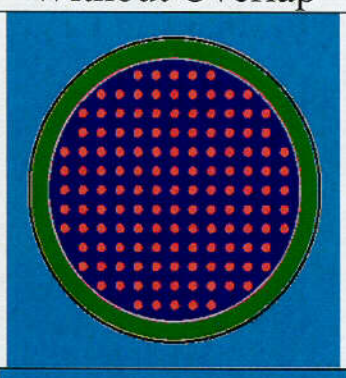
Triangular Lattice XY	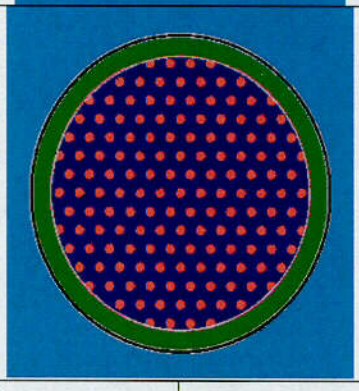	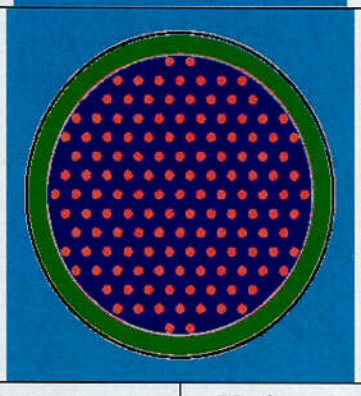
XZ Views (at Y = 0.0)	Square  Triangular 	Square 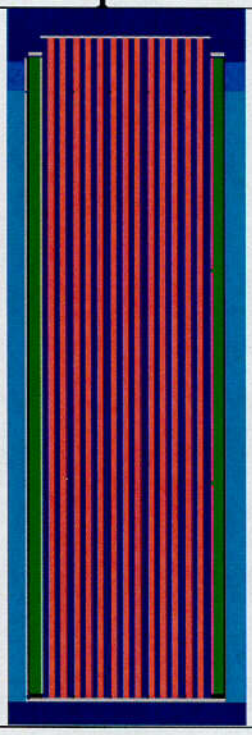 Triangular 

*55kgs UO_2 at a W/F = 4.50

C10

Figure 6.6d –NPC Container Square and Triangular 17X17 Fuel Rod Lattice* Models With the Virtual Fill Option

Model	VFO Lattice		Regular Lattice with Overlap	
Square Lattice XY	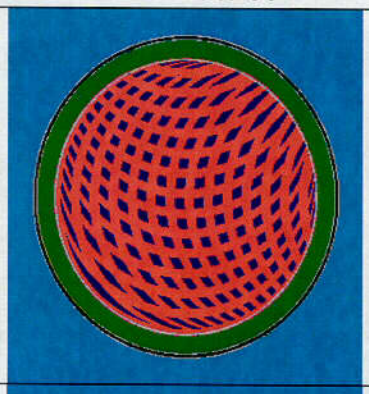		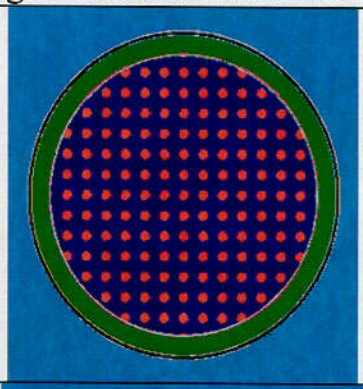	
Triangular Lattice XY			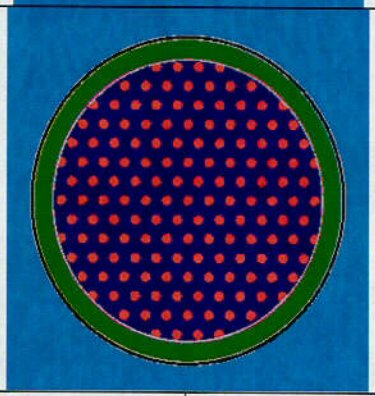	
XZ Views (at Y = 0.0)	**Square**	**Triangular**	**Square**	**Triangular**
	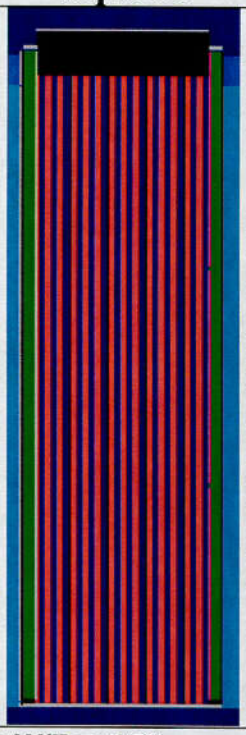			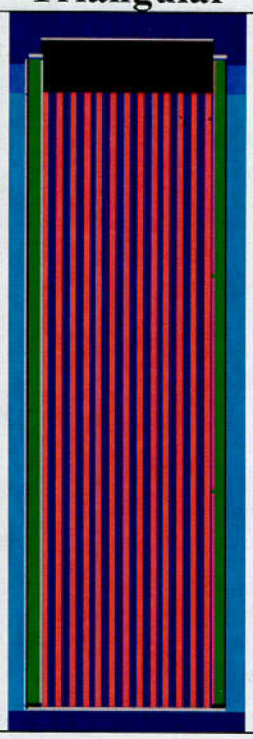

*55kgs UO_2 at a W/F = 4.50

C11

The Virtual Fill Option (VFO) has been used in this analysis because it permits modeling of fuel lattices with a very large number of cylindrical elements (rods). Since only one geometry unit is actually used for the lattice (and the lattice is created by mirror reflection boundary conditions on the unit) the size of the array that can be modeled is essentially unlimited.

This analytic capability is required when analyzing the most reactive fuel lattice without regard to particle size outer diameter (OD) or W/F ratio since the optimum outer rod diameter for 5.00% enriched UO_2 rods is in the range of 0.05 inches to 0.15 inches. Explicit modeling of fixed arrays of these sizes of cylindrical elements in the ICCAs would require hundreds of thousands of elements in the lattice. In the present analysis, the range of cylindrical diameters analyzed for the optimum case is derived from four separate particle size diameters through optimum heterogeneity (e.g., 0.20", 0.10", 0.05", and 0.025" diameters). Example 2D plots for these cases are shown in Figure 6.6e (the XZ models are those for the square lattices; the models for the triangular lattices are similar).

This analysis demonstrates that optimum heterogeneity occurs at (or very near) particle size diameter of 0.100". An actual 'random' array of particles of unrestricted diameter is no more reactive than the 'ordered' arrays of heterogeneous cylindrical elements analyzed herein under optimum diameter and spacing (W/F ratio) conditions. This is the basis of applying these results to heterogeneous fuel mixtures of unrestricted particles sizes.

Figure 6.6e – NPC Container Models for the VFO Analysis of Optimum Rod Diameters*

Rod Diameter (Inches)	XY Square Lattices	XZ Model (Y = 0)	XY Triangular Lattices
0.025	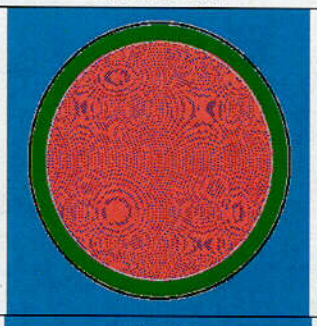		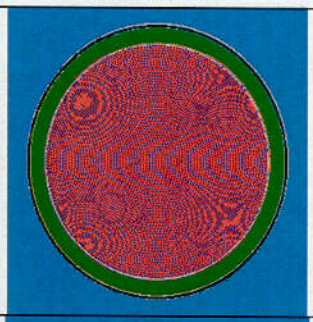
0.050	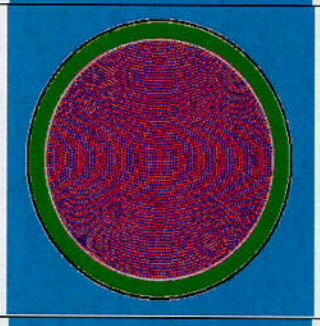		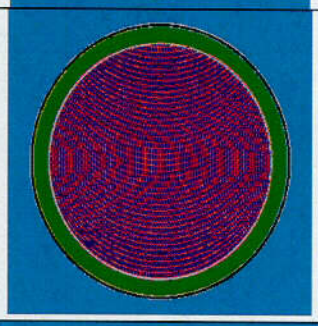
0.100	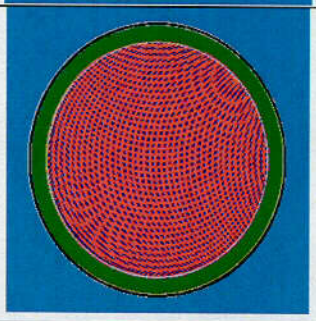		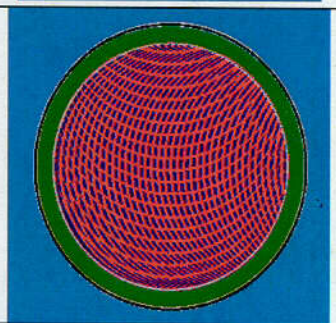
0.200	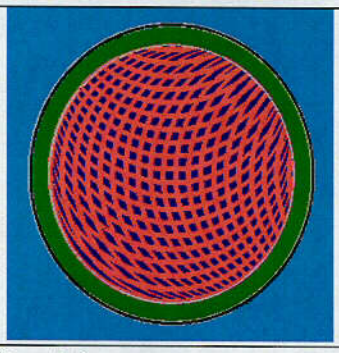		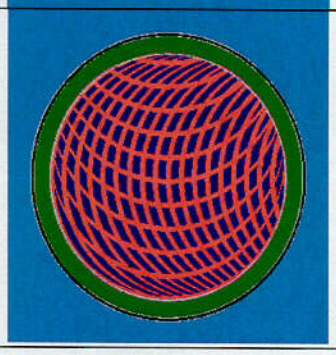

*46 kgs UO_2 at W/F = 5.2

C12

6.3.4 UNDAMAGED AND DAMAGED PACKAGE ARRAYS

Two basic package array model constructs are included in this evaluation - undamaged and damaged.

6.3.4.1 Undamaged Package Arrays with Homogeneous UO_2 and H_2O

In the undamaged array case for homogeneous UO_2 and H_2O, 60 kgs theoretical UO_2 compound plus variable water moderation is modeled through optimal moderation conditions in which the ICCA becomes effectively "full". No restriction on water moderation in the undamaged model is required, provided that each ICCA is limited to not greater than 60 kgs total material weight.

Table 6.7 provides the calculated fuel height for 60 kgs UO_2 compound and water mixtures within the ICCA inner canister as a function of weight fraction H_2O added (up through optimum, full ICCA conditions). In these undamaged models, homogeneous theoretical density UO_2 compound density is used (rho_uo2 = 10.96 g/cc). The weight fraction H_2O corresponding to a full ICCA occurs at wt.fr._h2o = 0.28504.

Table 6.7 Fuel Material Specifications – Undamaged Package Array (60 kgs UO_2 + H_2O theoretical mixture, unrestricted H2O)

COM	WF-W	FR.ENR	DFACT	RHOMIX gm/cc	RHOC gm/cc	RHOU gm/cc	UFACT	G-BIAS	K-BIAS	H/5	H/U x10	HEIGHT cm	
	RADIUS = 10.814 CM				FUEL MASS = 60.000 KG								
UO2	.150	.05000	1.0000	4.3945	3.7354	3.2925	.88144	0.0002	0.0125	104	53	43.721	
UO2	.200	.05000	1.0000	3.6631	2.9305	2.5830	.88144	-.0020	0.0098	148	75	55.729	
UO2	.250	.05000	1.0000	3.1404	2.3553	2.0761	.88144	-.0044	0.0070	197	100	69.339	
UO2	.260	.05000	1.0000	3.0533	2.2594	1.9915	.88144	-.0049	0.0065	208	105	72.281	
UO2	.270	.05000	1.0000	2.9708	2.1687	1.9116	.88144	-.0054	0.0059	219	111	75.304	
UO2	.280	.05000	1.0000	2.8927	2.0828	1.8358	.88144	-.0059	0.0053	230	117	78.411	
UO2	.285	.05000	1.0000	2.8549	2.0411	1.7992	.88144	-.0062	0.0050	236	119	80.01	(*)

(*) ICCA full condition, wf-w = 0.28504

The homogeneous UO_2 and H_2O models for undamaged arrays consist of infinite arrays of normal condition NPC packages. Per the applicable IAEA and 10 CFR §71.59 standards, the undamaged package arrays are evaluated with the individual units close-packed modeling of the 5N = infinite arrays is accomplished by using a single unit with mirror boundary conditions on all 6 sides, which is conservative relative to the model for a fully reflected finite system.

Figures 6.7a-6.7f depict the models used to assess normal conditions of transport, and illustrate the increasing fuel height – up to the 80.01 cm maximum - as the weight fraction of H_2O (WF-W) is increased. These sample plots apply to the 60 kg UO_2 mass limit.

The package was subjected to the tests specified in IAEA and 10 CFR §71.71, normal conditions of transport, and, as reported in Chapters 2, *Structural Evaluation* and Chapter 3, *Thermal*, the geometric form of the package was not substantially altered. No water leakage into the ICCAs occurred, and no substantial reduction in the effectiveness of the packaging was observed. The damage incurred will not affect the technical evaluation, and the package contents under normal conditions of transport will be less reactive than the contents under hypothetical accident (damaged) conditions.

Figure 6.7a – Infinite undamaged array: 60 kgs UO_2 + 15% H2O, theoretical mixture

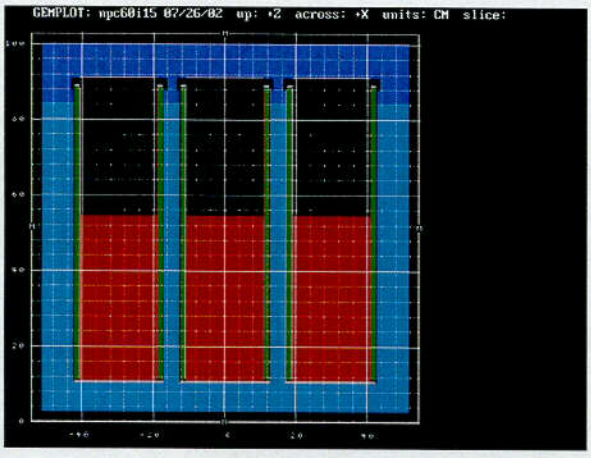

Figure 6.7b – Infinite undamaged array: 60 kgs UO_2 + 20% H_2O, theoretical mixture

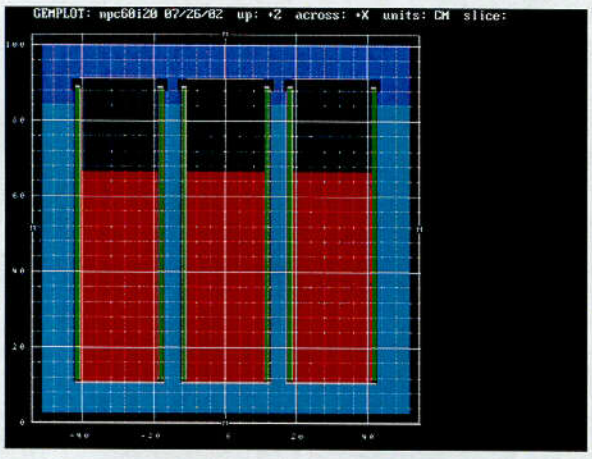

C13

Figure 6.7c – Infinite undamaged array: 60 kgs UO_2 + 25% H_2O, theoretical mixture

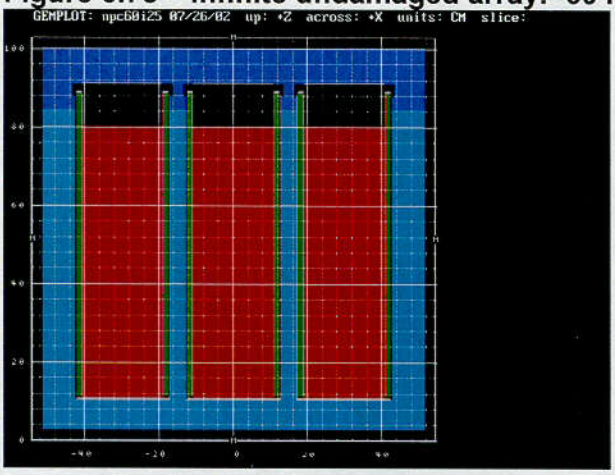

Figure 6.7d – Infinite undamaged array: 60 kgs UO_2 + 26% H_2O, theoretical mixture

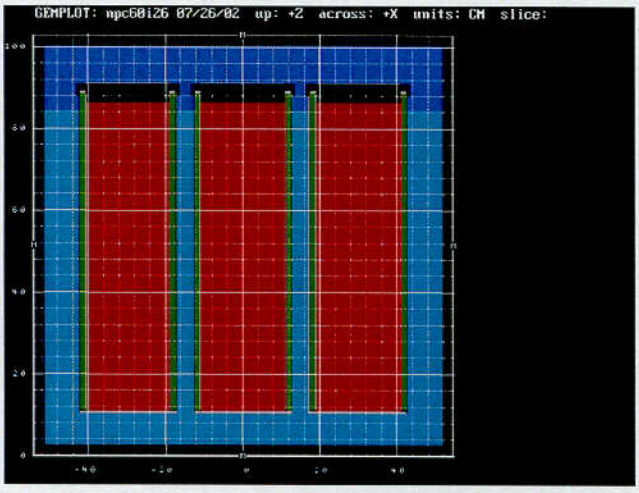

Figure 6.7e – Infinite undamaged array: 60 kgs UO_2 + 27% H_2O, theoretical mixture

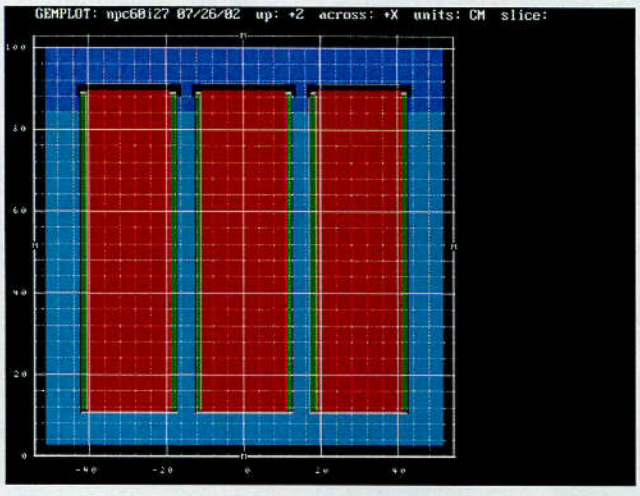

C14

Figure 6.7f – Infinite undamaged array: 60 kgs UO_2 + 28.504% H_2O, theoretical mixture (ICCA full)

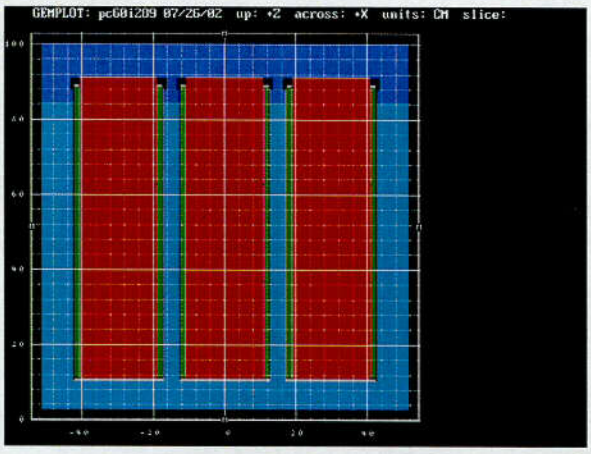

6.3.4.2 Undamaged Package Arrays with Heterogeneous UO_2 Rods in H_2O

The container model for undamaged arrays with heterogeneous UO_2 right circular cylinder elements in H_2O is the same as that shown in Figures 6.7a through 6.7f, but with the fuel lattices as described in Section 6.3.3.2. As in the homogeneous case, the undamaged arrays were modeled as infinite by mirror reflecting the single package at its six (6) boundaries.

6.3.5 DAMAGED PACKAGE ARRAYS

6.3.5.1 Damaged Package Arrays with Homogeneous UO_2 and H_2O

The NPC package was subjected to the tests specified in IAEA and 10 CFR §71.73, Hypothetical Accident Condition (HAC) testing and the geometric form of the package was not substantially altered. The four individual Certification Test Units (CTUs) were fabricated that underwent testing summarized in detail in Section 2.7, *Hypothetical Accident Conditions*.

Certification Test Units CTU-1 and CTU-2 were subjected to required IAEA and 10 CFR §71.73(c)(4) thermal excursion with an average flame temperature of 1,475 °F (800 °C) for a period of at least 30 minutes. In both tests, the fuel was ignited and the test item was subjected to a minimum of 30 minutes of a fully engulfing hydrocarbon pool fire.

A modified CTU-1 unit with reinforced corners was retest of the CTU-3 HAC test sequence (CG-over lid-corner orientation). A 10-guage (0.135-inch) doubler plate was added to reinforce the corners. CTU-1 was subjected to a Jet-A pool fire test. The Jet-A fuel was placed in the tank at a level sufficient to initiate the burn. Additional fuel was pumped into the tank during the testing as necessary to maintain the burn for 30-minutes. During the CTU-1 Jet-A burn test, the overall average flame temperature was 1,809 deg. F (in excess of the required 1,475 deg. F). The maximum surface temperature recorded was recorded as 2,319 deg. F.

C15

The CTU-1 residual foam thickness measurements are reported in Appendix 2.10.1.7.1.6. The –x (left), +x (right), -y (rear), and +y (front) average cube face residual foam thickness values were determined to be 1.01, 1.71, 2.19, and 0.89-inches, respectively. The –z (bottom) and +z (top lid) average thickness' were 0.23, and 3.09-inches, respectively. The cube face averages were modeled to assess observed CTU-1 non-uniform foam burn effects on package reactivity.

For CTU-2, a diesel fuel pool fire test was used. During the CTU-2 diesel burn test, the overall average flame temperature was 1,972 °F (in excess of the required 1,475 °F). The maximum surface temperature recorded was recorded as 2,308 °F.

The CTU-2 residual foam thickness measurements are reported in Appendix 2.10.1.7.2.6. The –x (left), +x (right), -y (rear), and +y (front) average cube face residual foam thickness values were determined to be 0.26, 1.41, 0.23, and 0.58-inches, respectively (refer to Appendix 2.10.1.7.2.6). The –z (bottom) and +z (top lid) average thickness' were 0.0, and 3.0-inches, respectively. The cube face averages were modeled to assess observed CTU-2 non-uniform foam burn effects on package reactivity.

For the final damaged package array model, the maximum observed foam burn is uniformly applied on all six faces of the cube. This results in zero residual foam on all six faces of the cube as measured from the ICCA radial and axial centerline. The total face burn model construct conservatively bounds the observed package performance under HAC testing. This is underscored by the fact that the minimum hydrogen content in both the poly and foam regions is used, and the maximum 10% density tolerance is applied in all foam regions.

In all damaged package array models, a 2% reduction in polyethylene density (0.92 * 0.98) is uniformly applied. This reduction in density effectively covers the observed 0.6% weight loss and 0.25% mass allowance for minimum specified poly height of 30.3" verses the modeled 30.375" height.

The minor x-y and x-z movement of the 3 × 3 ICCA array contained within the OCA are compensated by the physical deformation of the OCA body itself, coupled with the conservatism's described in Section 6.3.1.5, Models- Actual Package Differences.

The observed damage incurred to the packaging and its contents did not affect this technical evaluation - as the packaging and its contents post HAC testing is determined to be within the bounding assumptions and analyzed conditions of this evaluation.

The damaged package array models consist of finite, near cubic 5x5x6 close packed arrays (2N = 150) to minimize neutron leakage. Additional close packed arrays using a 6x5x5 (2N = 150) and 9x9x2 (2N =162) are assessed to confirm the aspect ratio of the basic 5x5x6 array is most reactive.

In all cases, the close packed array is surrounded by 12" (30.48-cm) full-density water reflector. As required by IAEA and 10 CFR §71.59, the damaged packages are evaluated as if each package was subjected to the tests specified in 10 CFR §71.73, hypothetical accident conditions, with optimum interspersed moderation, and full water reflection.

The damaged package Inner Containment Canister Assembly (ICCA) contents are modeled per Section 6.3.1.4, *Materials*, Table 6.6.

The UO_2 compound mass per canister, internal moderation, observed foam burn conditions (CTU-1, CTU-2), and maximum foam burn conditions are modeled to determine an acceptable package Transport Index (TI) based on criticality control.

In addition, supplemental NPC damaged package array models are constructed based on the limiting acceptable payload and foam burn conditions derived above to study certain reactivity effects. These sensitivity studies include:

Effect of the package array shape (aspect ratio) on system reactivity. A 6 × 5 × 5 array (2N = 150) and a 9 × 9 ×x 2 array (2N = 162) are both assessed using the limiting burn condition and acceptable payload.

Effect of internal moderator content and payload contained in the UO_2 + H_2O mixture region contained within the ICCA.

Effect of 100% foam burn and subsequent replacement by optimal interspersed water moderation. In this set, the water density is varied from void through 12.5% of full density water to determine the hydrogen content necessary to demonstrate safety of the package, and determine if the damaged package is over or under-moderated.

Effect of ICCA center-to-center movement on reactivity for a specified damaged condition. For these cases, the nominal 11.75" (29.8450 cm) center-to-center ICCA spacing is uniformly reduced by 1/8" (0.3175 cm) increments to 11.25" (28.575 cm) to quantify the effect (if any) on ICCA spacing within the damaged package.

Effect of including external Type 304L stainless steel structure used for fork truck lifting of the package. This structure is quantified and effectively "smeared" onto the bottom layer of the OCA body.

Effect of polyethylene gap as determined from the physical measurements of the ICCA's post HAC testing is assessed to confirm the modeled poly height and density assumptions. The modeled poly height of is reduced by 75 mils to minimum specified height of 30.3". The maximum gap formation at top/bottom is also modeled and compared with the modeled limiting damaged package array calculation.

The following 2D images are provide to clarify the damaged package array model constructs and associated sensitivity studies:

- Figure 6.8a and 6.8b depicts horizontal/vertical slices of the damaged 5 × 5 × 6 package array to determine acceptable UO_2 equivalent payload under postulated damaged conditions of transport, using the observed CTU-1 and CTU-2 non-uniform foam burn conditions, respectively.

- Figure 6.8c depicts horizontal/vertical slices of the damaged 5 × 5 × 6 package array to determine acceptable UO_2 equivalent payload under postulated damaged conditions of transport, applying the maximum burn condition.
- Figures 6.8d and 6.8e depict horizontal/vertical slices of the damaged 6 × 5 × 5 and 9 × 9 × 2 package array size respectively, to confirm the close packed 5 × 5 × 6 aspect ratio is the most reactive array configuration.
- Figure 6.8f depicts horizontal/vertical slices of the damaged 5 × 5 × 6 package array used to quantify the required hydrogen content necessary for demonstrating package safety.
- Figure 6.8g depicts horizontal zoom of the damaged 5 × 5 × 6 package array for the 11.25" (28.575 cm) ICCA center-to-center spacing to quantify the ICCA (x,y) movement effect.
- Figure 6.8h depicts vertical zoom of the damaged 5 × 5 × 6 damaged package array that include the additional external stainless steel structure.
- Figure 6.8i depicts vertical top/bottom zoom of the damaged 5 × 5 × 6 damaged package array that includes the maximum polyethylene gap formation.

Figure 6.8a – Fully reflected damaged 5x5x6 package array: 60 kgs UO_2 + H_2O mixture, CTU-1 observed non-uniform burn (horizontal and vertical views)

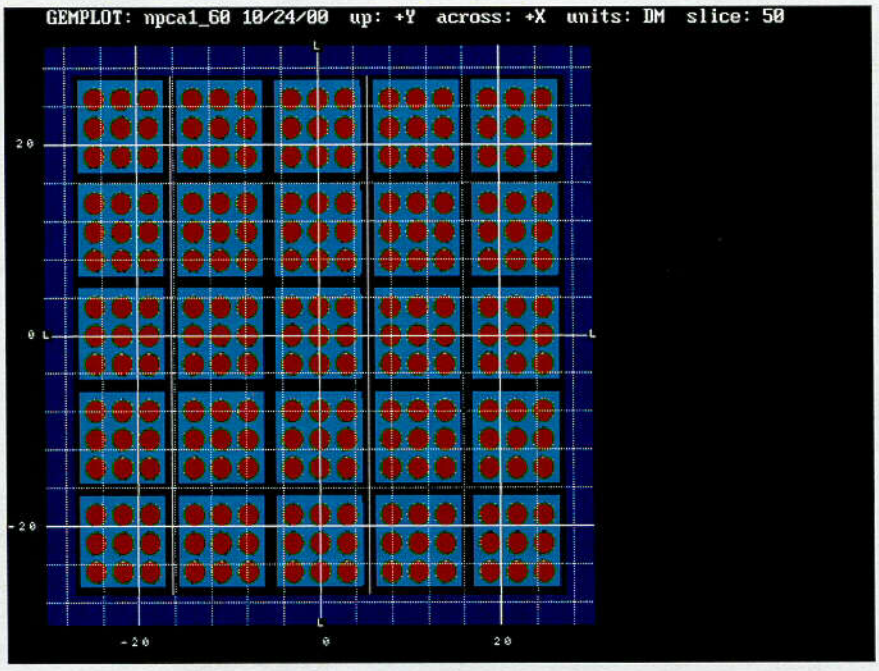

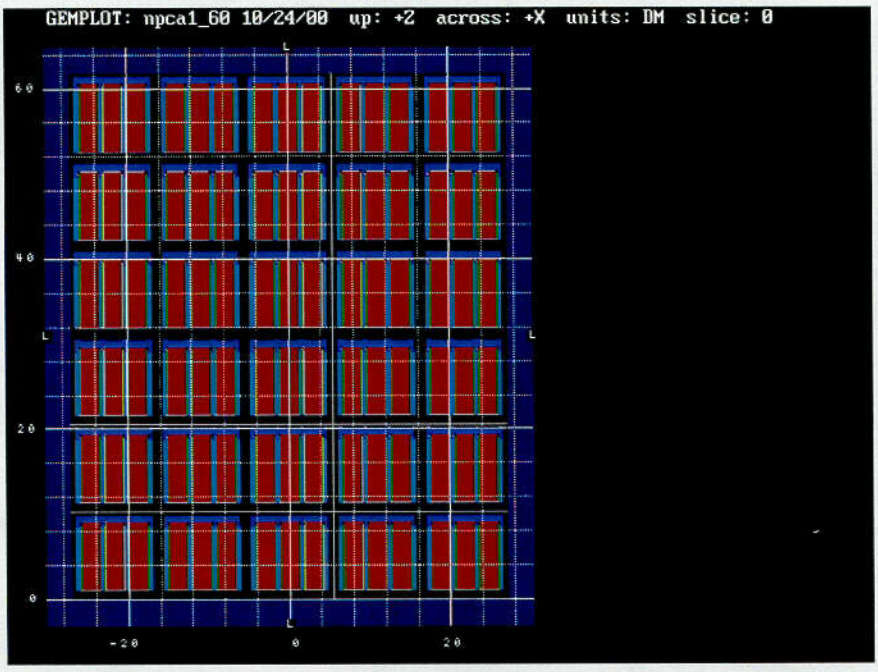

C16

Figure 6.8b – Fully reflected damaged 5x5x6 package array: 60 kgs UO_2 + H_2O mixture, CTU-2 observed non-uniform burn (horizontal and vertical views)

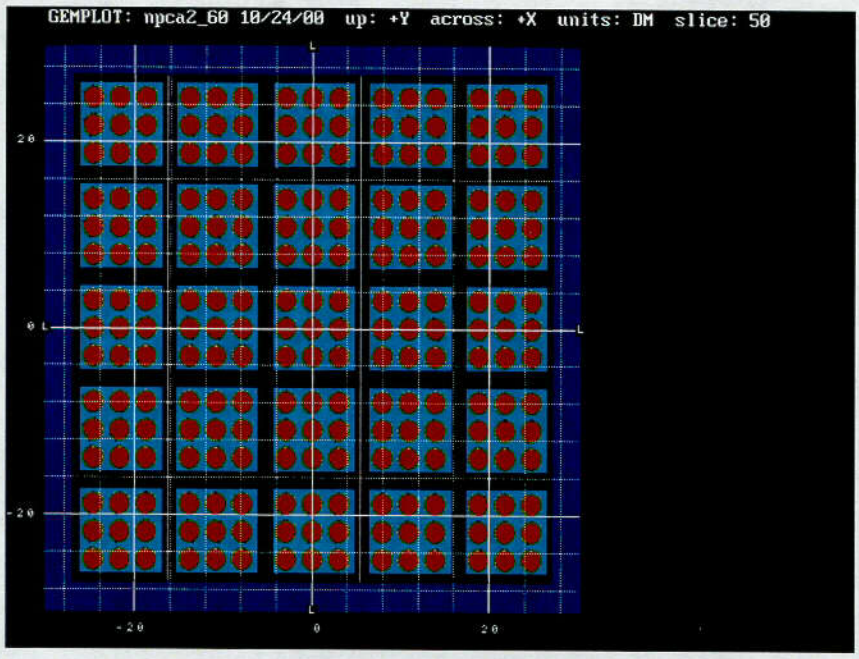

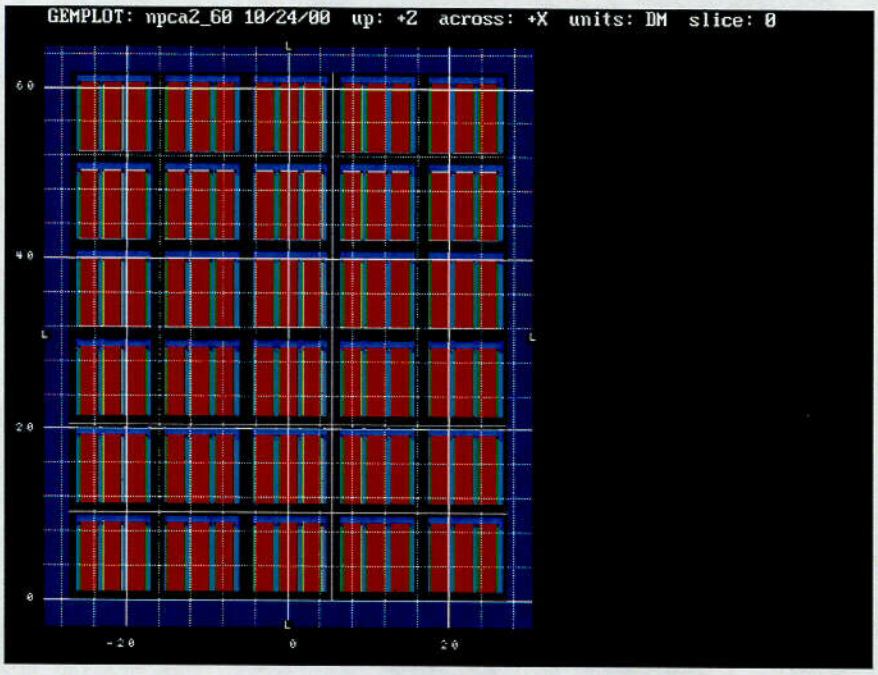

C17

Figure 6.8c – Fully reflected damaged 5x5x6 package array: 60 kgs UO_2 + H_2O mixture, maximum burn (horizontal and vertical views)

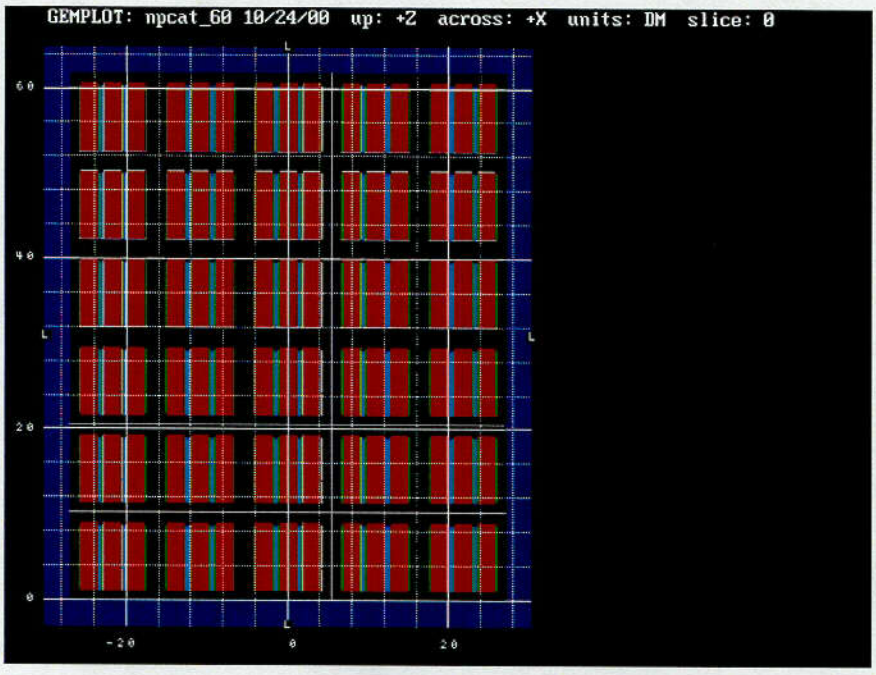

C18

Figure 6.8d – Fully reflected damaged 6 × 5 × 5 package array: 60 kgs UO_2 + H_2O mixture, maximum burn (horizontal and vertical views)

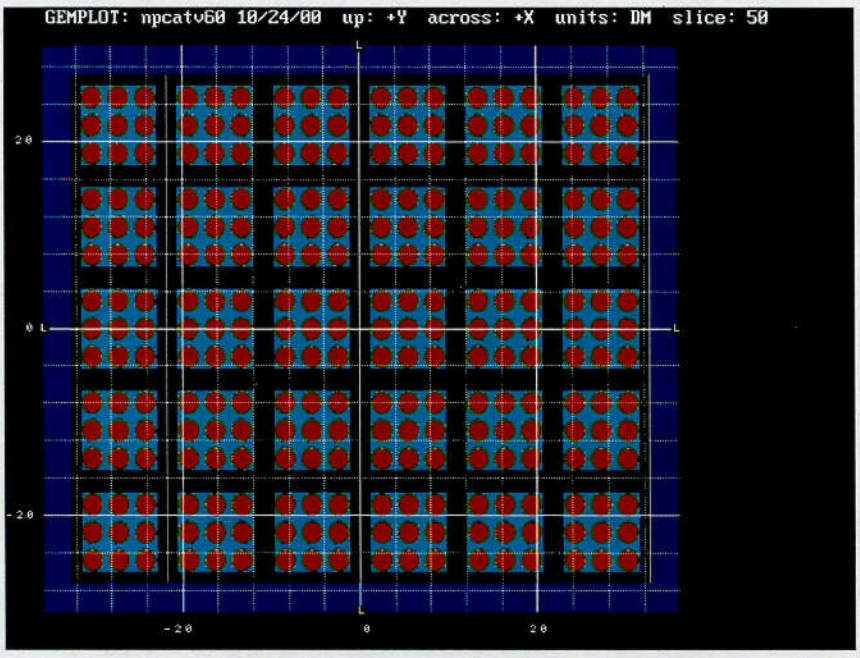

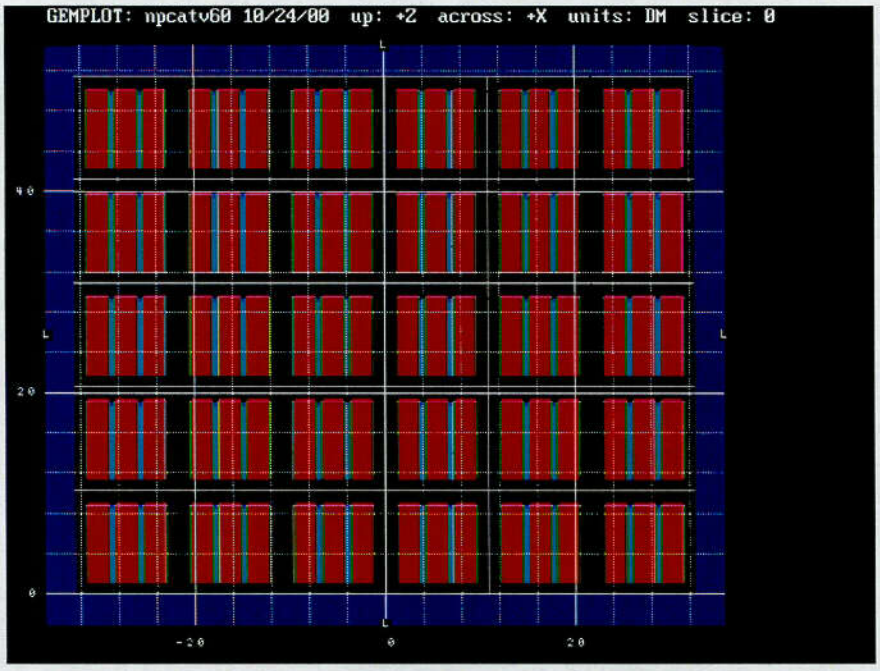

C19

Figure 6.8e – Fully reflected damaged 9 × 9 × 2 package array: 60 kgs UO_2 + H_2O mixture, maximum burn (horizontal and vertical views)

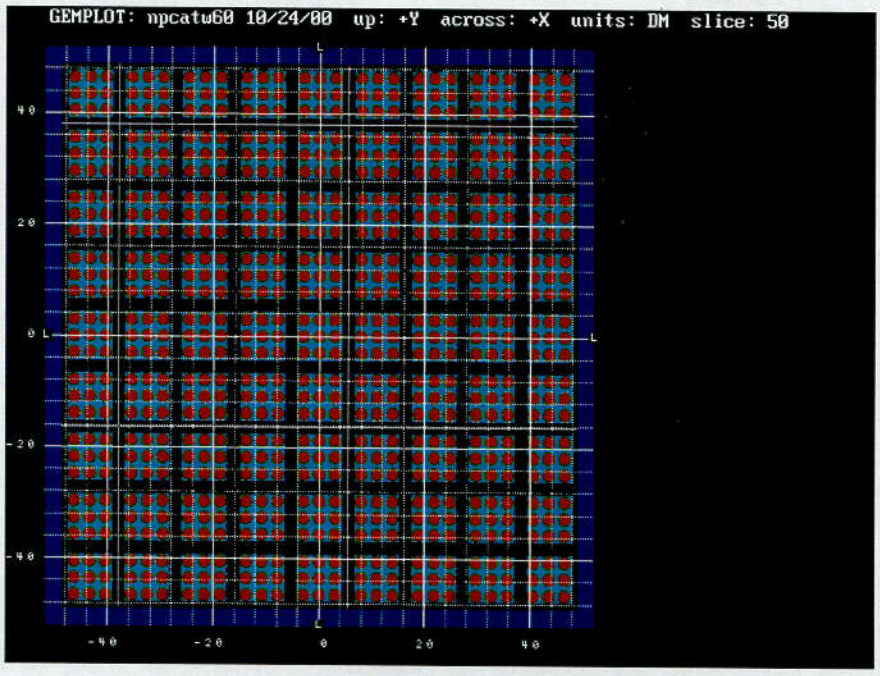

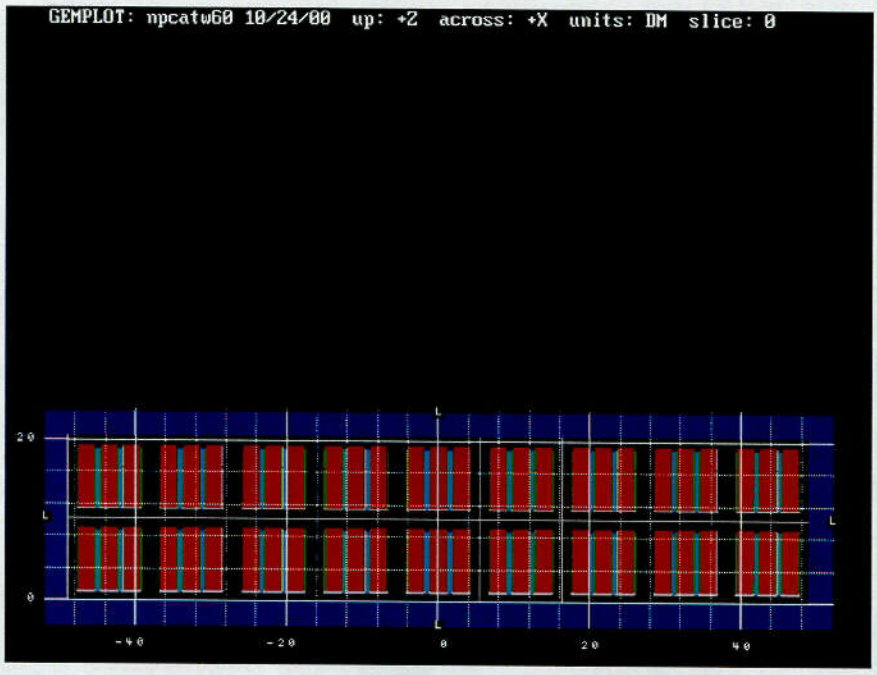

C20

Figure 6.8f – Fully reflected damaged 5 × 5 × 6 package array: 60 kgs UO_2 + H_2O mixture, 100% foam burn, void replacement (horizontal and vertical views)

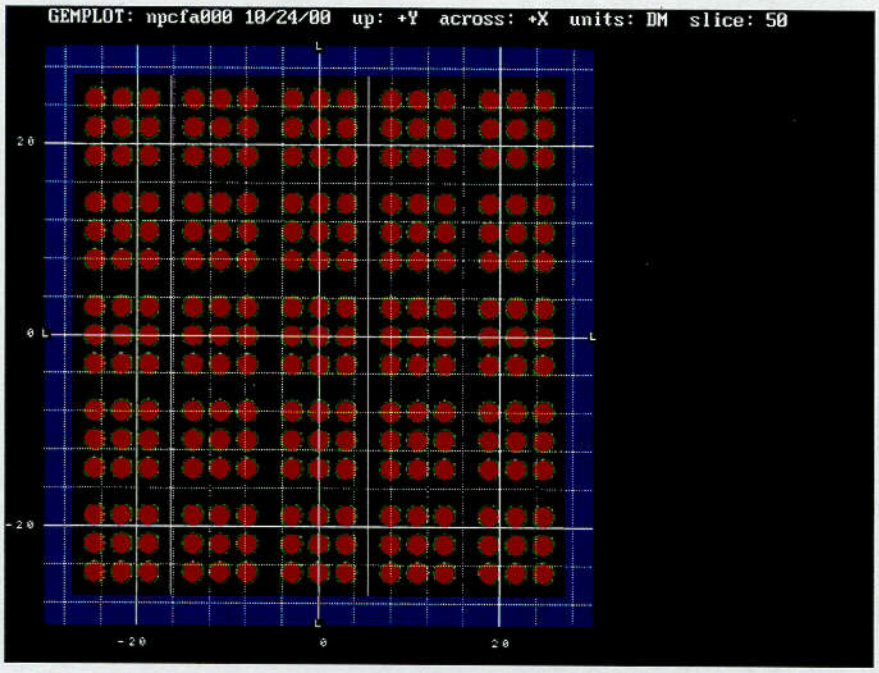

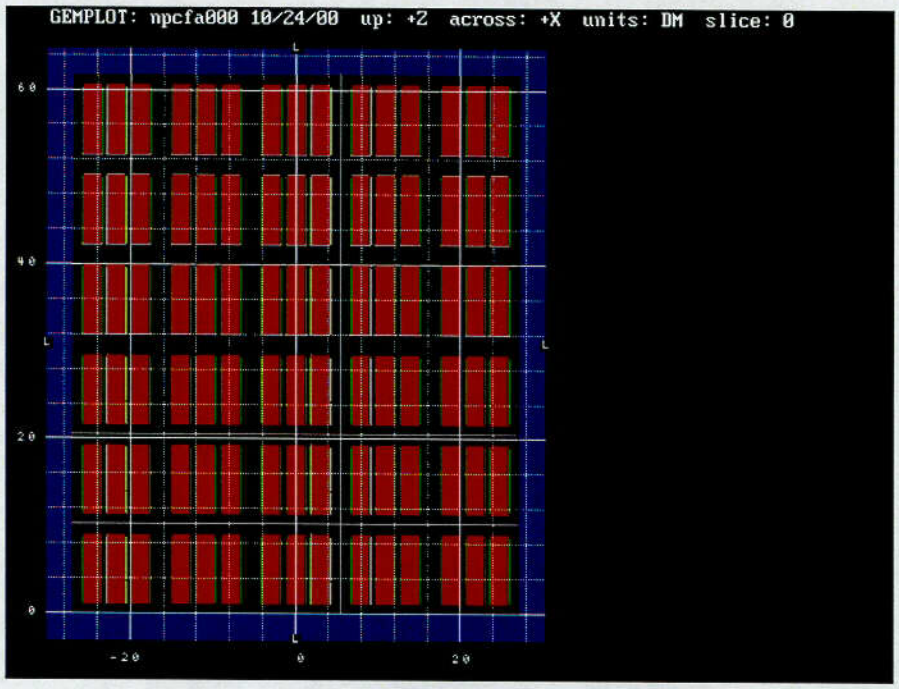

C21

Figure 6.8g – Fully reflected damaged 5 × 5 × 6 package array: 60 kgs UO_2 + H_2O mixture, maximum burn, 11.25" c-c ICCA spacing (horizontal zoom, lower left array corner)

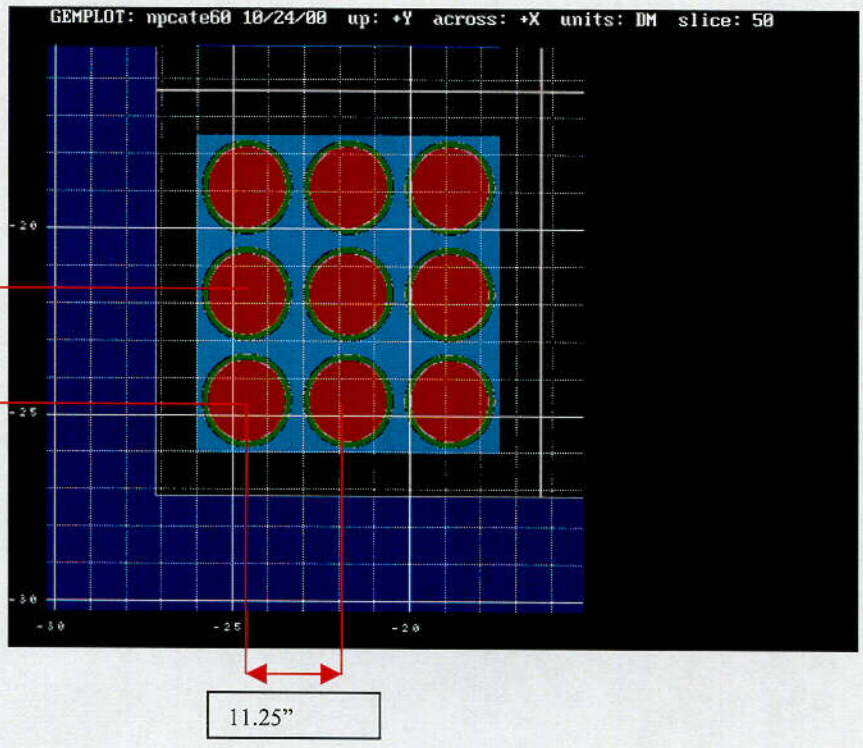

Figure 6.8h – Fully reflected damaged 5 × 5 × 6 package array: 60 kgs UO_2 + H_2O mixture, maximum burn, external structure add-on to bottom of OCA body (vertical zoom, lower left array corner)

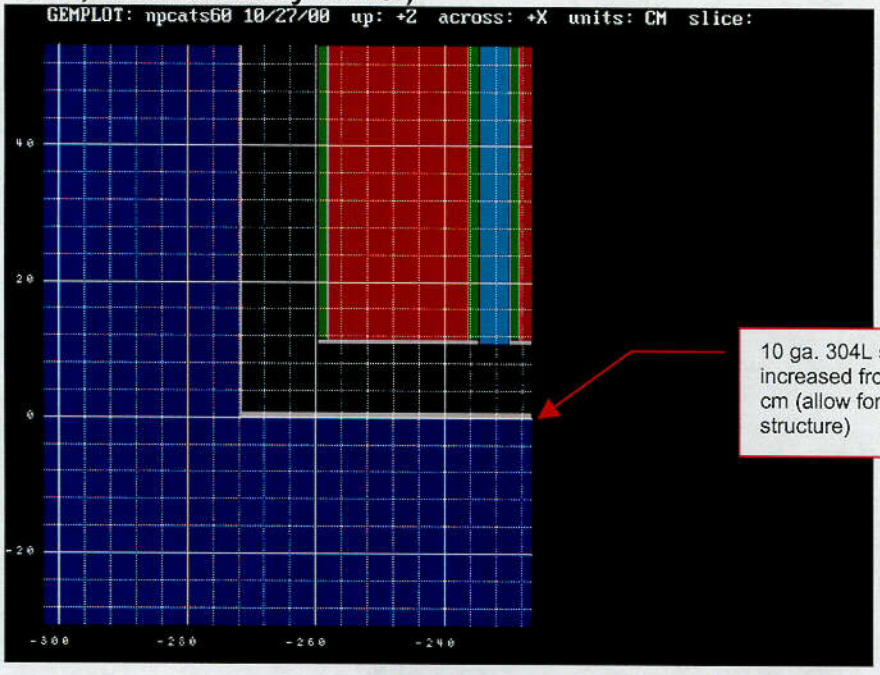

C22

Figure 6.8i – Fully reflected damaged 5x5x6 package array: 60 kgs UO_2 + H_2O mixture, maximum burn, observed maximum poly gap at top/bottom (vertical zoom, ICCA)

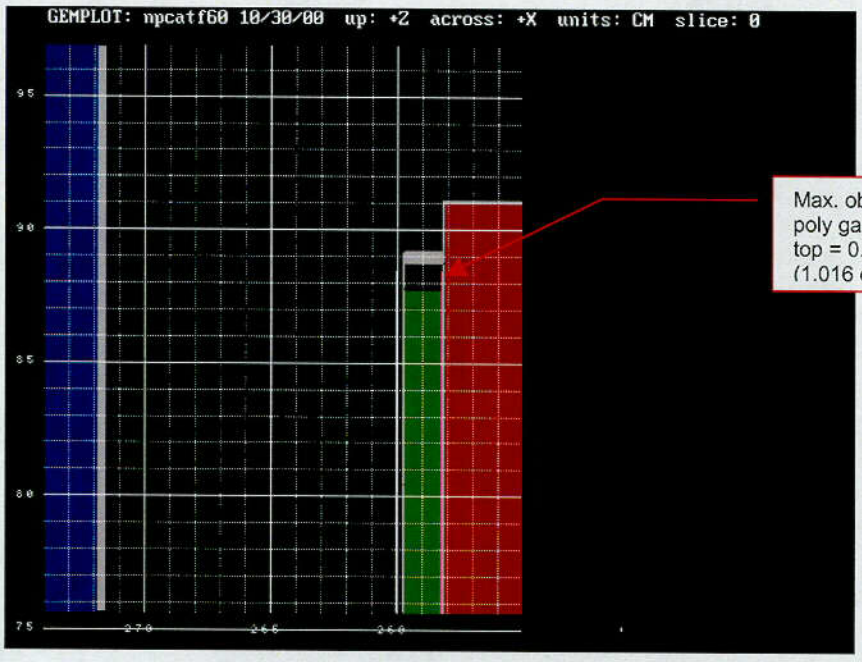

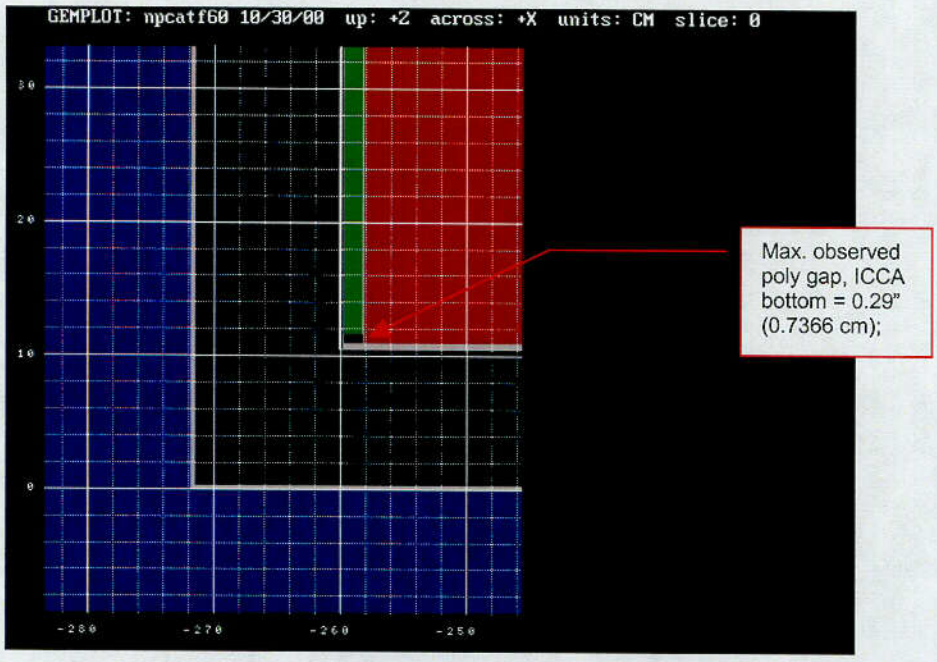

C23

6.3.5.2 Damaged Package Arrays with Heterogeneous UO_2 in H_2O

Damaged package arrays with heterogeneous UO_2 cylindrical elements (rods) have been analyzed with the same applicable worse case container array model as used in the homogeneous analyses. This is the array model shown in Figure 6.8c in the preceding section. The models for the heterogeneous lattices for these cases are the same as described in Section 6.3.3.2.

6.4 METHOD OF ANALYSIS

GEMER, a proprietary Global Nuclear Fuel company criticality analysis computer code was used in the analysis of these computational models (Ref. 1). All calculations were performed on verified workstations using Pentium processors running under Windows NT.

6.4.1 COMPUTER CODE SYSTEM

GEMER is a Monte Carlo program, which solves the neutron transport equation as an eigenvalue or a fixed source problem including the neutron-shielding problem. GEMER adds an advanced geometry input package to the problem solving capability of the Monte Carlo code that is very similar in capability to KENO Va.

6.4.2 CROSS SECTIONS AND CROSS-SECTION PROCESSING

GEMER uses cross-sections processed from the ENDF/B-IV library. These cross-sections are prepared in 190-group format and the values in the resonance region may have the form of the resonance parameters or Doppler broadened multigroup cross-section. This treatment of cross-sections with explicit resonance parameters is especially suited to the analysis of uranium compounds in the form of heterogeneous accumulations or lattices. Thermal scattering of hydrogen is represented by the $S(\alpha,\beta)$ data in the ENDF/B-IV library. The types of reactions considered in the Monte Carlo calculation are fission, elastic, inelastic, and (n,2n) reactions; the absorption is implicitly treated by reducing the neutron weight by the non-absorption probability on each collision.

6.4.3 GEOMETRY MODELING OF FUEL REGIONS

The previous Section 6.3 gives a detailed description of the NPC shipping container geometry models used in this analysis. This section expands on the descriptions of the fuel regions, especially regions containing lattices of cylindrical fuel elements (rods). As noted in the prior sections, the provision for heterogeneous fuel in the NPC is conservatively based on the analysis of lattices of UO_2 fuel in the form of right circular cylinder elements (rods) in the ICCAs. Both square and triangular lattices have modeled in the heterogeneous cases, together with consideration of lattice boundary conditions in which cylindrical elements in the lattices are either permitted or not permitted to overlap the internal ICCA wall boundary.

6.4.3.1 The INTERS and GEMER VFO Geometry Options

In addition to its standard geometry capabilities, the GEMER Monte Carlo code has two additional geometry options that are particularly useful in modeling rod lattices. The first is a special regular geometry construct called INTERS. As shown in Figure 6.9a, the INTERS region is a CUBOID with quarter cylinders missing along two opposite XY edges. The centerline of this region always passes through the X=0, Y=0 origin. Like regular geometry regions such as CUBOIDs or CYLINDERs, INTERS regions may be nested within each other, but the last region in the Box must be a CUBOID. The purpose of the INTERS region is to permit modeling of a triangular lattice of cylindrical rods by use of simple regular geometry input. This can be done two ways. One is to mirror reflect the INTERS box on its ±X and ±Y axes. (The +Z, -Z dimensions then define the height of the rods in the lattice.) The second way is to use two separate INTERS regions that differ by the location of quarter cylinder cutouts. As provided for by the INTERS input parameters, one region can be described by cutouts onn the –X,+Y and +X,-Y edges, and the second with the cutouts at the –X,-Y and +X,+Y edges. Placing these two regions in alternate X and Y locations in an array will then create a two-dimensional triangular lattice of cylinders. Because of its geometry definition, the INTERS constructs are for all practical purposes limited to use either with infinite triangular lattices, or with lattices in which the geometry is permitted to overlap a region (e.g. an ICCA) that the lattice is contained in. (GEMER does not currently have a boundary condition that would prevent overlap of part of an INTERS region.)

Figure 6.9a – The INTERS Geometry Region

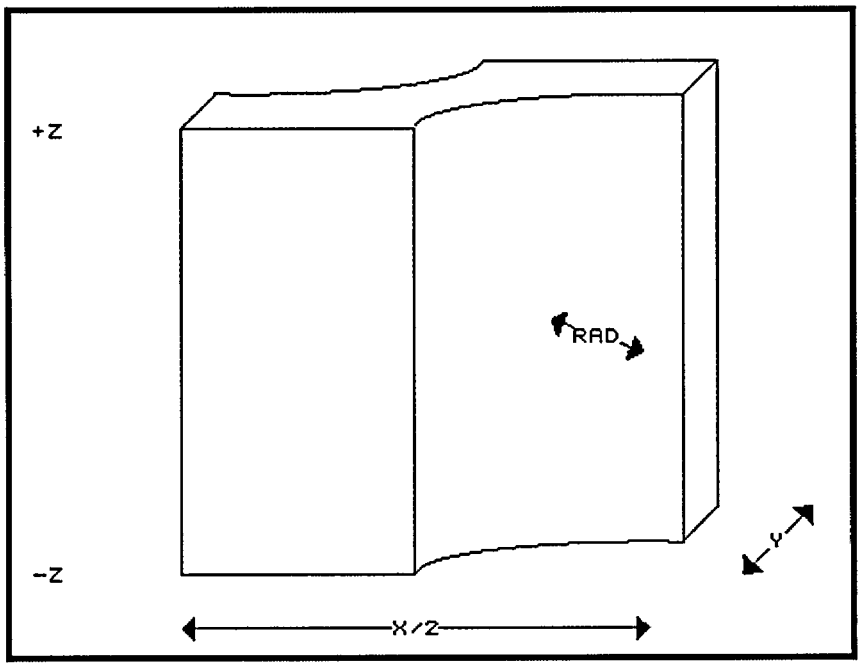

The second GEMER geometry option is the Virtual Fill Option (VFO). This option allows geometry regions to be automatically filled with a virtual representation of a separate region. As depicted in Figure 6.9b, the VFO of a complete Box Type (the "FILL REGION") that is itself mirror reflected on all six of its sides, allows placing in a larger region (the "BIG REGION") which is any regulary geometry region. When a neutron enters the Big Region, it is translated into the Fill Region and tracked via the standard Monte Carlo methods (e.g. importance weighing, splitting, Russian roulette) in the Fill Region until the code determines that the neutron's path has reached one of the Big Region's boundaries. It is then translated back to the Big Region where regular tracking resumes. This option is called "Virtual" because in reality, no Fill Region exists (i.e. is stored in the run-time memory) until a neutron enters the Big Region. When a neutron is translated into the Fill region, it is randomly located and then remains in this region, reflecting from wall to wall, until its track would take it back out of the Big Region. This wall-to-wall reflection effectively presents a fixed array of the Fill Region Boxes to the neutron tracking and hence can be used to model both square pitch and triangular pitch (via the INTERS Box) lattices in the Fill Region. One feature of note about VFO is that since each neutron entering the Big Region is randomly placed in the Fill Region, each neutron sees the same overall Fill Region lattice, but each of these lattices has a different location for its central unit. Over an entire calculation, the effect of this is to average the results of the tracking over all possible central locations.

Figure 6.9b – The Virtual Fill Option

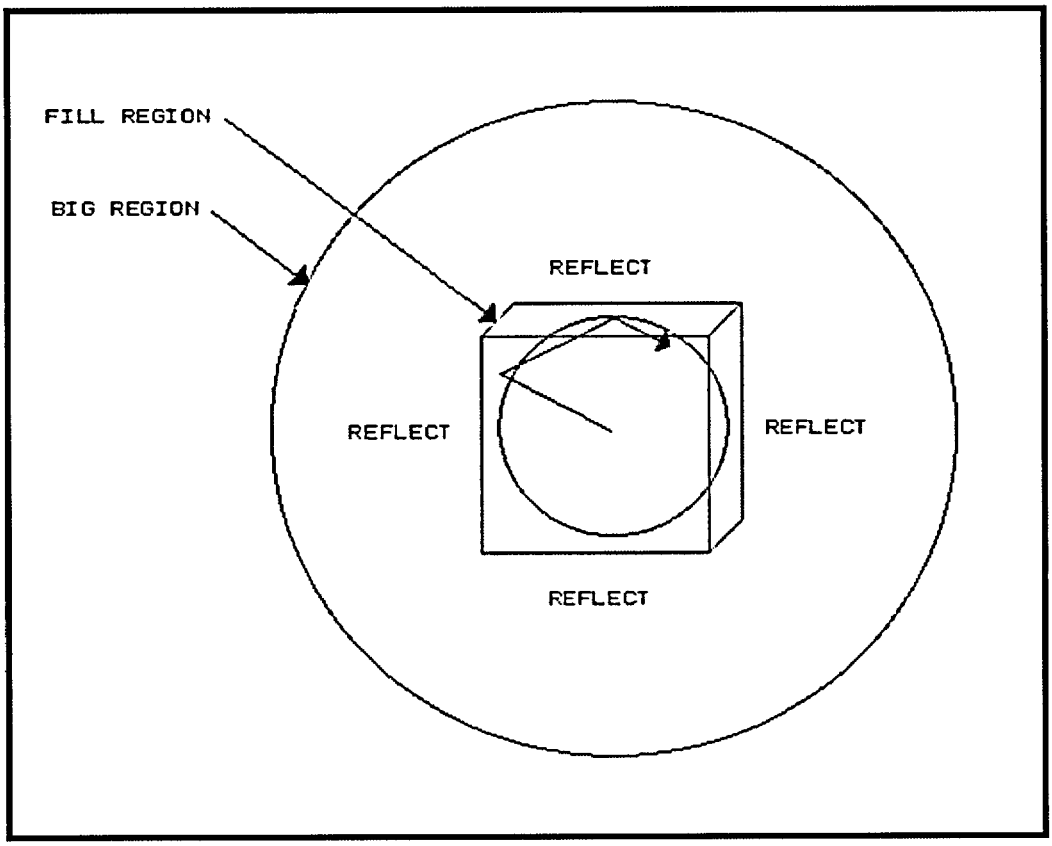

6.4.3.2 Water to Fuel Volume Ratios and Rod to Rod Spacings in Lattices of Fuel Rods

In uniform but heterogeneous fuel regions, the relative amount of moderator is specified as the Water to Fuel volume ratio (W/F ratio) in the unit cell. For uniform square and triangular pitched arrays of cylindrical (unclad) fuel rods in which the unit cells are two dimensional squares or triangles (since the heights of the rods in a given lattice are all the same), these W/F ratios are determined completely by the radii of the fuel rods and the center-to-center spacings between adjacent units. Figure 6.9c shows examples of the unit cells (the areas bounded by the dotted lines) for these two types of arrays from which it can be seen that the relationship between the W/F ratios and the radii (R_f) and spacings (L) are:

$$\text{Square Lattices: } W/F = \frac{L^2 - \pi \times R_f^2}{\pi \times R_f^2}$$

and

$$\text{Triangular Lattices: } W/F = \frac{0.866 \times L^2 - \pi \times R_f^2}{\pi \times R_f^2}$$

[0.866 in these equations is Sqrt(3.0)/2.0.]

Comparing these two formulas, it can be seen that if a Square and Triangular lattice with the same diameter fuel rods have the same W/F ratios, the triangular lattice will have a greater pitch (i.e. L) between rods. In the ICCAs, this means that for the same W/F ratios, triangular lattices will have fewer rods and thus for the same fissile mass, will be taller.

Figure 6.9c – Square and Triangular Lattices

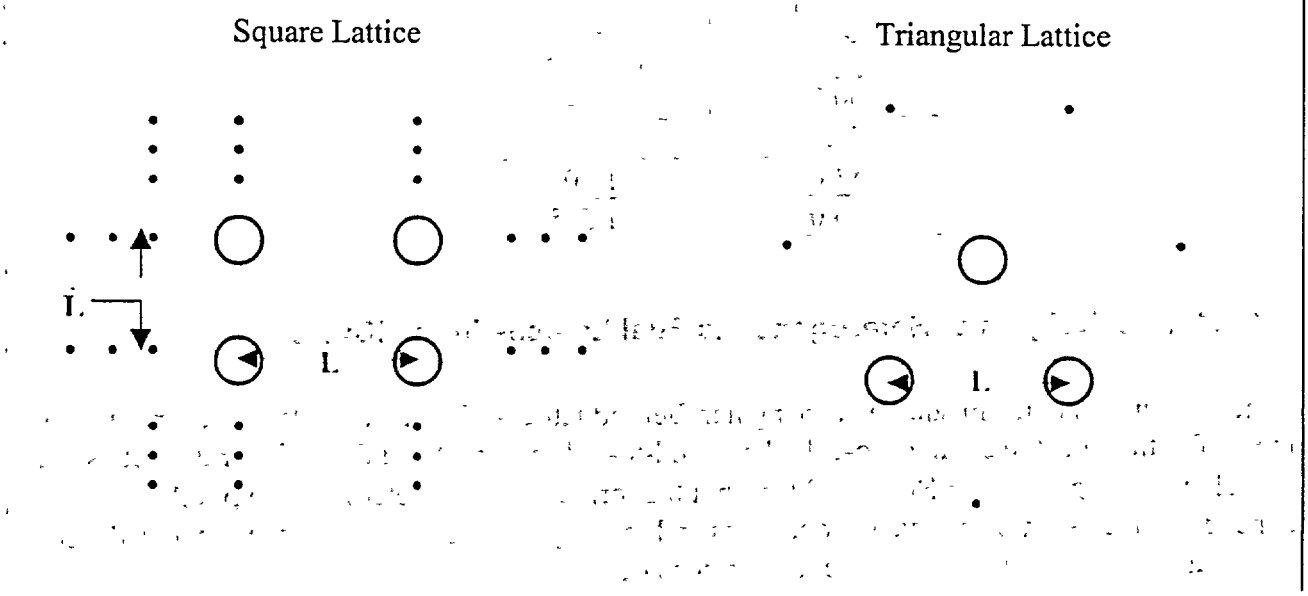

6.4.3.3 Fuel Heights of Homogeneous Fuel Mixtures in the ICCAs

A brief description is given is Section 6.3.1.4 of the treatment of homogeneous UO_2 and water mixtures in the ICCA fuel region. In summary, this method is

i. For a (binary) fuel mixture with a given weight fraction of H_2O, determine the corresponding UO_2 density, ρ, assuming a maximum theoretical density of UO_2 of 10.96 gm/cm^3.

ii. For a given mass, M, of UO_2 in the ICCA, determine the Volume, V, of the $UO_2 + H_2O$ mixture by

$$\rho \times V = M$$

iii. Since the ICCA is cylindrical, V is equal to the base area, $\pi \times R_{ICCA}^2$, times the height, h, of the mixture, and hence

$$H = M/(\rho \times \pi \times R_{ICCA}^2).$$

Since the maximum height in the ICCA is 80.01 cm, and its radius is 10.8141 cm, this means that for a given UO_2 mass there is a minimum UO_2 density below which the contents of the ICCA will be less than the specified mass. The following Table 6.8 tabulates these minimum densities for the mass limits applicable to this analysis.

Table 6.8 Minimum UO_2 Densities for Homogeneous UO_2 and H_2O Mixtures in the ICCA

UO_2 Mass Limit (kgs)	Minimum UO_2 Density (gm/cm^3)
60.0	2.041
55.0	1.871
53.0	1.803
46.0	1.565

6.4.3.4 Fuel Heights of Heterogeneous Fuel Lattices in the ICCAs

In heterogeneous uniform square or triangular fuel rod lattices, the fuel heights are still related to the W/F ratios (i.e. the cylinder-to-cylinder or rod-to-rod spacings) and the cylinder diameters via the relationship $\rho \times$ Area $\times$ Height = Mass, but the formula used to determine the $\rho \times$ Area depends on the assumed boundary conditions and the way in which the regions are modeled. In this analysis, three different cases have been considered.

Case 1 is for arrays in which it is assumed that the right circular cylinder fuel elements (rods) can overlap the (ICCA) boundary. This assumption means that if a given fuel element in the lattice is such that part of it overlaps the ICCA region boundary, the external overlap part is deleted from the model but the part internal to the ICCA is kept. For this exact modeling, $\rho = 10.96$ gm/cm^3 and the Area is given by the sum of the partial areas of the rods that overlap the boundary + the sum of the areas of the internal rods that do not intersect the boundary. This latter sum is just N $\times A_R$, with N equal to the number of internal rods and A_R equal to the area of a single cylinder (i.e. $\pi \times R_f^2$). For the first term, the sum is more complicated since individual fuel cylinder elements will intersect the boundary at different points. However, the internal partial area of each cylindrical element can be determined by integration, and the integration can be made simple by considering the ICCA and fuel cylinder (rod) in question to be rotated so that the center of the overlapping rod is at X = 0.0. Figure 6.9d shows a depiction of the two situations that can result.

Figure 6.9d – Partial Areas of Overlapping Fuel Cylinders

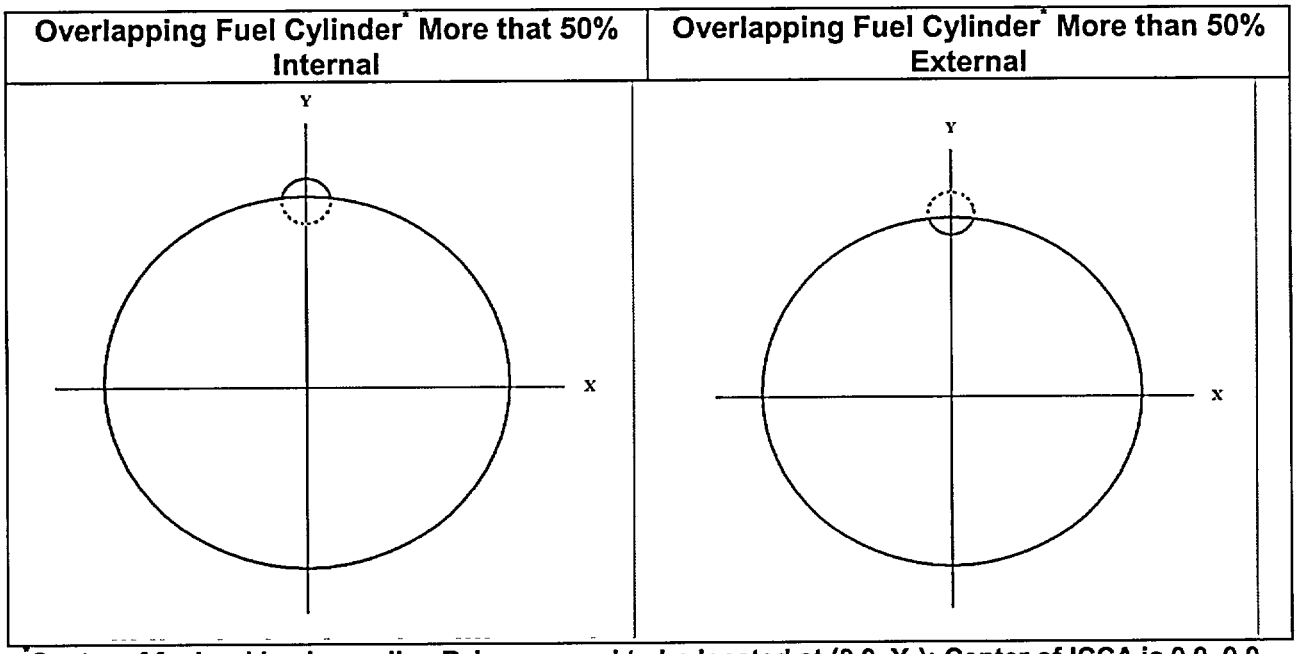

*Center of fuel rod having radius R_f is assumed to be located at (0.0, Y_0); Center of ICCA is 0.0, 0.0.

[N.B. "More than 50% Internal" or "More than 50% External" should be interpreted to mean that the curve for the ICCA boundary and the cylindrical fuel element intersects at a value of $Y \leq Y_0$ or $Y > Y_0$, respectively.] Separation into these two situations is necessary since the functional form of the overlapping rod used in the integration can only be the top half of the cylinder [i.e. $Y_{r1} = Y_0 + \text{Sqrt}(R_f^2 - X^2)$] or the bottom half [i.e. $Y_{r2} = Y_0 - \text{Sqrt}(R_f^2 - X^2)$]. The dotted line parts of the partial rods in Figure 6.9d are the parts not included in the area integration. In the "More than 50% Internal" situation, this integration is from X = 0.0 to $X = X_i$ (the +X point of intersection of the ICCA boundary and the cylindrical elment [rod] curve) of the quantity $(Y_{r1} - Y_{ICCA})$, with $Y_{ICCA} = \text{Sqrt}(R_{ICCA}^2 - X^2)$. If the result of this integral is A_p, the corresponding value for the internal partial area for the cylindrical fuel element is $A_R - 2 \times A_p$.

For the situation when more than 50% or the cylindrical fuel element (rod) is external, the integral is made from X = 0.0 to X_i of $Y_{ICCA} - Y_{r2}$, and the internal partial area of the fuel cylinder is equal to two times the value of this integral. Both of these integrals have results that can be expressed in closed form (involving arcsines), and hence the partial fuel cylinder determinations can readily be computed.

The 2nd array case considered is that of fuel element (rod) lattices in which the elements in the lattice are not permitted to overlap the ICCA boundary. If any part of a fuel cylinder intersects the ICCA boundary at any point, it is deleted from the array. All fuel cylinders are thus completely internal, and the total fuel area is just $N \times A_R$. As in case 1, the density ρ for this case is 10.96 gm/cm^3.

The third case is that in which the fuel element (rod) lattices are modeled with the Virtual Fill Option (VFO). In this case, each neutron that enters the internal ICCA fuel region sees a fuel rod lattice with an overlapping boundary condition like that in Case 1, but each lattices of these has a randomly location in the XY plane so that each will have a different number of overlapping and internal rods. Since the effect of this over an entire calculation is to average the arrays over all locations, the method used to determine the lattice heights is that used for the homogeneous case. This is done by correlating the given W/F ratio of the heterogeneous lattice with an equivalent WF H_2O for a homogeneous mixture by the relationship

$$\text{WF } H_2O = \frac{\text{W/F}}{10.96 + \text{W/F}},$$

which then determines the UO_2 density in the equivalent homogeneous mixture. [Note that this WF H_2O determined by this method is independent of the diameter of the fuel rod.]

6.4.4 CODE INPUT

All problems were started with a flat initial neutron distribution over the fissile material regions only. Except as noted, calculations were run with 200 generations of 2000 neutrons each, skipping the first 10 generations before starting the statistical output processing, for a total of 380,000 histories used in the final eigenvalue calculation. Appendix 6.9 contains sample GEMER input files for both the homogeneous and heterogeneous cases considered in this analysis.

6.4.5 CONVERGENCE OF CALCULATIONS

Problem convergence was determined by examining plots of k_{eff} by generation run and skipped, as well as the final k_{eff} edit tables. No abnormal trends were observed to indicate non-convergence of the eigenvalue solution. Representative convergence plots for the individual damaged single package, undamaged array, and damaged array models are shown in Figures 6.10a- 6.10d. (The plots shown are for cases with homogeneous UO_2 and H_2O mixtures, but the results are also representative of the results for heterogeneous lattices.)

Figure 6.10a – Sample k_{eff} convergence: damaged unit – npcut_25.in

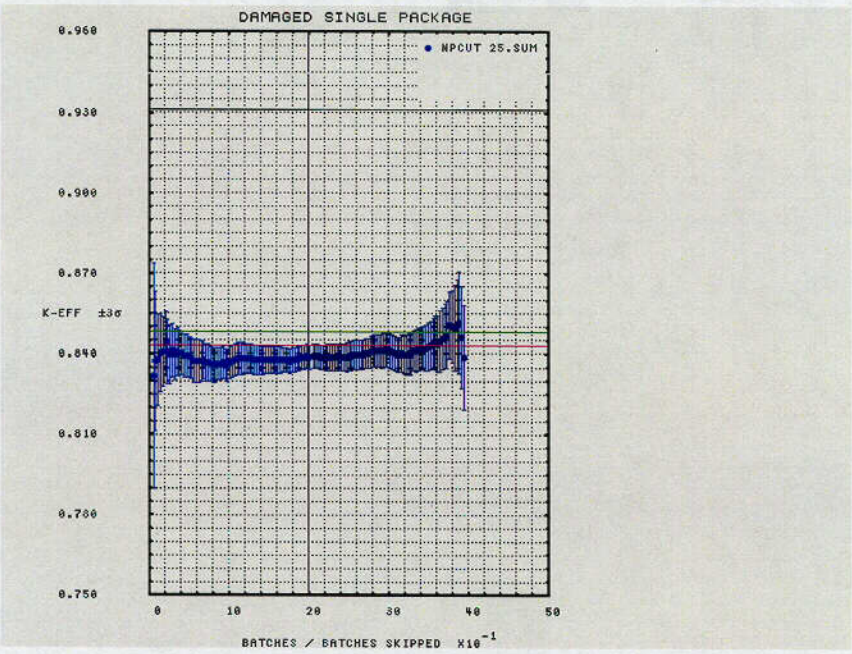

Figure 6.10b – Sample k_{eff} convergence: undamaged array - npc60i28.in

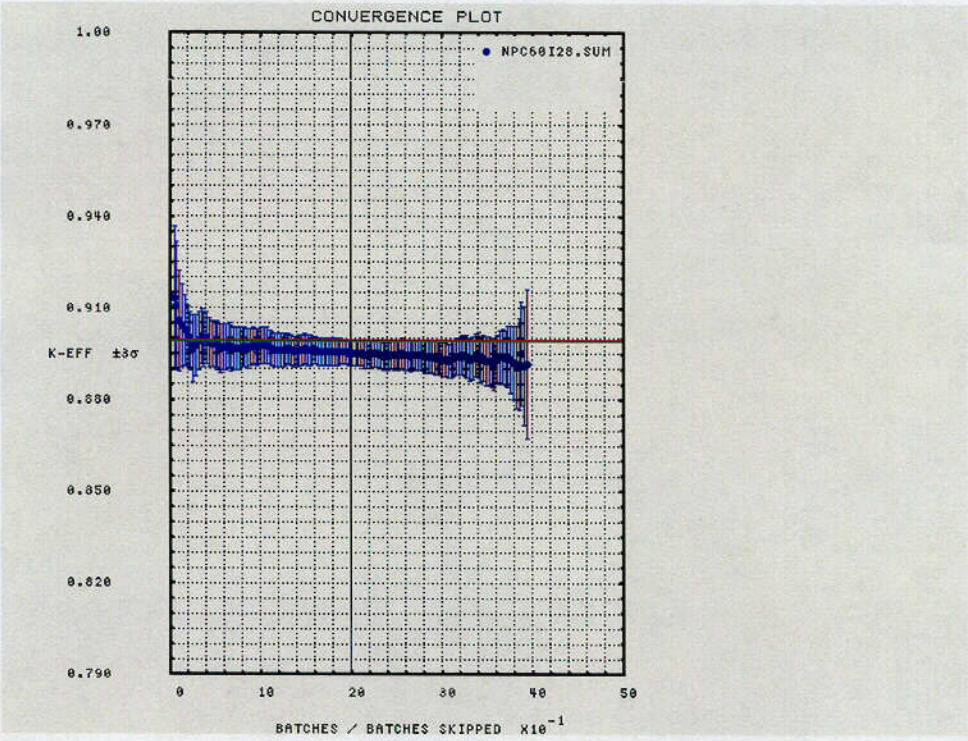

C24

Figure 6.10c – Sample k_{eff} convergence: damaged array – npca2_60.in (CTU-2 observed burn)

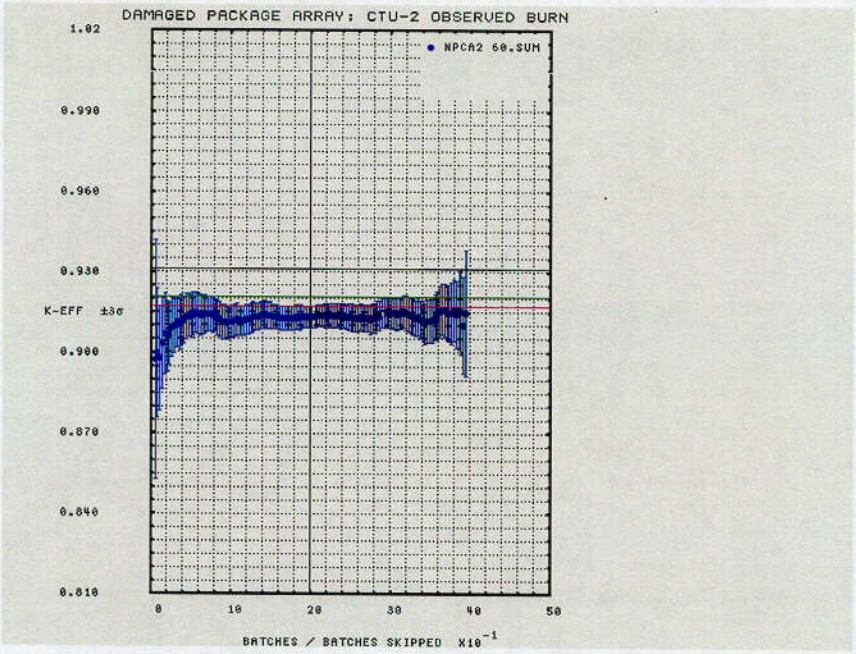

Figure 6.10d – Sample k_{eff} convergence: damaged array - npcat_60.in (maximum burn)

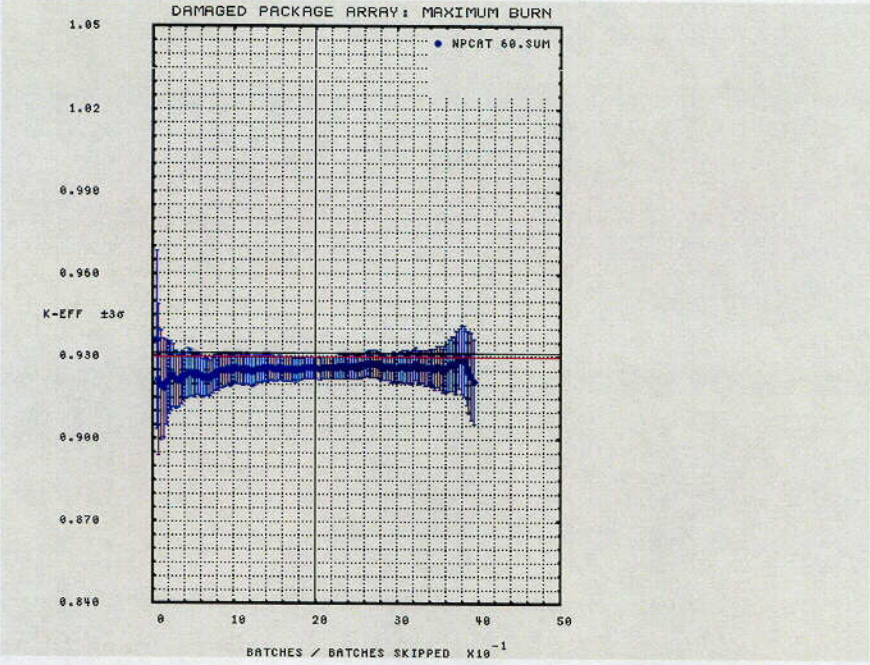

C25

6.5 VALIDATION

The following general relationship for establishing the acceptance criteria for the NPC package (Ref. 4).

$$k_c - \Delta k_u \geq k_{eff} + 2\sigma + \Delta k_m$$

where,

k_c = mean value of k*eff* resulting from calculation of benchmark critical experiments
Δk_u = an allowance for the calculational uncertainty
Δk_m = a required margin of subcriticality (0.05 used)
k_{eff} = the calculated value obtained for the package or array of packages
σ = is the standard deviation of the keff value obtain with Monte Carlo analysis

If the calculational bias $\beta = k_c - 1$, the bias is negative if $k_c < 1$, and positive if $k_c > 1$. Thus, the acceptance criteria may be rewritten as,

$$1.00 + \beta - \Delta k_u \geq k_{eff} + 2\sigma + 0.05$$

or

$$k_{eff} + 2\sigma \leq 0.95 - \Delta k_u + \beta.$$

Validation of GEMER consists of performing calculation of benchmark experiments including the area of applicable to the uranium oxides. Bias for GEMER and the ENDF/B-IV library has been established for the area of applicability for the NPC package (refer Appendix). The uranium oxide bias determined is no greater than 0.009 ($\Delta k_u - \beta$) at a 99% confidence level (Ref. 2). For uranium nitrate compounds, the bias determined is not greater than 0.0125 ($\Delta k_u - \beta$) at a 99% confidence level. The uranium oxide bias with cadmium is no greater than 0.01888 ($\Delta k_u - \beta$) at a 95% confidence level (refer Appendix 6.8, Validation of GEMER).

The area of applicability for the homogeneous and heterogeneous uranium oxide benchmark calculations is enrichment ranges from 1.29 to 9.83 weight percent U-235, W/F ratios from 0.5 to 10.0 and H/U-235 ratio 41 to 866. The area of applicability for the uranium oxide with cadmium benchmark calculations is enrichment ranges from 2.35 to 4.98 weight percent U-235 and H/U-235 ratio 260-488.

Using the above general equation for the upper safety limit (USL) and requirements of 10 CFR 71, calculations are considered subcritical, if the following condition is satisfied:

$$k_{eff} + 2\sigma \leq 0.95 - \Delta k_u + \beta$$

For this evaluation, the NPC package and it contents are considered subcritical if the following condition is satisfied:

$$k_{eff} + 2\sigma \leq 0.931$$

6.6 CRITICALITY CALCULATIONS AND RESULTS

This evaluation demonstrates the subcriticality of single packages (Section 6.6.1) and arrays of packages (Section 6.6.2) during both normal and hypothetical accident conditions of transport for fissile material contents that are representable as homogeneous or heterogeneous mixtures of UO_2 and H_2O. For the types of fissile materials listed in Table 6.1, with the specified mass limits, the determined Transport Index (TI) for criticality control of damaged and undamaged shipment is given in Section 6.6.3, *Transport Index*.

All calculations were performed at the maximum allowable U-235 enrichment (5.00 wt %) to ensure optimum reactivity, and the maximum k_{eff}s resulting from these analyses are summarized in Table 6.9. A complete listing of all results is included in Tables 6.16 through 6.20 in Appendix 6.10.

6.6.1 DAMAGED SINGLE PACKAGES

Calculations show that a single package remains subcritical under general requirements for fissile material packages, under both normal conditions of transport, and under hypothetical accident conditions. To meet the general requirements for fissile material package, a package must be designed and its contents so limited, that it would be subcritical under the most reactive configuration of material, optimum moderation, and close reflection of the containment system by water on all sides or surrounding materials of the packaging.

6.6.1.1 Damaged Single Package with Homogeneous UO_2 and H_2O

Figure 6.11 shows the reactivity of a damaged single package for CTU-1, CTU-2, and maximum observed foam burn conditions. A third order regression fit of the Keff $\pm 2\sigma$ results are shown for each fit. The figure demonstrates the damaged single package remains subcritical under the most reactive configuration of material, optimum moderation, and close reflection of the containment system by water on all sides or surrounding materials of the packaging. The damaged single package is demonstrated to be a favorable geometry unit. The limiting condition occurs for the maximum foam burn condition.

The effect of replacing the void (burn region) with full density water is also demonstrated to have a small effect for the damaged single package. This is expected due to optimal internal fuel moderation treatment and close proximity of the water reflector.

From Table 6.16 in Appendix 6.10, the maximum calculated $k_{eff} + 2\sigma$ - bias results for the damaged single package are:

FILENAME	K-EFF	SIGMA	K+2S	BIAS	K+2S-B
npcu1_25	0 8452	0.0013	0.8478	- 0189	0.8666
npcu2_25	0 8407	0.0013	0.8433	- 0189	0.8622
npcut_25	0.8405	0 0014	0.8432	-.0189	0.8621
npcutw25	0.8476	0 0015	0.8506	-.0189	0 8694

Table 6.9 – NPC Calculated *Keff* Summary

A. Single Container Cases*

Rod Type	Lattice	File Name	k_{eff}	σ	k_{eff}+2σ	Bias (B)	k_{eff}+2σ - B	Rod Type	Lattice	File Name	k_{eff}	σ	k_{eff}+2σ	Bias (B)	k_{eff}+2σ - B
		60 Kgs Homogeneous Single Container Case													
NA	NA	Npcutw25	0.8475	0.0015	0.8506	-0.0189	0.8694								
		55 Kgs Heterogeneous Single Container Case with Overlap								53 Kgs Heterogeneous Single Container Case with Overlap					
17X17	Square	ESSP-420	**0.85195**	0.00143	0.85481	-0 01890	**0.87371**	17X17	Square	ESSN-437	**0.84788**	0.00138	0.85064	-0.01890	**0.86954**
17X17	Triangular	ESTP-400	0.85358	0.00141	0.85640	-0.01890	0.87530	17X17	Triangular	ESTN-437	0.8499	0.00137	0.85265	-0.01890	0.87155
10X10	Square	ETSP-410	**0.84464**	0.00130	0.84724	-0.01890	**0.86614**	10X10	Square	ETSN-400	**0.84441**	0.00152	0.84745	-0.01890	**0.86635**
10X10	Triangular	ETTP-430	0.84806	0.00148	0.85102	-0.01890	**0.86992**	10X10	Triangular	ETTN-437	**0.84546**	0.00133	0.84812	-0.01890	**0.86702**
9X9	Square	ENSP-410	**0.84113**	0 00134	0 84381	-0.01890	**0.86271**	9X9	Square	ENSN-437	**0.83796**	0 00140	0.84076	-0 01890	**0.85966**
9X9	Triangular	ENTP-430	**0.84217**	0.00151	0.84519	-0.01890	**0.86409**	9X9	Triangular	ENTN-410	**0.83982**	0.00135	0.84252	-0.01890	**0.86142**
8X8	Square	EESP-420	**0.83597**	0.00135	0.83867	-0.01890	**0.85757**	8X8	Square	EESN-400	**0.83275**	0.00139	0.83553	-0.01890	**0.85443**
8X8	Triangular	EETP-410	**0.83736**	0.00129	0.83994	-0.01890	**0.85884**	8X8	Triangular	EETN-420	**0.83385**	0 00145	0.83675	-0.01890	**0.85565**
		55 Kgs Heterogeneous Single Container Case without Overlap								53 Kgs Heterogeneous Single Container Case without Overlap					
17X17	Square	OSSP-480	**0.84764**	0.00128	0.85020	-0.01890	**0.86910**	17X17	Square	OSSN-480	**0.84512**	0 00143	0.84798	-0.01890	**0.86688**
17X17	Triangular	OSTP-410	**0.85091**	0 00139	0.85369	-0 01890	**0.87259**	17X17	Triangular	OSTN-420	0.84833	0.00157	0.85147	-0 01890	**0.87037**
10X10	Square	OTSP-437	**0.84222**	0 00134	0.84490	-0 01890	**0.86380**	10X10	Square	OTSN-437	**0.83676**	0.00140	0.83956	-0.01890	**0.85846**
10X10	Triangular	OTTP-410	**0.84648**	0.00142	0.84932	-0 01890	**0.86822**	10X10	Triangular	OTTN-410	**0.84175**	0.00138	0.84451	-0.01890	**0.86341**
9X9	Square	ONSP-400	**0.84056**	0.00142	0.84340	-0.01890	**0.86230**	9X9	Square	ONSN-410	**0.83529**	0.00149	0.83827	-0.01890	**0.85717**
9X9	Triangular	ONTP-470	**0.83397**	0 00136	0.83669	-0.01890	**0.85559**	9X9	Triangular	ONTN-460	**0.83184**	0.00133	0.83450	-0.01890	**0.85340**
8X8	Square	OESP-400	**0.82941**	0.00140	0.83221	-0.01890	**0.85111**	8X8	Square	OESN-400	**0.82773**	0.00153	0.83079	-0 01890	**0.84969**
8X8	Triangular	OETP-420	**0.83805**	0 00148	0.84101	-0.01890	**0.85991**	8X8	Triangular	OETN-420	**0.83446**	0.00147	0.83740	-0.01890	**0.85630**
		55 Kgs Heterogeneous Single Container Case with VFO								53 Kgs Heterogeneous Single Container Case with VFO					
17X17	**Square**	**VSSP-400**	**0.85223**	**0.00144**	**0.85511**	**-0.01890**	**0.87401**	17X17	Square	VSSN-400	0.84788	0.00151	0.85090	-0 01890	**0.86980**
17X17	Triangular	VSTP-460	0.85248	0.00154	0.85556	-0.01890	**0.87446**	17X17	Triangular	VSTN-400	**0.84909**	0.00146	0.85201	-0.01890	**0.87091**
10X10	Square	VTSP-410	**0.84517**	0.00143	0.84803	-0.01890	**0.86693**	10X10	Square	VTSN-420	**0.84343**	0.00135	0.84613	-0.01890	**0.86503**
10X10	Triangular	VTTP-410	**0.84900**	0.00136	0.85172	-0.01890	**0.87062**	10X10	Triangular	VTTN-440	**0.84402**	0.00145	0.84692	-0.01890	**0.86582**
9X9	Square	VNSP-400	**0.84079**	0 00132	0.84343	-0.01890	**0.86233**	9X9	Square	VNSN-400	**0.83652**	0.00143	0.83938	-0.01890	**0.85828**
9X9	Triangular	VNTP-400	**0.84181**	0.00150	0.84481	-0 01890	**0.86371**	9X9	Triangular	VNTN-440	**0.83967**	0.00144	0.84255	-0.01890	**0.86145**
8X8	Square	VESP-400	**0.83521**	0.00131	0.83783	-0.01890	**0.85673**	8X8	Square	VESN-400	**0.83352**	0.00135	0.83622	-0.01890	**0.85512**
8X8	Triangular	VETP-430	**0.83642**	0.00147	0.83936	-0.01890	**0.85826**	8X8	Triangular	VETN-400	**0.83305**	0.00135	0.83575	-0.01890	**0.85465**

* Maximum Values Shown with Green Background

B. Undamaged Array Cases*

Rod Type	Lattice	File Name	k_{eff}	σ	$k_{eff}+2\sigma$	Bias (B)	$k_{eff}+2\sigma$ - B	Rod Type	Lattice	File Name	k_{eff}	σ	$k_{eff}+2\sigma$	Bias (B)	$k_{eff}+2\sigma$ - B
		60 Kgs Homogeneous Undamaged Array Case													
NA	NA	Npcat6012	0.8956	0.0013	0.8982	-0.0189	0.9171								
		55 KGs Heterogeneous Undamaged Array Case with Overlap								53 KGs Heterogeneous Undamaged Array Case with Overlap					
17X17	Square	DSSP-400	**0.89437**	0.00127	0.89691	-0 01890	**0.91581**	17X17	Square	DSSN-400	**0.89271**	0.00138	0 89547	-0 01890	**0.91437**
17X17	Triangular	DSTP-437	0.89798	0.00128	0.90054	-0.01890	0.91944	17X17	Triangular	DSTN-400	0.89336	0.00146	0.89628	-0.01890	**0.91518**
10X10	Square	DTSP-400	**0.88984**	0.00133	0.89250	-0.01890	**0.91140**	10X10	Square	DTSN-410	**0.88681**	0.00144	0.88969	-0.01890	**0.90859**
10X10	Triangular	DTTP-420	0.89023	0.00139	0.89301	-0.01890	**0.91191**	10X10	Triangular	DTTN-430	**0.88958**	0.00143	0.89244	-0.01890	**0.91134**
9X9	Square	DNSP-410	**0.88563**	0.00134	0 88831	-0.01890	**0.90721**	9X9	Square	DNSN-410	**0.88232**	0.00130	0.88492	-0.01890	**0.90382**
9X9	Triangular	DNTP-400	**0.88619**	0.00149	0.88917	-0.01890	**0.90807**	9X9	Triangular	DNTN-420	**0.88310**	0 00129	0.88568	-0.01890	**0.90458**
8X8	Square	DESP-400	**0.88283**	0.00128	0.88539	-0.01890	**0.90429**	8X8	Square	DESN-410	**0.87831**	0.00137	0.88105	-0 01890	**0.89995**
8X8	Triangular	DETP-400	**0.88162**	0.00140	0.88442	-0.01890	**0.90332**	8X8	Triangular	DETN-420	0.87802	0.00147	0.88096	-0 01890	**0.89986**
		55 KGs Heterogeneous Undamaged Array Case without Overlap								53 KGs Heterogeneous Undamaged Array Case without Overlap					
17X17	Square	CSSP-430	**0.89233**	0.00141	0.89515	-0.01890	**0.91405**	17X17	Square	CSSN-470	0 88851	0.00139	0.89129	-0.01890	**0.91019**
17X17	Triangular	CSTP-430	0.89407	0.00164	0.89735	-0.01890	**0.91625**	17X17	Triangular	CSTN-430	**0.89308**	0.00129	0.89566	-0.01890	**0.91456**
10X10	Square	CTSP-437	**0.88294**	0.00138	0.88570	-0.01890	**0.90460**	10X10	Square	CTSN-400	**0.88125**	0.00139	0.88403	-0 01890	**0.90293**
10X10	Triangular	CTTP-400	**0.89104**	0.00135	0.89374	-0.01890	**0.91264**	10X10	Triangular	CTTN-410	**0.88590**	0.00141	0.88872	-0 01890	**0.90762**
9X9	Square	CNSP-420	**0.88232**	0.00137	0 88506	-0.01890	**0.90396**	9X9	Square	CNSN-420	**0.87967**	0.00140	0.88247	-0.01890	**0.90137**
9X9	Triangular	CNTP-420	**0.87670**	0.00127	0 87924	-0.01890	**0.89814**	9X9	Triangular	CNTN-420	**0.87457**	0 00125	0.87707	-0.01890	**0.89597**
8X8	Square	CESP-400	**0.87068**	0.00133	0.87334	-0.01890	**0.89224**	8X8	Square	CESN-400	**0.86695**	0.00125	0.86945	-0.01890	**0.88835**
8X8	Triangular	CETP-410	**0.87997**	0.00145	0.88287	-0.01890	**0.90177**	8X8	Triangular	CETN-420	**0.87874**	0.00141	0.88156	-0.01890	**0.90046**
		55 KGs Heterogeneous Undamaged Array Case with VFO								53 KGs Heterogeneous Undamaged Array Case with VFO					
17X17	Square	BSSP-450	**0.89451**	0.00134	0.89719	-0.01890	**0.91609**	17X17	Square	BSSN-400	**0.89142**	0.00140	0.89422	-0.01890	**0.91312**
17X17	Triangular	BSTP-420	**0.89628**	0.00146	0 89920	-0.01890	**0.91810**	17X17	Triangular	BSTN-430	0.89470	0.00130	0.89730	-0.01890	0.91620
10X10	Square	BTSP-410	0.88797	0.00151	0.89099	-0.01890	**0.90989**	10X10	Square	BTSN-410	**0.88608**	0.00136	0.88880	-0 01890	**0.90770**
10X10	Triangular	BTTP-437	**0.88990**	0.00143	0.89276	-0 01890	**0.91166**	10X10	Triangular	BTTN-420	**0.88801**	0.00142	0.89085	-0.01890	**0.90975**
9X9	Square	BNSP-420	**0.88459**	0.00131	0.88721	-0.01890	**0.90611**	9X9	Square	BNSN-400	**0.88220**	0.00131	0.88482	-0.01890	**0.90372**
9X9	Triangular	BNTP-400	**0.88639**	0.00124	0.88887	-0.01890	**0.90777**	9X9	Triangular	BNTN-440	**0.88238**	0 00142	0.88522	-0.01890	**0.90412**
8X8	Square	BESP-420	**0.87958**	0.00129	0.88216	-0.01890	**0.90106**	8X8	Square	BESN-410	**0.87553**	0.00139	0.87831	-0.01890	**0.89721**
8X8	Triangular	BETP-400	**0.88143**	0 00142	0.88427	-0.01890	**0.90317**	8X8	Triangular	BETN-400	**0.87932**	0.00131	0.88194	-0.01890	**0.90084**

* Maximum Values Shown with Green Background

C. Damaged Array Cases*

Rod Type	Lattice	File Name	k_{eff}	σ	k_{eff}+2σ	Bias (B)	k_{eff}+2σ - B	Rod Type	Lattice	File Name	k_{eff}	σ	k_{eff}+2σ	Bias (B)	k_{eff}+2σ - B
		60 Kgs Homogeneous Damaged Array Case													
NA	NA	Spent 60	0.9275	0.0012	0.9299	-0.0189	0.9488								
		55 KGs Heterogeneous Damaged Array Case with Overlap								53 KGs Heterogeneous Damaged Array Case with Overlap					
17X17	Square	SS55-470	**0.92778**	0.00128	0.93034	-0.0189	**0.94924**	17X17	Square	SS53-520	**0.92239**	0.00143	0.92525	-0.0189	**0.94415**
17X17	Triangular	ST55-437	**0.92766**	0.00118	0.93002	-0.0189	**0.94892**	17X17	Triangular	ST53-460	**0.92417**	0.00128	0.92673	-0.0189	**0.94563**
10X10	Square	TS55-460	**0.91822**	0 00144	0.92110	-0.0189	**0.94000**	10X10	Square	TS53-460	**0.91475**	0.00133	0.91741	-0.0189	**0.93631**
10X10	Triangular	TT55-450	**0.92071**	0.00138	0.92347	-0.0189	**0.94237**	10X10	Triangular	TT53-440	**0.91582**	0.00132	0.91846	-0.0189	**0.93736**
9X9	Square	NS55-460	**0.91434**	0.00139	0.91712	-0.0189	**0.93602**	9X9	Square	NS53-440	**0.90949**	0.00138	0.91225	-0.0189	**0.93115**
9X9	Triangular	NT55-430	**0.91469**	0.00135	0.91739	-0.0189	**0.93629**	9X9	Triangular	NT53-500	**0.90879**	0.00128	0.91135	-0.0189	**0.93025**
8X8	Square	ES55-410	**0.90675**	0.00122	0.90919	-0.0189	**0.92809**	8X8	Square	ES53-430	**0.90091**	0.00123	0.90337	-0.0189	**0.92227**
8X8	Triangular	ET55-450	**0.90882**	0 00139	0.91160	-0 0189	**0.93050**	8X8	Triangular	ET53-420	**0.90444**	0.00133	0.90710	-0 0189	**0.92600**
		55 KGs Heterogeneous Damaged Array Case without Overlap								53 KGs Heterogeneous Damaged Array Case without Overlap					
17X17	Square	OSSP-430	0.92607	0.00131	0.92869	-0.0189	**0.94759**	17X17	Square	OSSN-480	**0.92213**	0.00140	0.92493	-0.0189	**0.94383**
17X17	Triangular	OSTP-440	**0.92629**	0.00143	0.92915	-0.0189	**0.94805**	17X17	Triangular	OSTN-430	**0.92038**	0.00142	0.92322	-0.0189	**0.94212**
10X10	Square	OTSP-430	**0.91271**	0 00138	0.91547	-0 0189	**0.93437**	10X10	Square	OTSN-470	**0.90916**	0.00129	0.91174	-0 0189	**0.93064**
10X10	Triangular	OTTP-437	**0.91928**	0 00126	0.92180	-0 0189	**0.94070**	10X10	Triangular	OTTN-410	**0.91296**	0.00138	0.91572	-0 0189	**0.93462**
9X9	Square	ONSP-410	**0.91320**	0.00132	0.91584	-0.0189	**0.93474**	9X9	Square	ONSN-420	**0.90637**	0.00140	0.90917	-0.0189	**0.92807**
9X9	Triangular	ONTP-520	**0.90778**	0.00122	0.91022	-0.0189	**0.92912**	9X9	Triangular	ONTN-490	**0.90790**	0.00136	0.91062	-0.0189	**0.92952**
8X8	Square	OESP-400	**0.89670**	0 00136	0 89942	-0 0189	**0.91832**	8X8	Square	OESN-500	**0.89400**	0 00149	0 89698	-0 0189	**0.91588**
8X8	Triangular	OETP-410	**0.90943**	0.00128	0.91199	-0.0189	**0.93089**	8X8	Triangular	OETN-410	**0.90299**	0.00132	0.90563	-0.0189	**0.92453**
		55 KGs Heterogeneous Damaged Array Case with VFO								53 KGs Heterogeneous Damaged Array Case with VFO					
17X17	Square	SS55-460	**0.92745**	0.00144	0.93033	-0.0189	**0.94923**	17X17	Square	SS53-450	**0.92132**	0.00137	0.92406	-0.0189	**0.94296**
17X17	Triangular	ST55-486	**0.92801**	0.00136	0.93073	-0.0189	**0.94963**	17X17	Triangular	ST53-470	**0.92198**	0.00130	0.92458	-0.0189	**0.94348**
10X10	Square	TS55-480	**0.91840**	0 00139	0.92118	-0 0189	**0.94008**	10X10	Square	TS53-486	**0.91233**	0 00138	0 91509	-0.0189	**0.93399**
10X10	Triangular	TT55-470	**0.91984**	0.00139	0.92262	-0.0189	**0.94152**	10X10	Triangular	TT53-460	**0.91603**	0.00138	0.91879	-0.0189	**0.93769**
9X9	Square	NS55-420	0.91206	0.00146	0.91498	-0.0189	**0.93388**	9X9	Square	NS53-430	**0.90676**	0.00121	0.90918	-0.0189	**0.92808**
9X9	Triangular	NT55-470	**0.91613**	0.00144	0.91901	-0.0189	**0.93791**	9X9	Triangular	NT53-437	**0.90957**	0.00141	0.91239	-0.0189	**0.93129**
8X8	Square	ES55-430	**0.90468**	0.00141	0.90750	-0.0189	**0.92640**	8X8	Square	ES53-400	**0.90223**	0.00126	0.90475	-0.0189	**0.92365**
8X8	Triangular	ET55-450	**0.90883**	0.00143	0.91169	-0.0189	**0.93059**	8X8	Triangular	ET53-440	**0.90455**	0.00135	0.90725	-0.0189	**0.92615**

* Maximum Values Shown with Green Background

D. Unrestricted Rod Diameter Cases*

Rod Diameter (Inches)	Lattice	File Name	k_{eff}	σ	$k_{eff}+2\sigma$	Bias (B)	$k_{eff}+2\sigma$ - B
		46 Kgs Heterogeneous Single Container Case with VFO					
0.200	Square	MSSL-450	**0.84629**	0.00145	0.84919	-0.01890	**0.86809**
0.200	Triangular	MSTL-500	**0.84902**	0.00134	0.85170	-0.01890	**0.87060**
0.100	Square	MTSL-540	**0.85424**	0.00146	0.85716	-0.01890	**0.87606**
0.100	Triangular	MTTL-600	**0.85120**	0 00146	0.85412	-0.01890	**0.87302**
0.050	Square	MNSL-520	**0.84886**	0.00147	0.85180	-0.01890	**0.87070**
0.050	Triangular	MNTL-600	**0.84713**	0.00141	0.84995	-0 01890	**0.86885**
0.025	Square	MESL-600	**0.84060**	0.00133	0.84326	-0.01890	**0.86216**
0.025	Triangular	METL-560	**0.84035**	0.00141	0.84317	-0.01890	**0.86207**
		46 Kgs Heterogeneous Undamaged Array Case with VFO					
0.200	Square	AASL-486	**0.88897**	0.00142	0.89181	-0.01890	**0.91071**
0.200	Triangular	AATL-437	**0.89076**	0.00145	0.89366	-0.01890	**0.91256**
0.100	Square	ABSL-520	**0.89600**	0.00133	0.89866	-0.01890	**0.91756**
0.100	Triangular	ABTL-490	**0.89307**	0.00152	0 89611	-0.01890	**0.91501**
0.050	Square	ACSL-560	**0.88834**	0.00138	0.89110	-0.01890	**0.91000**
0.050	Triangular	ACTL-600	**0.88882**	0.00126	0.89134	-0.01890	**0.91024**
0.025	Square	ADSL-560	**0.88223**	0.00135	0.88493	-0.01890	**0.90383**
0.025	Triangular	ADTL-544	**0.88161**	0.00152	0.88465	-0.01890	**0.90355**
		46 Kgs Heterogeneous Damaged Array Case with VFO					
0.200	Square	AS46-540	**0.91869**	0.00129	0.92127	-0.01890	**0.94017**
0 200	Triangular	AT46-500	**0.91880**	0.00130	0.92140	-0.01890	**0.94030**
0.100	Square	BS46-600	**0.92574**	0.00128	0.92830	-0.01890	**0.94720**
0.100	Triangular	BT46-600[1]	**0.92768**	0.00050	0.92868	-0.01890	**0.94758**
0 050	Square	CS46-616	**0.92402**	0.00128	0.92658	-0.01890	**0.94548**
0.050	Triangular	CT46-616	**0.92449**	0.00131	0.92711	-0.01890	**0.94601**
0.025	Square	DS46-616	**0.91810**	0.00124	0.92058	-0.01890	**0.93948**
0.025	Triangular	DT46-600	**0.91908**	0.00127	0.92162	-0.01890	**0.94052**

* Maximum Values Shown with Green Background
[1] 3800000 Neutron Histories

In these cases, homogeneous theoretical UO_2 (max. density = 10.96) of unlimited mass remains subcritical under optimum moderation. The reactivity of the single package system depends the effectiveness of the fuel in competing with other materials, such as the cadmium, hydrogen, stainless steel or water reflector, for absorption of thermal neutrons.

Figure 6.11 – NPC damaged single package results – 60 kgs Homogeneous UO_2 + H_2O

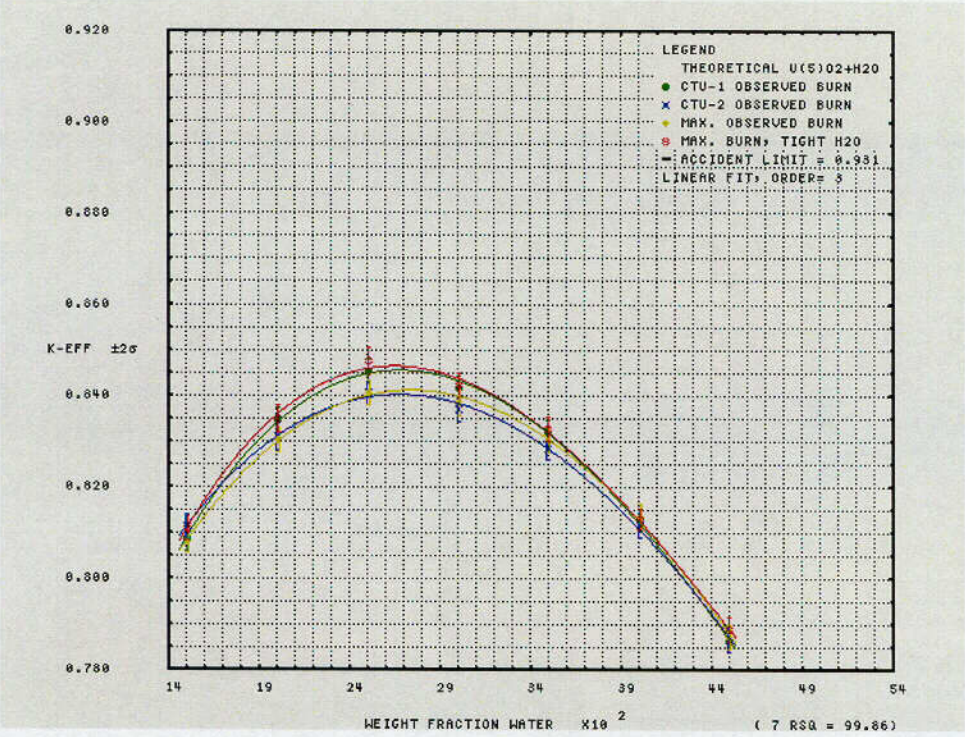

6.6.1.2 Damaged Single Package with Heterogeneous UO_2 in H_2O

Figures 6.12a through 6.12h show the reactivity of damaged single packages for the 55 . 53 and 46 kg UO_2 per ICCA cases described in the preceding sections. These plots (and the other plots of heterogeneous cases presented in the following sections) were generated in the same fashion as the ones for the homogeneous cases, utilizing a third order regression fit of the k_{eff} $\pm 2\sigma$ results. The figures demonstrate that with the specified pellet OD versus ICCA UO_2 mass limits, 0.34" for 55 kg, 0.30" for 53 kg and unlimited pellet diameter for 46 kg, the damaged single package remains subcritical under the most reactive configuration of material, W/F ratio, lattice array type (square or triangular), lattice boundary conditions (overlap or no overlap) and close reflection of the containment system by water on all sides in the surrounding materials in the packaging. As for the homogeneous case, the damaged single package is thus demonstrated to be a favorable geometry unit. The limiting conditions occur for the maximum foam burn condition with W/F ratios ~4 for the 55 and 53 kg case and around W/F ~5 for the 46 kg unlimited particle size diameter case.

C26

Figure 6.12a – NPC damaged single package k*eff* vs. W/F Ratio (10X10 pellet type, square pitch, 55 kgs UO2 / ICCA)

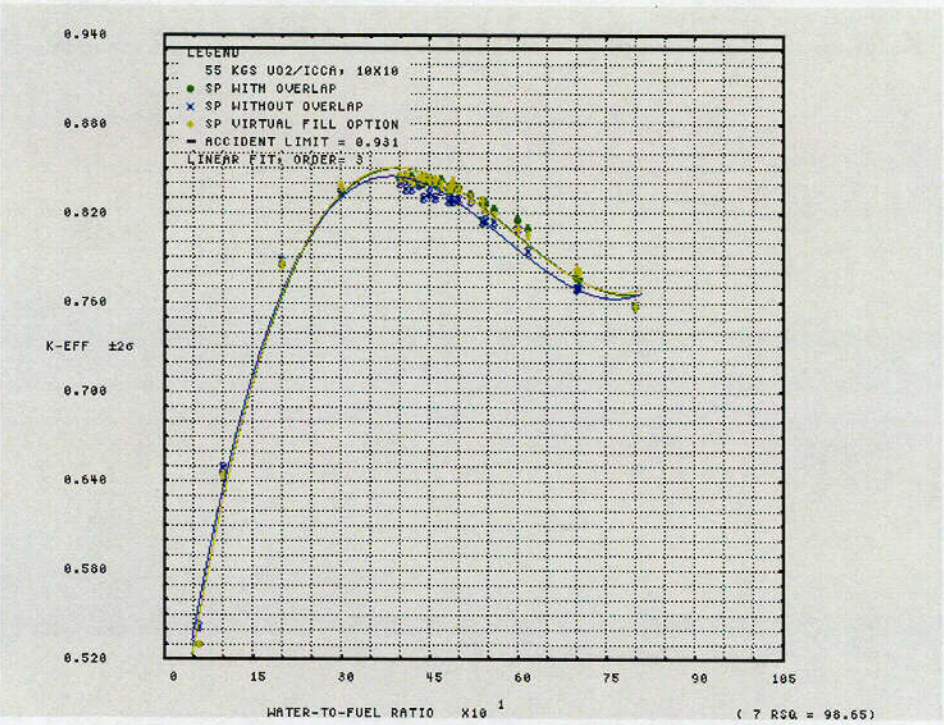

Figure 6.12b – NPC damaged single package k*eff* vs. W/F Ratio (10X10 pellet type, triangular pitch, 55 kgs UO2 / ICCA)

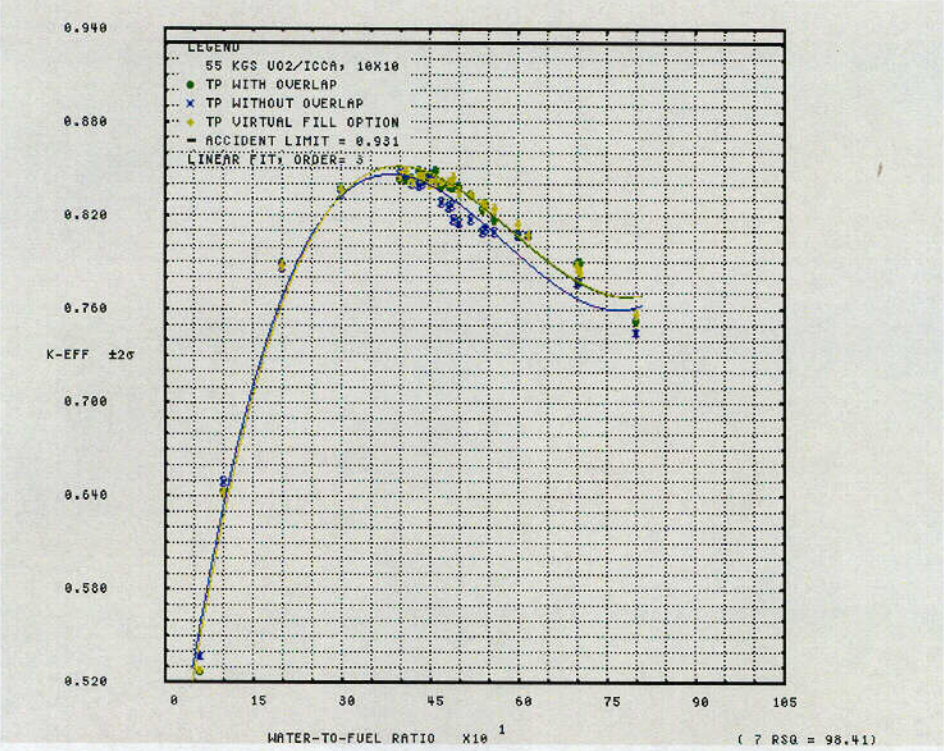

C27

Figure 6.12c – NPC damaged single package k*eff* vs. W/F Ratio (reactivity comparison vs. pellet size, triangular pitch, 55 kgs UO_2/ICCA, VFO)

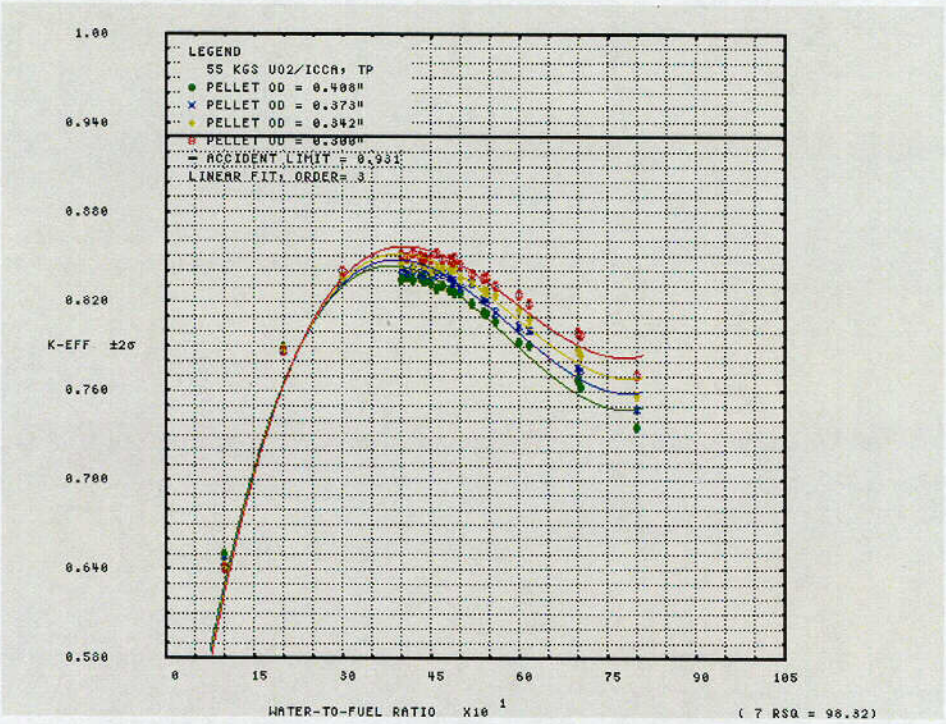

Figure 6.12d – NPC damaged single package k*eff* vs. W/F Ratio (17X17 pellet type, square pitch, 53 kgs UO_2/ICCA)

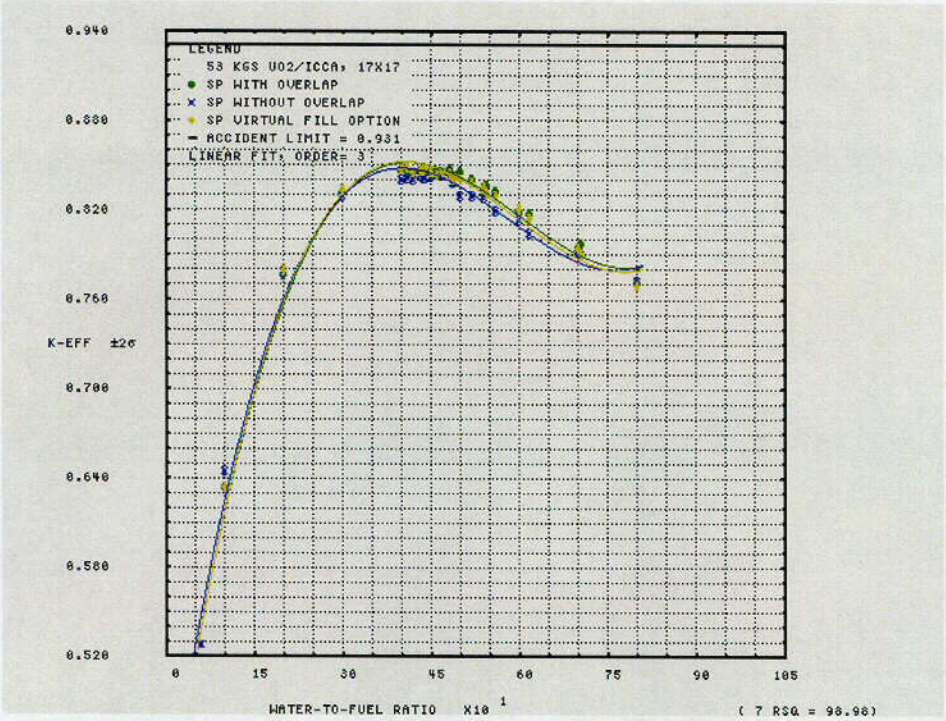

C28

Figure 6.12e – NPC damaged single package k*eff* vs. W/F Ratio (17X17 pellet type, triangular pitch, 53 kgs UO_2/ICCA)

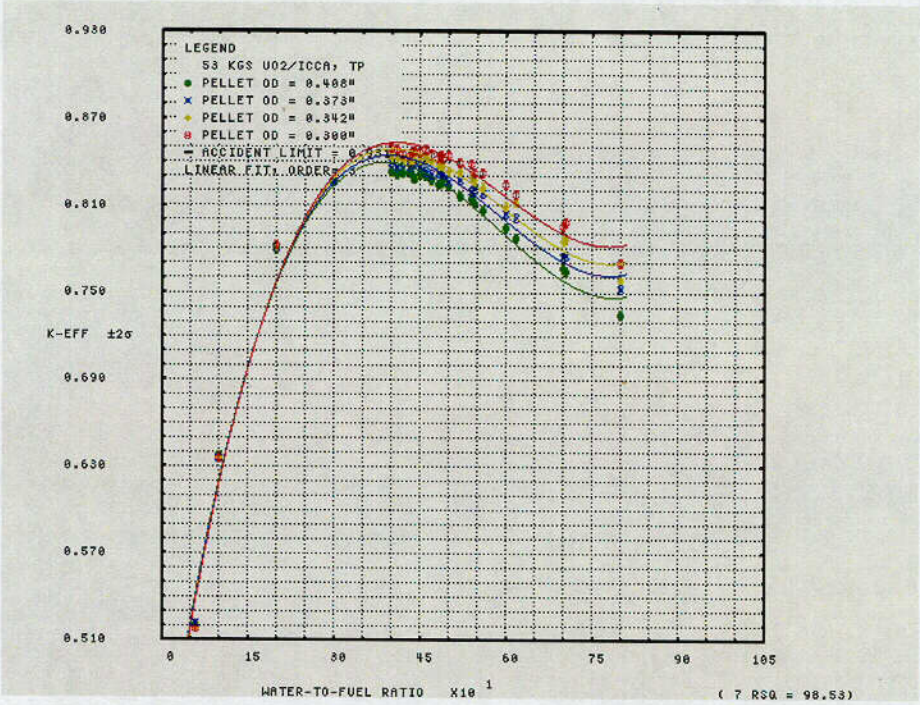

Figure 6.12f – NPC damaged single package k*eff* vs. W/F Ratio (reactivity comparison vs. pellet size for triangular pitch, 53 kgs UO_2/ICCA, VFO)

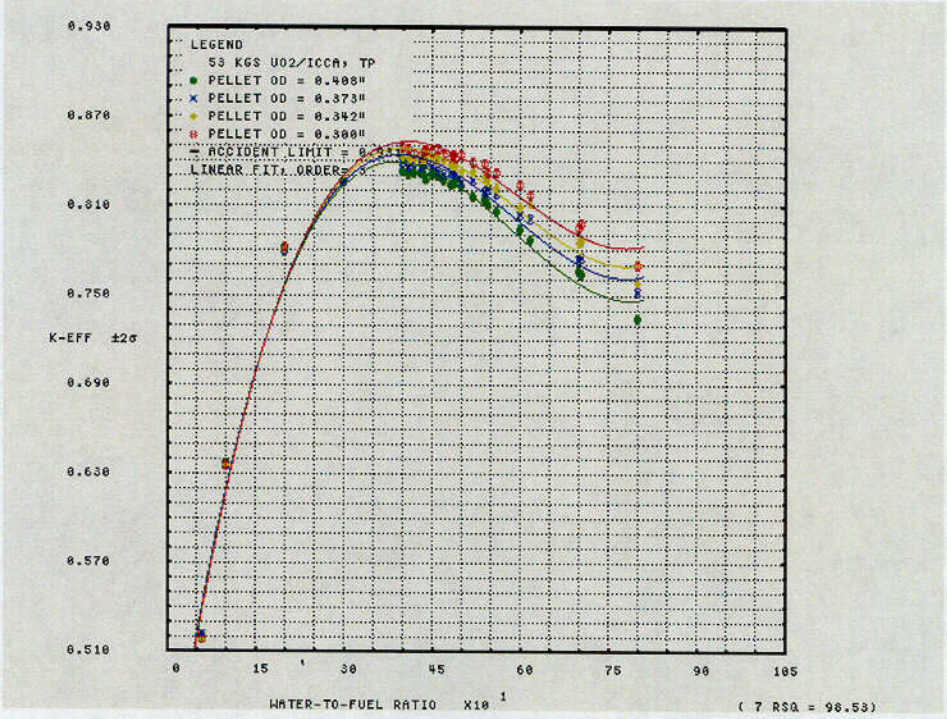

C29

Figure 6.12g – NPC damaged single package k*eff* vs. W/F Ratio (unrestricted particle size, square pitch, 46 kgs UO_2/ICCA)

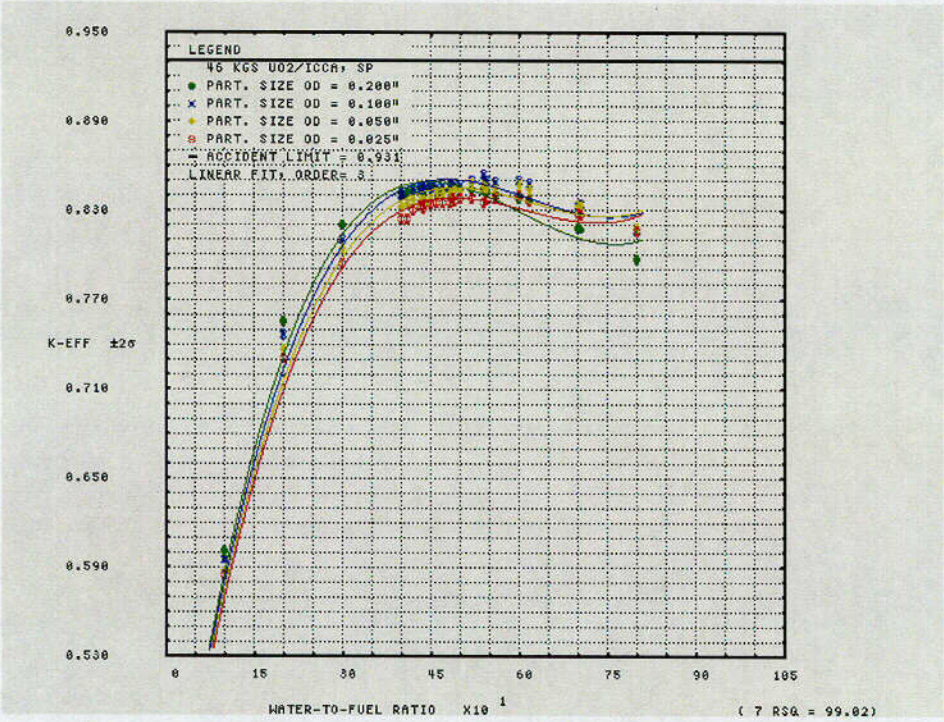

Figure 6.12h – NPC damaged single package k*eff* vs. W/F Ratio (unrestricted particle size, triangular pitch, 46 kgs UO_2/ICCA)

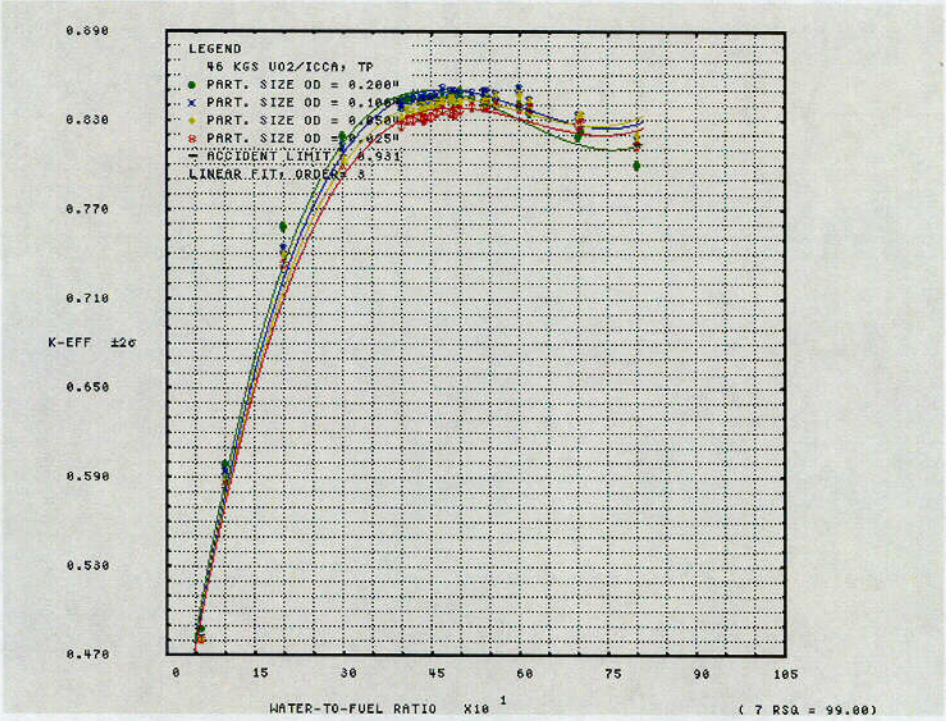

C30

From tables A and D in Table 6.9 above the maximum calculated $k_{eff} + 2\sigma$ - bias results for the damaged single package are:

FILENAME	UO2 MASS	K-EFF	SIGMA	K+2S	BIAS	K+2S-B
ESTP-400	55 kgs	0.8536	0.0014	0.8564	-.0189	0.8753
ESTN-437	53 kgs	0.8499	0.0014	0.8526	-.0189	0.8712
MTSL-540	46 kgs	0.8542	0.0015	0.8572	-.0189	0.8761

Several results shown in Figures 6.12a through 6.12h are generic to not only the damaged single container case but also the infinite undamaged array and 150 container damaged array cases. These are:

1. For the 55 and 53 kg UO_2 cases, the results using the VFO model are in excellent agreement with the results for the square and triangular lattices with overlap. This good agreement also expected to be even better in the cases for 46 kg UO_2 /ICCA (which cannot at present be explicitly modeled with GEMER's fix geometry capabilities) because of the large number of rods in each of the lattices (for the 0.200:, 0.100", 0.050" and 0.025" rod ODs).
2. The results for the 55 and 53 kg UO_2 cases without overlap are consistent lower than the same cases with overlap. (Note, however, that as described in section 6.4.3.4,the VFO cases are with overlap only.)
3. The entire set of results indicates that the optimum pellet diameter for the heterogeneous lattices is about 0.100". This is the explanation of why the 10X10 rod type results are the minimum allowable OD for the 55 kg UO_2 payload cases and the 17X17 pellet type results are the mimimun allowable OD for the lower 53 kg UO_2 payload cases (i.e. the 17X17 rod type has a 0.30" OD, the 10X10 rod type has a 0.34" OD, and the 9X9 and 8X8 rod types have progressively larger diameters of 0.376" and 0.408", respectively).
4. The triangular lattices usually tend to have the highest k_{eff}s, but their values do not differ greatly from the results for the square lattices. In a few cases the square lattices actually have larger keffs, which suggests that the differences are within statistical limits (2 to 4 σ, based on the number of different calculations made for this analysis).

6.6.2 DAMAGED PACKAGE ARRAYS

Calculations show that a damaged package array remains subcritical under general requirements for fissile material packages, for normal conditions of transport, and under hypothetical accident conditions. To meet the general requirements for fissile material packages, a fissile material package must be controlled to assure that an array of packages remains subcritical.

To enable this control, the designer shall derive a number "N" based on all of the following conditions being satisfied, assuming packages are stacked together in any arrangement and with close full reflection on all sides of the array by water such that: (a) 5N undamaged packages with nothing between the packages would be subcritical; (b) 2N damaged packages, if each package were subjected to tests specified in 10 CFR §71.73 would be subcritical with optimum interspersed hydrogenous moderation..

6.6.2.1 Damaged Package Arrays with Homogeneous UO_2 and H_2O

Figure 6.13 demonstrates a damaged NPC package array of size 5x5x6 (2N = 150) remains subcritical under CTU-1, CTU-2 observed non-uniform foam burn conditions. This figure also demonstrates the damaged package array remains subcritical under maximum foam burn conditions. A third order regression fit of the $k_{eff} \pm 2\sigma$ results are plotted as a function of ICCA payload.

The reactivity of the damaged package array depends on the effectiveness of the fuel in competing with other materials, such as the cadmium, hydrogen, stainless steel or water reflector for absorption of thermal neutrons. For damaged package array conditions, the amount of interstitial foam between packages becomes important to creating the required thermal spectrum necessary for effective thermal capture by cadmium.

The homogeneous UO_2 payload is varied from 40 - 65 kgs UO_2 equivalent per ICCA (360 – 585 kgs UO_2 per NPC package). In these damaged package array cases, the system becomes mass and geometry limited. The ICCA spacing is modeled at 11.75" (29.845 cm), while the nominal spacing between ICCAs is 12.00" (30.48 cm). All damaged package array models remain below the accident limit $k_{eff,USL} = 0.931$ for up to 60 kgs UO_2 per ICCA.

From Table 6.16 in Section 6.10, the maximum calculated $k_{eff} + 2\sigma$ - bias results for the undamaged package array at 60 kgs UO2 per ICCA are:

FILENAME	K-EFF	SIGMA	K+2S	BIAS	K+2S-B
npca1_60	0.9059	0.0013	0.9084	-.0189	0.9273
npca2_60	0.9141	0.0013	0.9167	-.0189	0.9356
npcat_60	0.9275	0.0012	0.9299	-.0189	0.9488

As expected, the maximum burn condition is demonstrated the most reactive damaged package array model, though the interstitial 7-lb/ft^3 foam region between ICCAs and the 0.570-inch polyethylene are sufficient to maintain the damaged package array subcritical (e.g., $k_{eff} + 2\sigma$ - bias < 0.95).

Figure 6.13 – NPC damaged package array k_{eff} vs. UO_2 mass per canister (CTU-1, CTU-2, and maximum observed foam burn conditions)

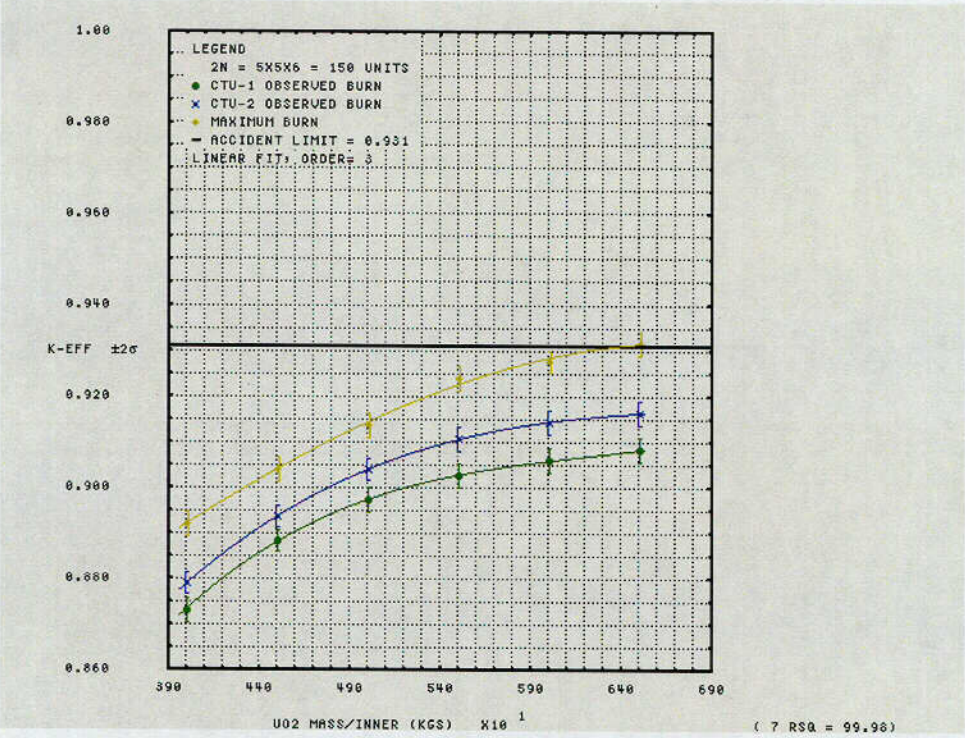

6.6.2.2 Damaged Package Arrays with Heterogeneous UO_2 in H_2O

Figures 6.14a through 6.14h show the reactivity of damaged package arrays for the 55.0, 53.0 and 46.0 kgs UO_2 per ICCA cases. The figures demonstrate that with the specified pellet OD versus ICCA UO_2 mass limits, 0.34" (or larger) for 55.0 kg UO2 payload, 0.30" (or larger) for 53.0 kg UO2 payload, and for unrestricted particle diameters, the maximum payload is demonstrated 46.0 kg UO2. In all caes, the damaged package array remains subcritical (i.e., have $k_{eff} + 2\sigma$ - bias < 0.95) under the most reactive configuration of material, W/F ratio, lattice array type (square or triangular), lattice boundary conditions (overlap or no overlap) and close reflection of the containment system by water on all sides in the surrounding materials in the packaging.

C31

Figure 6.14a – NPC damaged package array k*eff* vs. W/F Ratio (10X10 pellet type, square pitch, 55 kgs UO_2/ICCA)

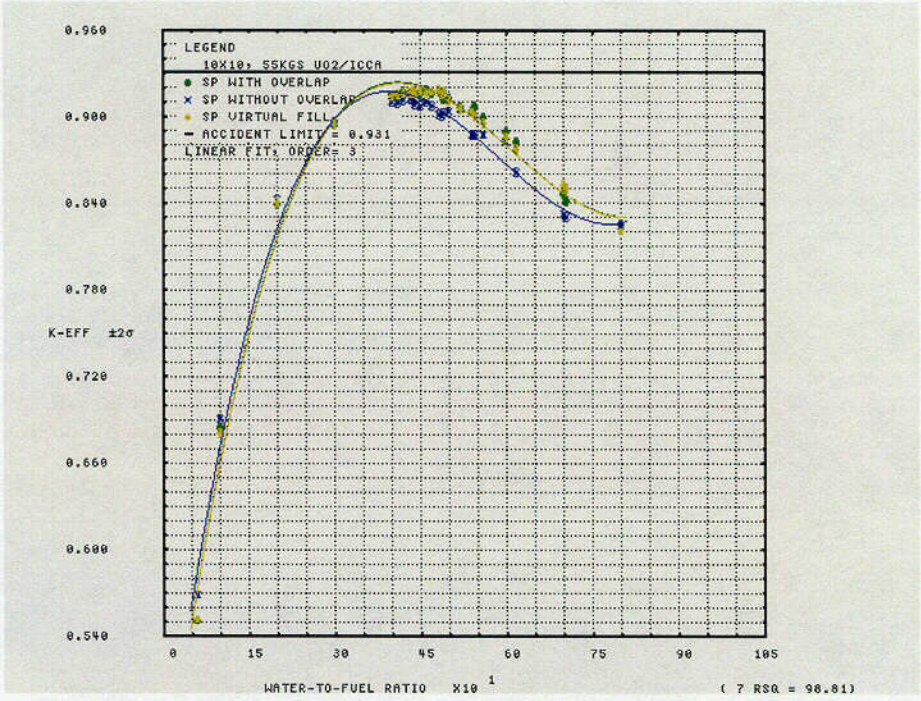

Figure 6.14b – NPC damaged package array k*eff* vs. W/F Ratio (10X10 pellet type, triangular pitch, 55 kgs UO_2/ICCA)

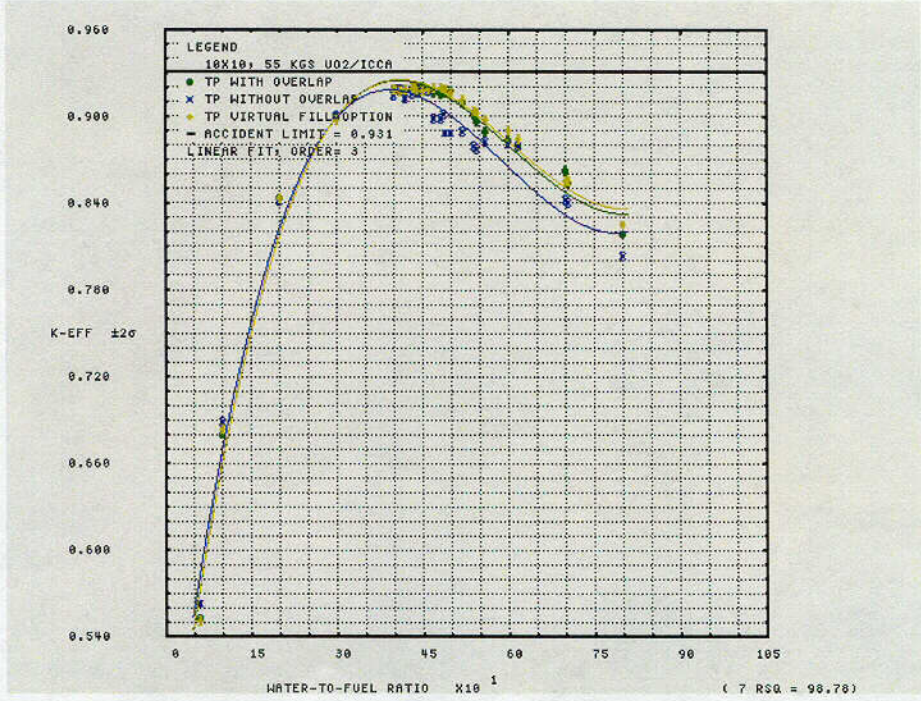

C32

Figure 6.14c – NPC damaged package array k*eff* vs. W/F Ratio (reactivity comparison vs. pellet size, triangular pitch, 55 kgs UO_2/ICCA, VFO)

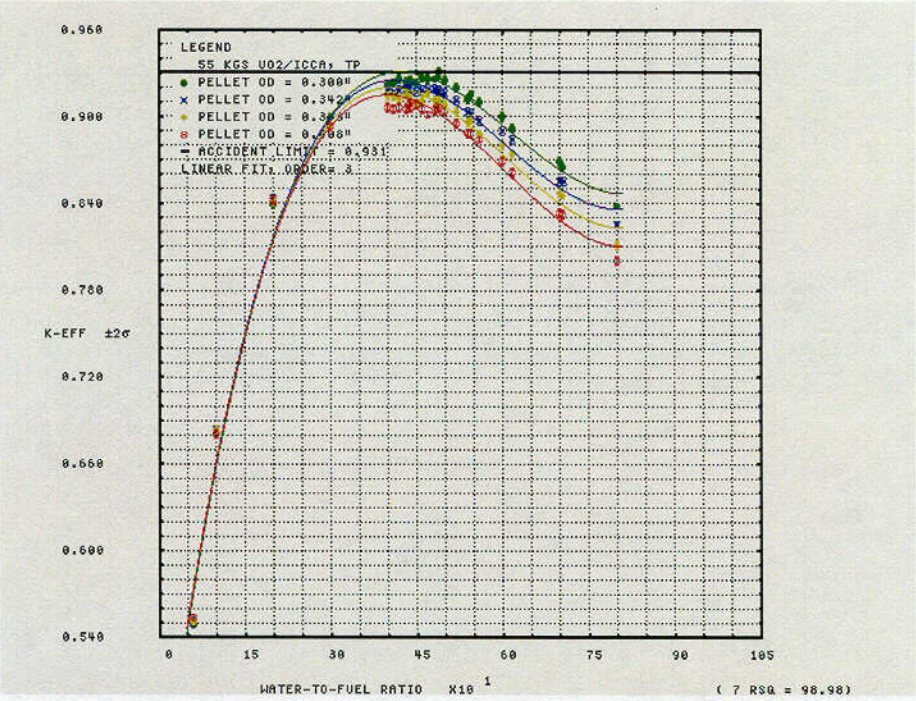

Figure 6.14d – NPC damaged package array k*eff* vs. W/F Ratio (17X17 pellet type, square pitch, 53 kgs UO_2/ICCA)

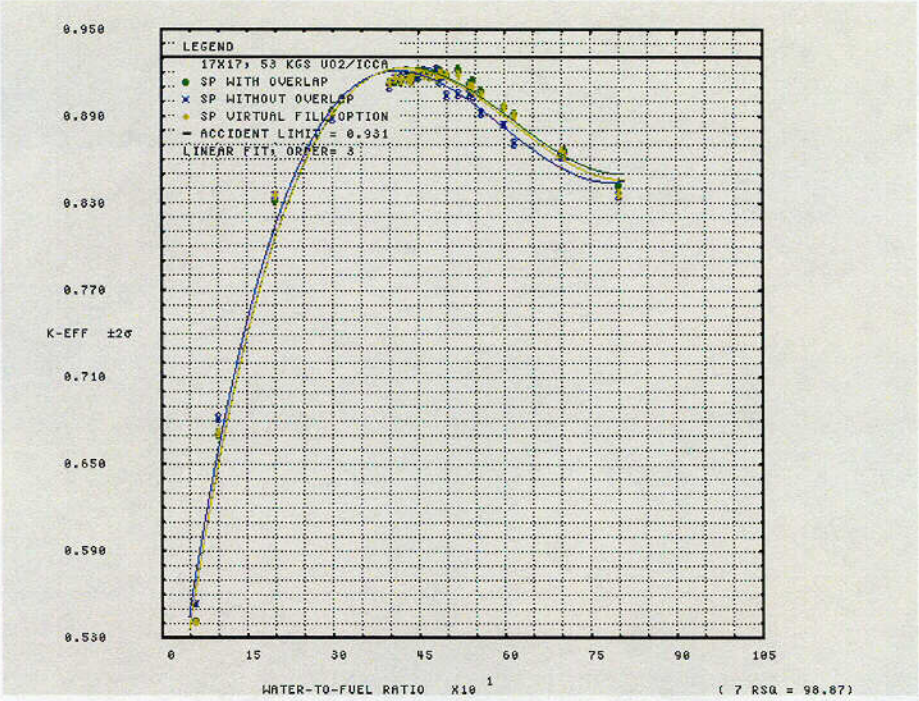

C33

Figure 6.14e – NPC damaged package array k*eff* vs. W/F Ratio (17X17 pellet type, triangular pitch, 53 kgs UO_2/ICCA)

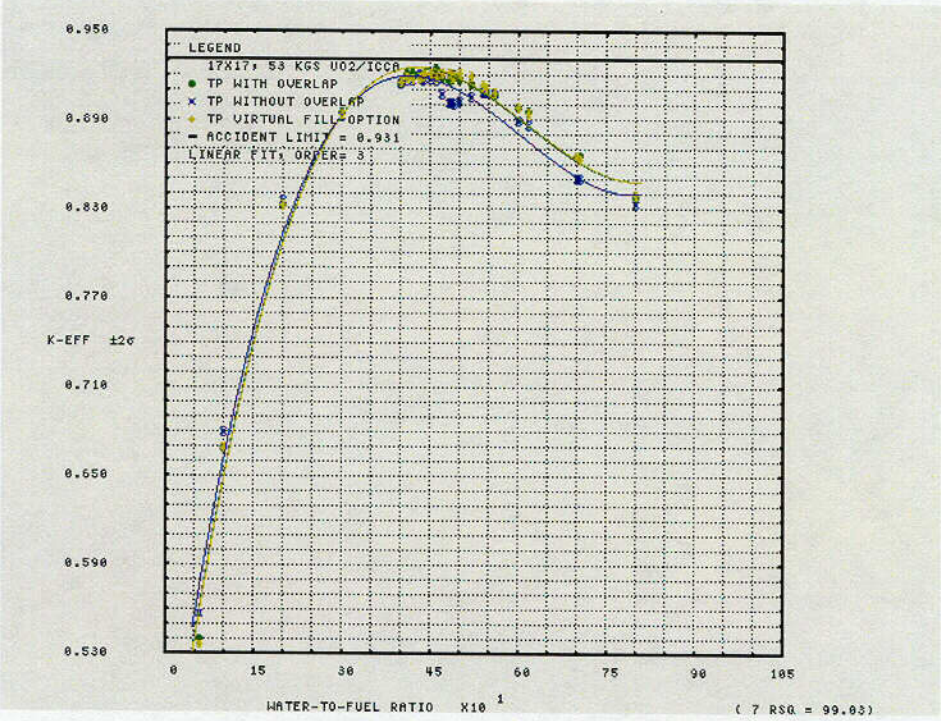

Figure 6.14f – NPC damaged package array k*eff* vs. W/F Ratio (reactivity comparison vs. pellet size for triangular pitch, 53 kgs UO_2/ICCA, VFO)

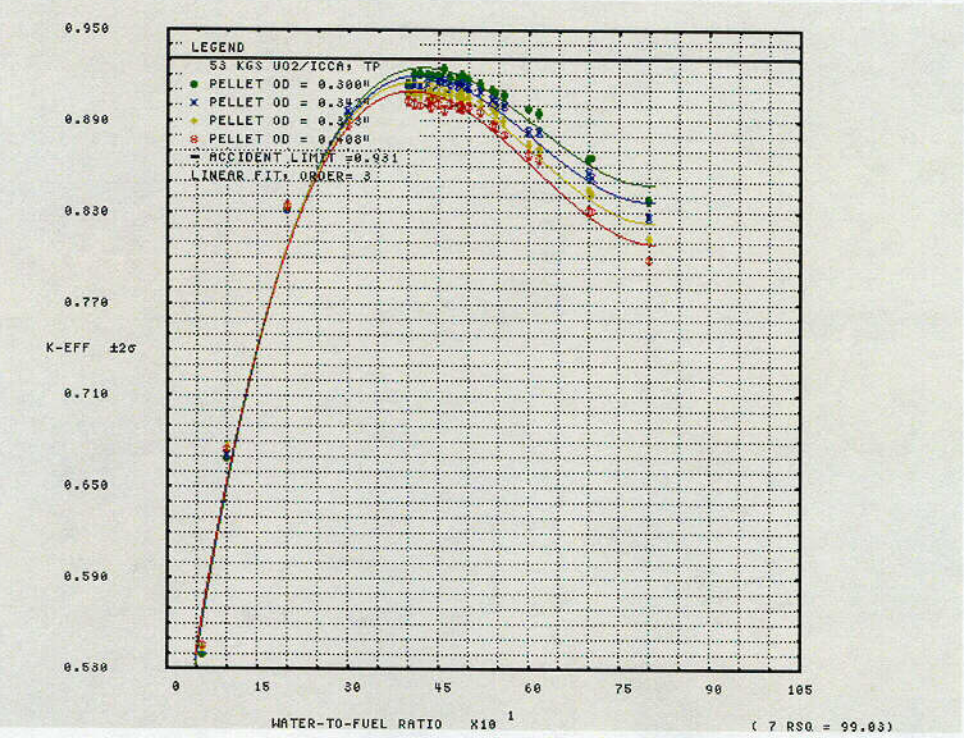

C34

Figure 6.14g – NPC damaged package array k*eff* vs. W/F Ratio (unrestricted particle size, square pitch, 46 kgs UO_2/ICCA)

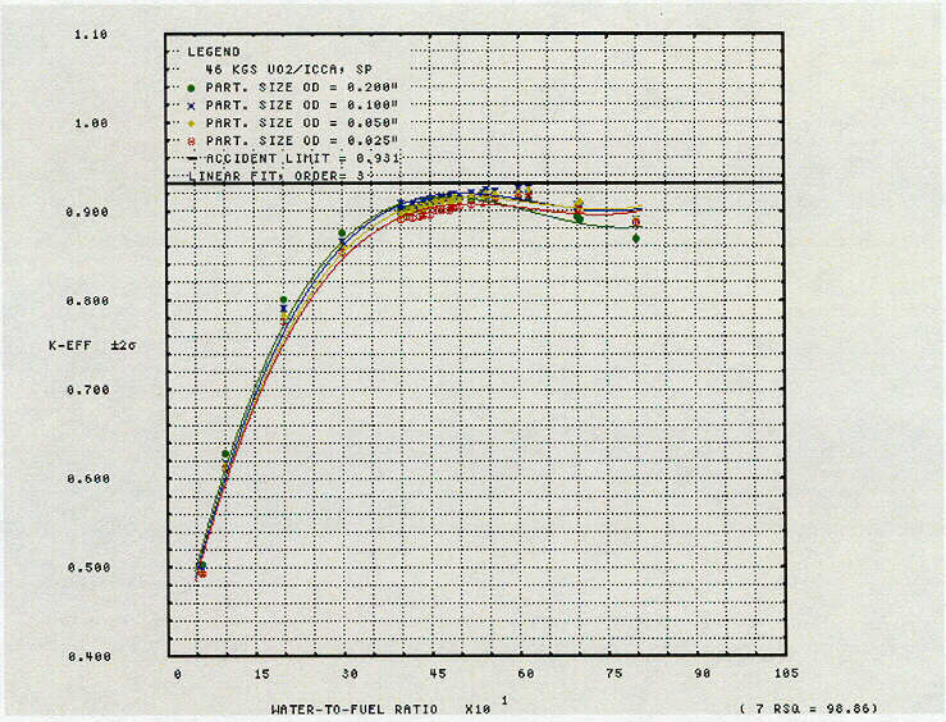

Figure 6.14h – NPC damaged package array k*eff* vs. W/F Ratio (unrestricted particle size, triangular pitch, 46 kgs UO_2/ICCA)

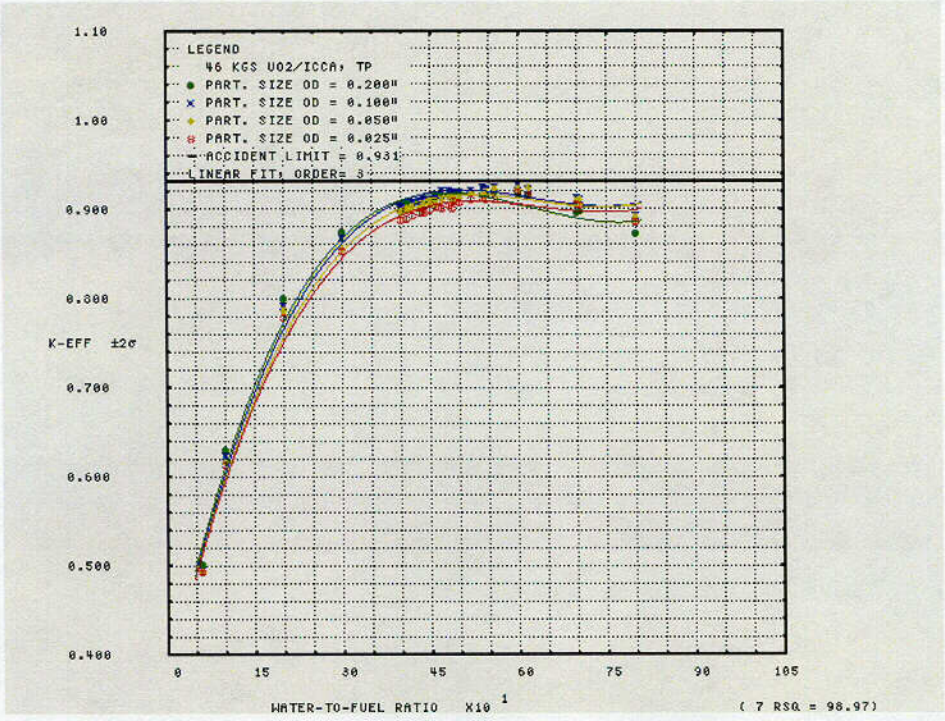

C35

From tables C and D in Table 6.9 above, the maximum calculated $k_{eff} + 2\sigma$ - bias results for the damaged package arrays are:

FILENAME	UO2 MASS	K-EFF	SIGMA	K+2S	BIAS	K+2S-B	
ST55-486*	55 kgs	0.9280	0.0014	0.9307	-.0189	0.9496	- a 17X17 Case
TT55-450	55 kgs	0.9207	0.0014	0.9235	-.0189	0.9424	- a 10X10 Case
ST53-460	53 kgs	0.9242	0.0013	0.9263	-.0189	0.9456	- a 17x17 Case
BT46-600	46 kgs	0.9277	0.0005	0.9287	-.0189	0.9476	- a 0.1" OD Case

*VFO Case; Also, SIGMA for case BT46-600 is based on 3,800,000 neutron histories

Notes 1-4 in Section 6.6.1.2 also apply to these results.

6.6.3 UNDAMAGED PACKAGE ARRAYS

6.6.3.1 Undamaged Package Arrays with Homogeneous UO_2 and H_2O

Figure 6.15 demonstrates that an undamaged NPC package array of unlimited size ($5N = \infty$) remains subcritical provided the UO_2 equivalent payload is restricted to 60 kgs per ICCA. The fuel mixture condition with 60 kgs UO_2 fuel containing a varying amount of added H_2O, as described in section 6.3.1.4, *Materials*, Table 6.5, has been evaluated. In this worse case condition, a third order regression fit of the Keff $\pm 2\sigma$ results are plotted as a function of WF H_2O from 0.140 to 0.290. It is noted that prior evaluations have demonstrated that mixtures with the 60 kgs UO_2 mass limit and a varying amount of H_2O are more reactive than mixtures that contain 60 kg total weight of UO_2 and H_2O.

From Table 6.16 in Section 6.10, the maximum calculated $k_{eff} + 2\sigma$ - bias results for the undamaged package array are:

FILENAME	K-EFF	SIGMA	K+2S	BIAS	K+2S-B	
npc60i26	0.8897	0.0014	0.8925	-.0189	0.9114	WF H_2O = 0.260
npc60i27	0.8956	0.0013	0.8982	-.0189	0.9171	WF H_2O = 0.270
npc60i28	0.8954	0.0012	0.8978	-.0189	0.9167	WF H_2O = 0.280

As shown, under normal conditions of transport, the UO_2 equivalent product is subcritical at an optimum WF of H_2O. Therefore, the NPC package is not required to be restricted in moderator content in the individual ICCAs, provided that the type and form of the moderator is no more effective than normal H_2O.

Figure 6.15 – NPC undamaged package array K*eff* vs. Weight Fraction H_2O (60 kgs UO2 compound/ICCA)

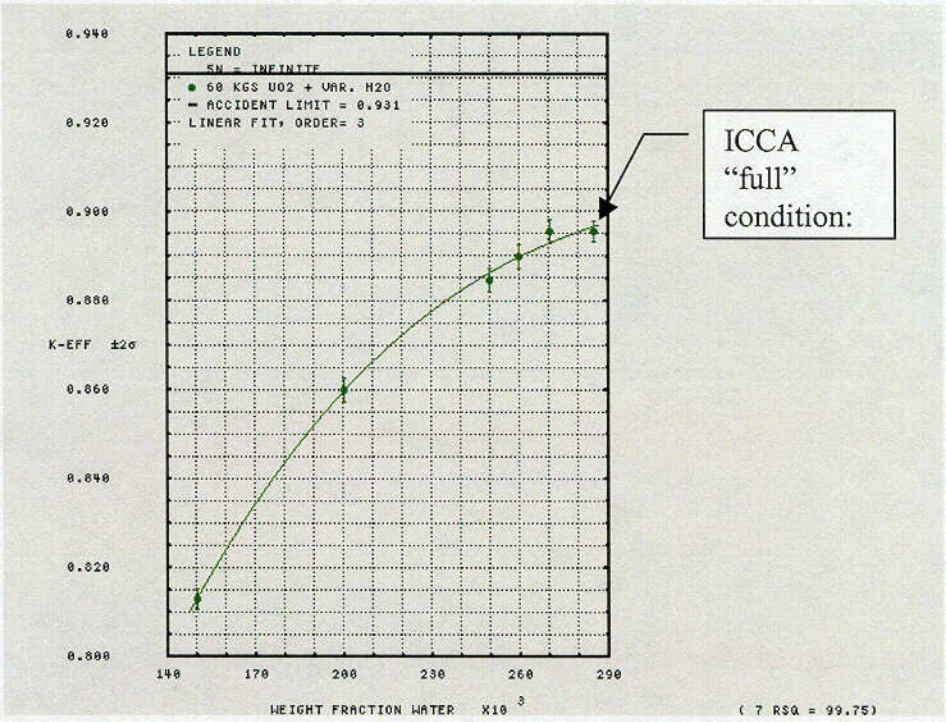

6.6.3.2 Undamaged Package Arrays with Heterogeneous UO_2 in H_2O

Figures 6.16a through 6.16h show the reactivity of undamaged package arrays for the 55, 53 and 46 kg UO_2 per ICCA cases described in the preceding sections. The figures demonstrate that with the specified pellet OD versus ICCA UO_2 mass limits, 0.34" for 55 kg, 0.30" for 53 kg and unlimited pellet diameter for 46 kg, the undamaged package arrays remain subcritical under the most reactive configuration of material, W/F ratio, lattice array type (square or triangular), lattice boundary conditions (overlap or no overlap) and close reflection of the containment system by water on all sides in the surrounding materials in the packaging.

C36

Figure 6.16a – NPC undamaged package array k*eff* vs. W/F Ratio (10X10 rod type, square pitch, 55 kgs UO_2/ICCA)

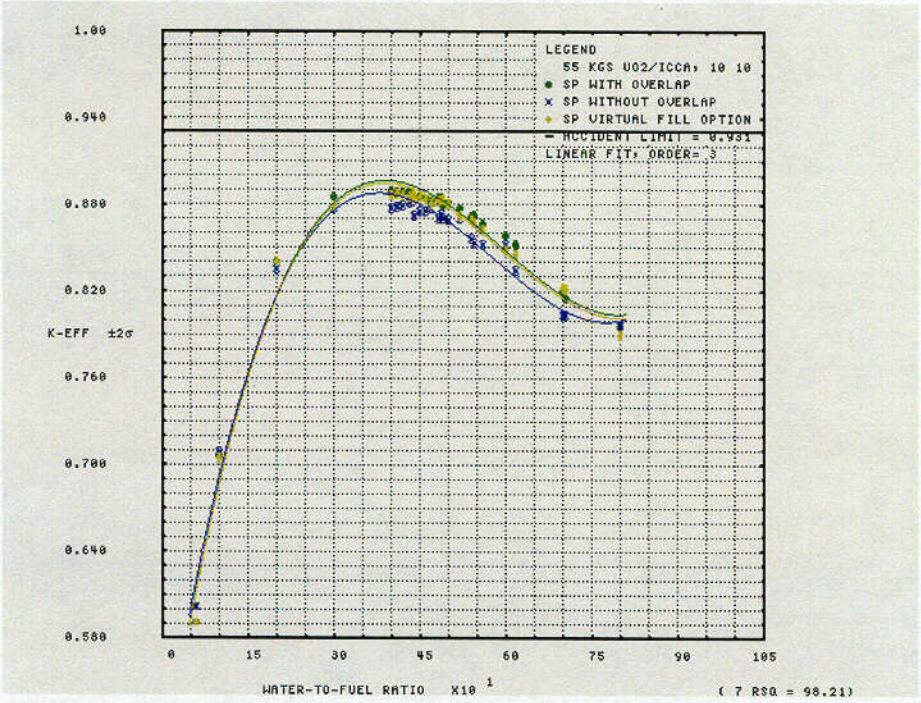

Figure 6.16b – NPC undamaged package array k*eff* vs. W/F Ratio (10X10 rod type, triangular pitch, 55 kgs UO_2/ICCA)

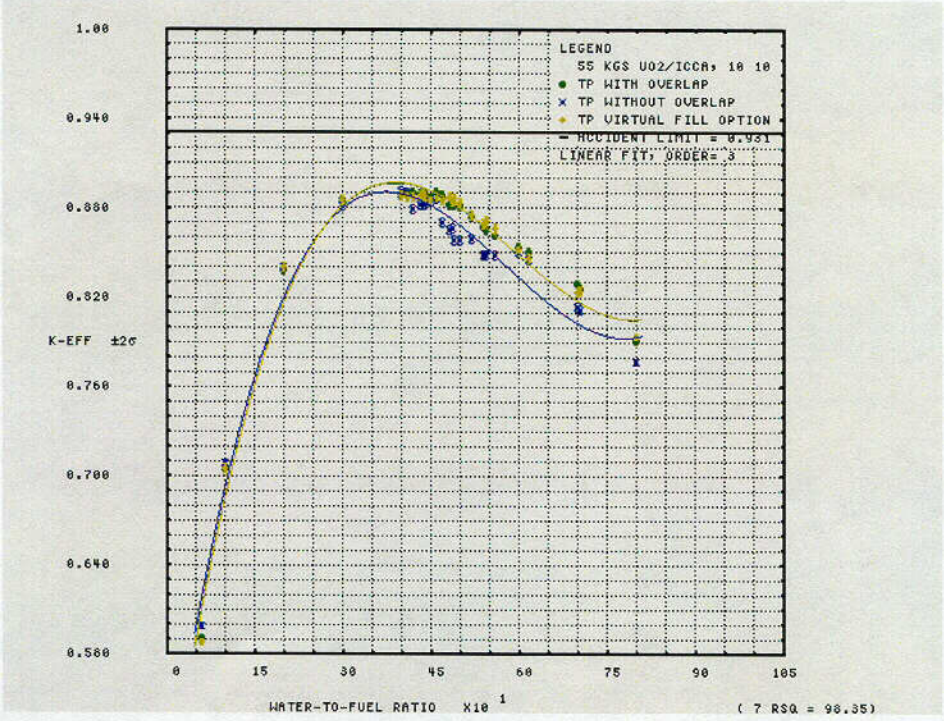

C37

Figure 6.16c – NPC undamaged package array k*eff* vs. W/F Ratio (reactivity comparison vs. pellet size, triangular pitch, 55 kgs UO_2/ICCA, VFO)

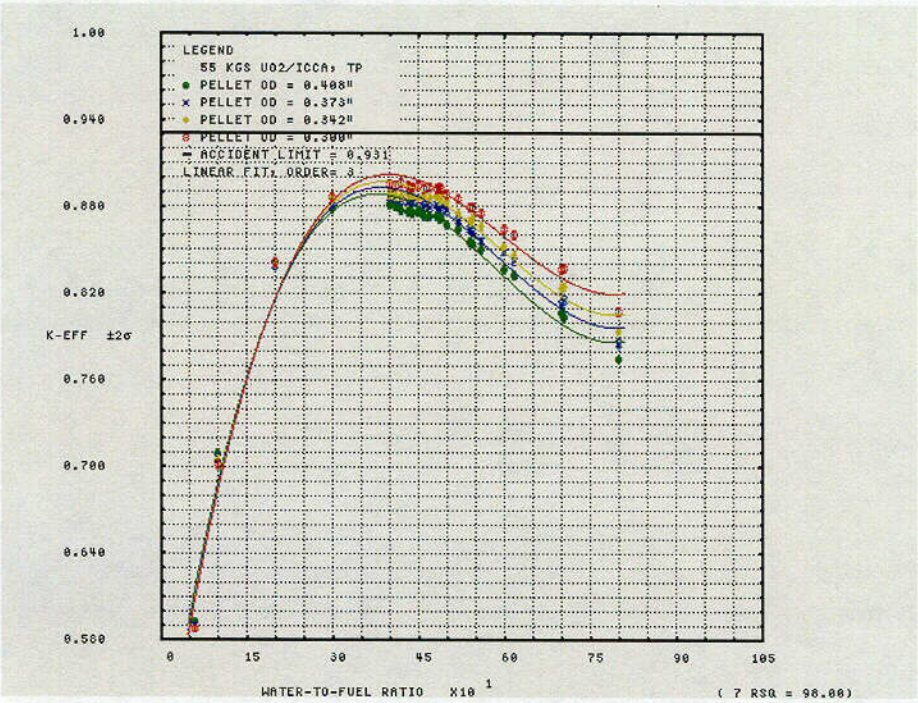

Figure 6.16d – NPC undamaged package array k*eff* vs. W/F Ratio (17X17 rod type, square pitch, 53 kgs UO_2/ICCA)

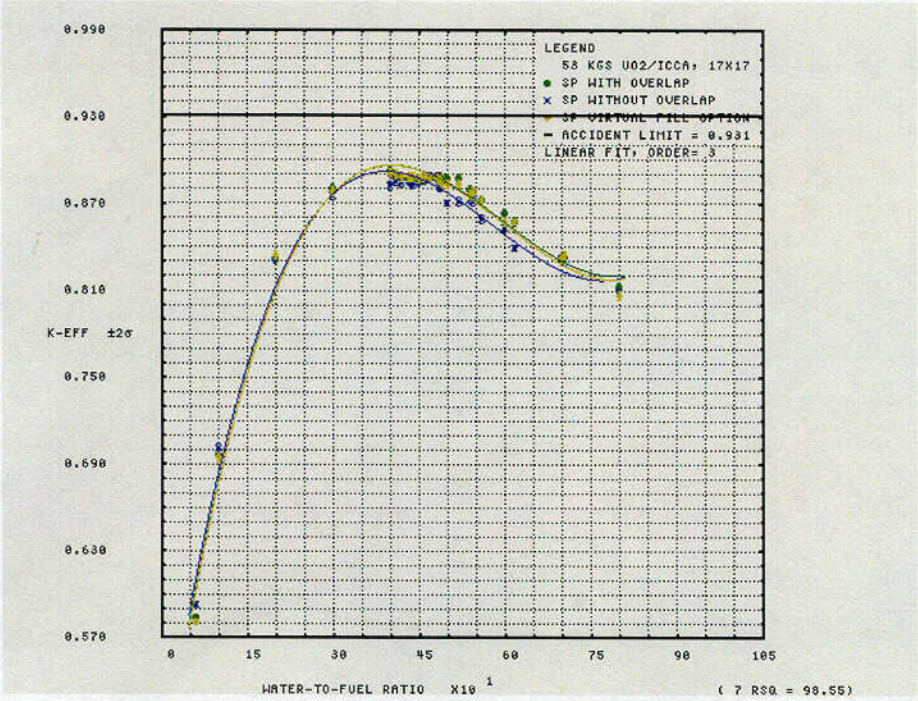

C38

Figure 6.16e – NPC undamaged package array k*eff* vs. W/F Ratio (17X17 rod type, triangular pitch, 53 kgs UO_2/ICCA)

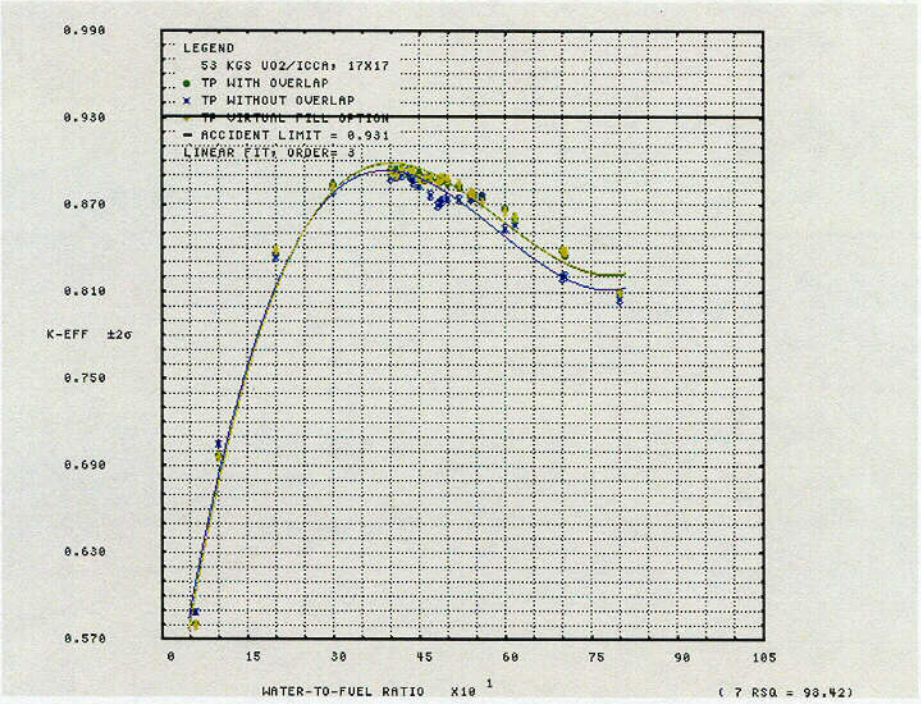

Figure 6.16f – NPC undamaged package array k*eff* vs. W/F Ratio (reactivity comparison vs. pellet size for triangular pitch, 53 kgs UO_2/ICCA, VFO)

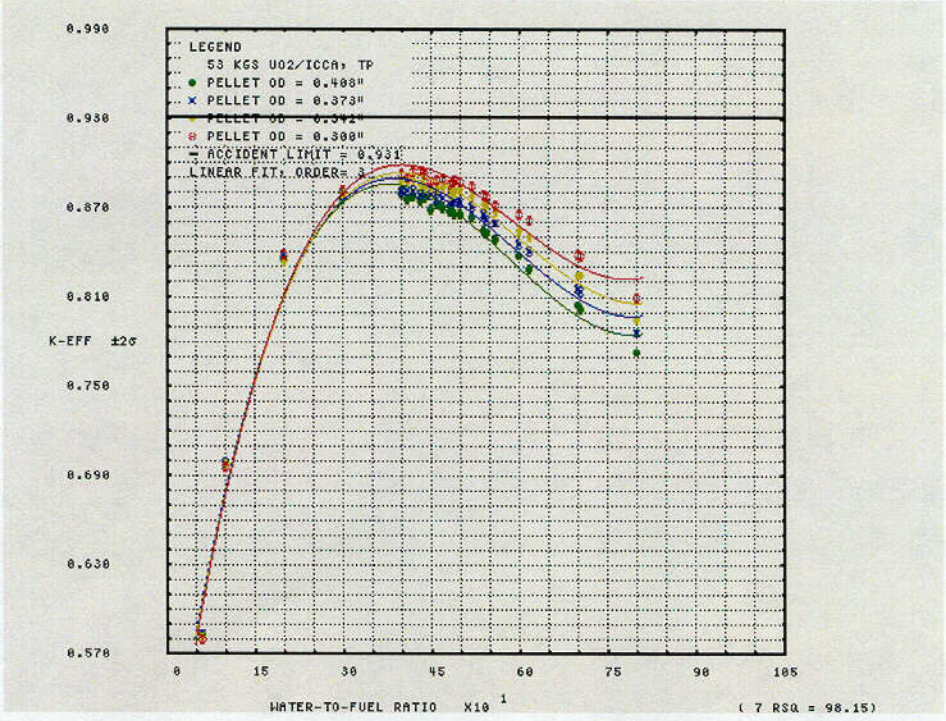

C39

Figure 6.16g – NPC undamaged package array k*eff* vs. W/F Ratio (unrestricted particle size, square pitch, 46 kgs UO_2/ICCA)

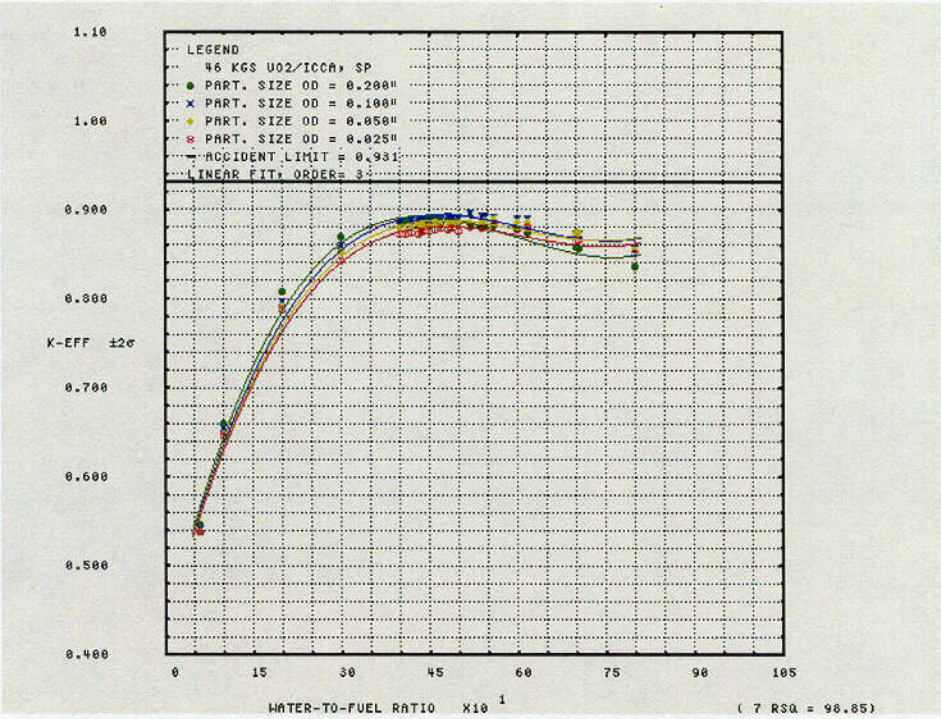

Figure 6.16h – NPC undamaged package array k*eff* vs. W/F Ratio (unrestricted particle size, triangular pitch, 46 kgs UO_2/ICCA)

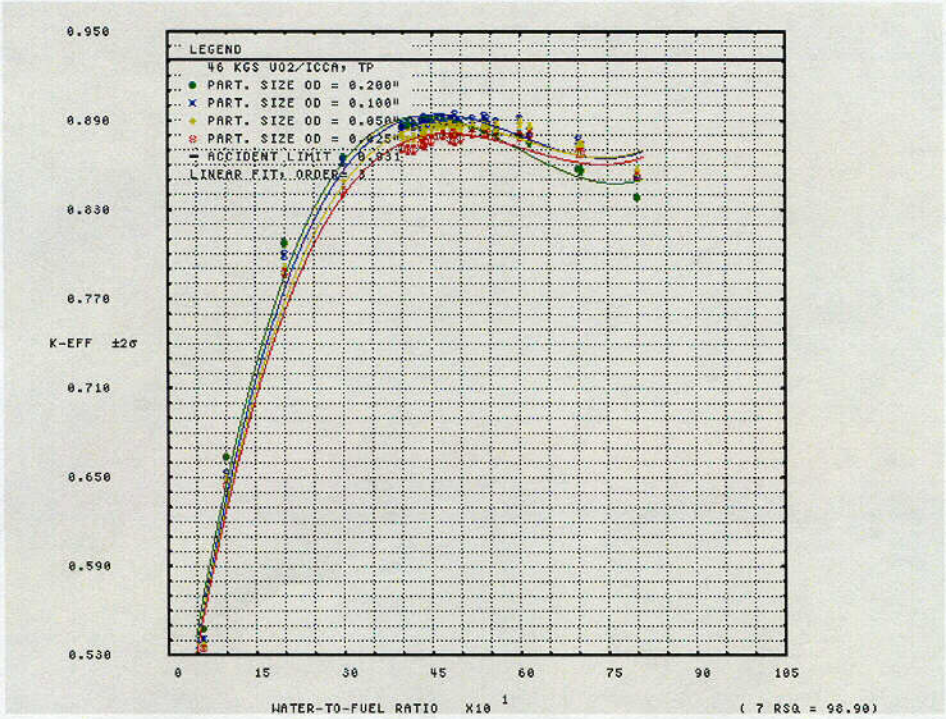

C40

From tables B and D in Table 6.9 above the maximum calculated $k_{eff} + 2\sigma$ - bias results for the undamaged package arrays are:

FILENAME	UO2 MASS	K-EFF	SIGMA	K+2S	BIAS	K+2S-B
DSTP-437	55 kgs	0.8980	0.0013	0.9005	-.0189	0.9194
BSTN-430*	53 kgs	0.8947	0.0013	0.8973	-.0189	0.9162
ABSL-520	46 kgs	0.8960	0.0013	0.8987	-.0189	0.9176

*VFO Case

Notes 1-4 in Section 6.6.1.2 also apply to these results.

6.6.4 SENSITIVITY STUDIES WITH HOMOGENEOUS UO2 + H2O

6.6.4.1 Sensitivity Study - Damaged Package Array Shape

As described in section 6.3.4.2, cases were run to confirm the most reactive aspect ratio of the damaged package array shape. The standard near cubic 5x5x6 array (case npcat_60.in) is confirmed representative of the most reactive configuration relative to the 6x5x5 (case npcatv60.in) and the 9x9x2 array (case npcatw60.in) for equivalent package payload and foam burn conditions. Though it is noted that there is little statistical difference between the 5x5x6 and 6x5x5 damaged package array models. From summary Table 6.16, the maximum calculated $k_{eff} + 2\sigma$ - bias results for the damaged package array shape study (60 kgs UO_2 per ICCA) are:

FILENAME	K-EFF	SIGMA	K+2S	BIAS	K+2S-B
npcat_60	0.9275	0.0012	0.9299	-.0189	0.9488
npcatv60	0.9274	0.0012	0.9298	-.0189	0.9487
npcatw60	0.9132	0.0012	0.9156	-.0189	0.9345

6.6.4.2 Sensitivity Study - Damaged Package Array Moderator Content and Payload

As described in section 6.3.1.4, Materials, Table 6.6, cases were also run to confirm the most reactive damaged package array internal ICCA moderation condition. Lower weight fraction water cases were run to confirm the most reactive condition occurs when the mixture height for this mass just fills the internal volume of the ICCA. From summary Table 6.16, the results are:

FILENAME	K-EFF	SIGMA	K+2S	BIAS	K+2S-B	
npcatx60	0.8102	0.0013	0.8128	-.0189	0.8317	(wf_h2o=0.15)
npcaty60	0.8671	0.0013	0.8697	-.0189	0.8886	(wf_h2o=0.20)
npcatz60	0.9081	0.0014	0.9108	-.0189	0.9297	(wf_h2o=0.25)
npcat_60	0.9275	0.0012	0.9299	-.0189	0.9488	(wf_h2o=0.28504)

The above results confirm the most reactive condition occurs when the mixture height just fills the ICCA volume (limiting damaged array case npcat_60.in, wtfr. H_2O = 0.28504).

If additional water is added such that UO_2 mass is driven out of the ICCA, Figure 6.13 in Section 6.6.2.2 demonstrates system reactivity will decrease. These results support the fact that any UO_2 payload distribution is acceptable provided the maximum mass in any one of the nine ICCAs does not exceed 60 kgs UO2 (52.9 kgs U). Relative to 60 kgs UO2, by lowering the UO2 payload in any ICCA would result in a less reactive damaged package array.

6.6.4.3 Sensitivity Study - Damaged Package Array 100% Foam Burn

Figure 6.17 determines the worth of the foam for the limiting damaged package array determined in Section 6.6.2, Package Arrays. In this figure, 100% internal foam burn is assumed, and replaced with variable density H_2O. The figure shows the void condition is the most reactive, and the damaged package array becomes safe ($k_{eff} + 2\sigma$ - bias < 0.931) when the interspersed hydrogenous reaches ~ 2.63% water equivalent (or greater).

The 60 kg UO_2 per ICCA damaged package array results for CTU-1, CTU-2, and maximum burn models are provided in Figure 6.17 for comparison purposes. The 6% hydrogen content in the inner 7-lb/ft^3-foam region is demonstrated sufficient to maintain the damaged package subcritical. In general, increasing hydrogen content between packages reduces the reactivity of the NPC damaged package containing optimally moderated UO_2 canisters. The damaged package therefore exhibits an over-moderated behavior.

This is substantiated by the fact that package reactivity increases as the foam burn depth (see Figure 6.13) is increased to its maximum observed condition. This effect also underscores the use of void for the ceramic fiberboard around the periphery, and the use of void for the postulated burn regions instead of low interspersed water moderation.

Figure 6.17 – NPC damaged package array k_{eff} vs. interspersed H_2O (100% foam burn condition)

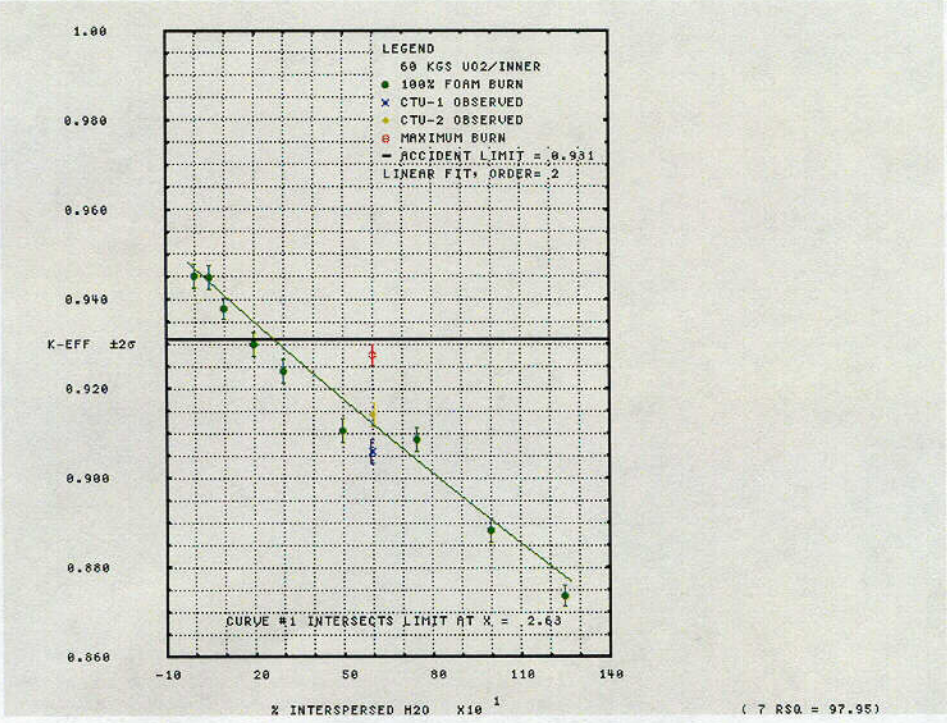

C41

6.6.4.4 Sensitivity Study - Damaged Package Array ICCA Spacing

Figure 6.18 demonstrates the damaged package reactivity behavior as a function of ICCA spacing. A second-order regression fit of the $K \pm 2\sigma$ results is shown. The 60 kg UO_2 per ICCA payload, maximum burn model is used as the basis for the center-to-center canister spacing study.

This figure demonstrates little sensitivity from movement of the ICCA from the standard center-to-center spacing of 11.75" (29.845 cm) to 11.25" (28.575 cm). Therefore, the 11.75" standard spacing is sufficiently conservative representation of the nominal ICCA spacing of 12" (30.48 cm). The reactivity of the damaged package array is not adversely affected by ICCA center-to center movement of up to ¾".

Figure 6.18 – NPC damaged package array k_{eff} vs. canister spacing

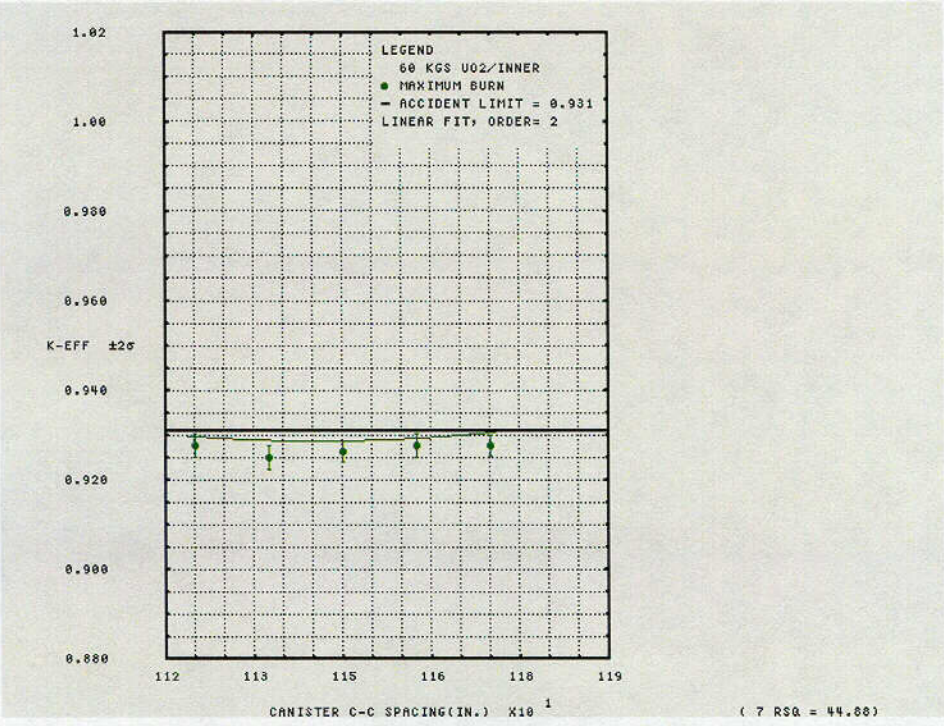

6.6.4.5 Sensitivity Study - Damaged Package Array Structure

The effect of adding certain external stainless steel structure into the limiting condition model is made to determine effect package reactivity. In particular the bottom of each NPC package is comprised of eight (8) 6x3x3/16" rectangular tubes, four (4) 6x1-1/2x19.25" connecting channels, and a 16-ga. 18x18" square doubler plate. A conservative estimate that includes maximum manufacturing tolerance of this structure mass associated is determined to be 40.8 kgs.

C42

If this mass of 40.8 kgs is then "smeared" over the bottom layer of the package, an additional thickness of 0.4365 cm may be included in the modeled bottom plate thickness [e.g., δh = mass_ss/(rho_ss*l*w) = 40,800/(7.9*108.7743*108.7743) = 0.4365 cm].
The reactivity comparison is made for the limiting damaged package array case using the acceptable 60 kg UO_2 per ICCA. From Table 6.16, the result is:

FILENAME	K-EFF	SIGMA	K+2S	BIAS	K+2S-B
npcat_60	0.9275	0.0012	0.9299	-.0189	0.9488
npcats60	0.9240	0.0012	0.9264	-.0189	0.9453

Relative to the limiting damaged package array model (npcat_60), the additional external Type 304L stainless steel (npcats60.in) structure on the bottom of the package results in a ~0.4% delta-k/k reactivity reduction.

6.6.4.6 Sensitivity Study - Damaged Package Array Poly Gap

The effect of polyethylene gap as determined from the physical measurements of the ICCAs post HAC testing is assessed to confirm the modeled poly height and density assumptions.

In the first case (npcatg60.in), the modeled polyethylene height of is reduced by 75 mils to the minimum specified height of 30.3" (the density remains constant at 0.92*0.98 to offset the 0.6 wt% maximum observed poly weight loss under accident conditions). No statistical change in reactivity relative to the limiting condition damaged package array model (npcat_60.in) resulted.

In the second case (npcatf60.in), the modeled polyethylene height surrounding all 9 ICCAs is reduced to correspond to the maximum observed gap conditions post HAC testing. The cumulative gap at the top plus bottom of the polyethylene wrap was measured for all ICCAs in CTU-1 and CTU-2. Maximum gap measurements for CTU-1 and CTU-2 test units are reported in Sections 2.10.1.7.1.6 and 2.10.1.7.2.6, respectively.

The maximum observed total gap was 0.40" top + 0.29" bottom = 0.69" and reported in certification test results Section 2.10.1.2, Summary. For this study, the top gap was increase from 1/8" (0.3175 cm) to its maximum of 0.4" (1.016 cm). The bottom gap was increased from 1/8" (0.3175 cm) to its maximum of 0.29" (0.7366 cm). Since the gap is explicitly modeled, the poly density of 0.92 g/cc is applied. Again, no statistical change in reactivity relative to the limiting condition damaged package array model resulted.

From Table 6.16, reactivity comparisons are as follows:

FILENAME	K-EFF	SIGMA	K+2S	BIAS	K+2S-B
npcat_60	0.9275	0.0012	0.9299	-.0189	0.9488
npcatg60	0.9271	0.0012	0.9296	-.0189	0.9484
npcatf60	0.9273	0.0013	0.9299	-.0189	0.9488

These results support the assumption that the 2% polyethylene density reduction factor applied to the damaged package array models are conservative and adequately address the observed polyethylene weight loss and model height.

Tables 6.16-6.20 provide a summary listing of all calculations made for the NPC package criticality safety demonstration.

6.6.5 TRANSPORT INDEX

The number of packages that remain below the upper safety limit determines the Transport Index (TI) for criticality control. For normal conditions of transport, an infinite array size ($5N = \infty$) remains subcritical. Under hypothetical accident conditions, the contents of 2N=150 packages would remain subcritical.

$$TI = 50/75 = 0.6667 \approx 0.7.$$

6.7 REFERENCES

1. "GEMER - Microcomputer Version Users Guide," JT Taylor, 4/20/94.
2. "Validation of the GEMER Monte Carlo Code for Applications with Enriched Uranium Fuels at GE Nuclear Fuels in Wilmington, NC", GENE Technical Report, WC Peters, 12/8/97.
3. "Criticality Safety Analysis: Evaluation of Cadmium Bias in the GEMER Code," Rev. 01, JF Zino, 1/27/2000.
4. "Recommendations for Preparing the Criticality Safety Evaluation of Transportation Packages," NUREG/CR-5661, ORNL/TM-11936, H.R. Dyer, C.V. Parks, April 1997.
5. U.S. Code of Federal Regulations, "Packaging and Transpiration of Radioactive Material," Part 71, Chapter I, Title 10, "Energy".
6. IAEA – Safety Standards Series: Regulations for the Safe Transport of Radioactive Material, Requirements, No. ST-1, 1996 Edition
7. International Handbook of Evaluated Criticality Safety Benchmark Experiments, NEA/NSS/DOC(95)03, NEA Nuclear Science Committee, Vol. IV, September 1999.
8. MCNP4C / MCNPDATA – A General Monte Carlo N-Particle Transport Code System, CCC-200, Radiation Shielding Information Center, Oak Ridge National Laboratory, July 2000.
9. MINITAB, Release 12.1, Minitab for Windows, Minitab Inc., ISBN 0-925636-35-5, 1996.

6.8 APPENDIX – VALIDATION OF GEMER

6.8.1 GEMER URANIUM BIAS

The GEMER Monte Carlo Code has been validated against an extensive set of critical benchmark experiments covering a broad range of enrichments, forms and densities of uranium, degrees of moderation and reflection, and types and amounts of neutron poisons (Ref. 2). Figure 6.19 shows a plot of this benchmark data along with a least square analysis of the code bias and statistical uncertainty.

Figure 6.19 – GEMER K_{eff}s vs. H/U-235 Ratios: 269 Benchmark Validation Set Rank 1 Eqn. 8002 [EXPONENTIAL] y = a + bexp(-x/c), where a= 0.99290588, b= 0.018116949, c= 90.332388

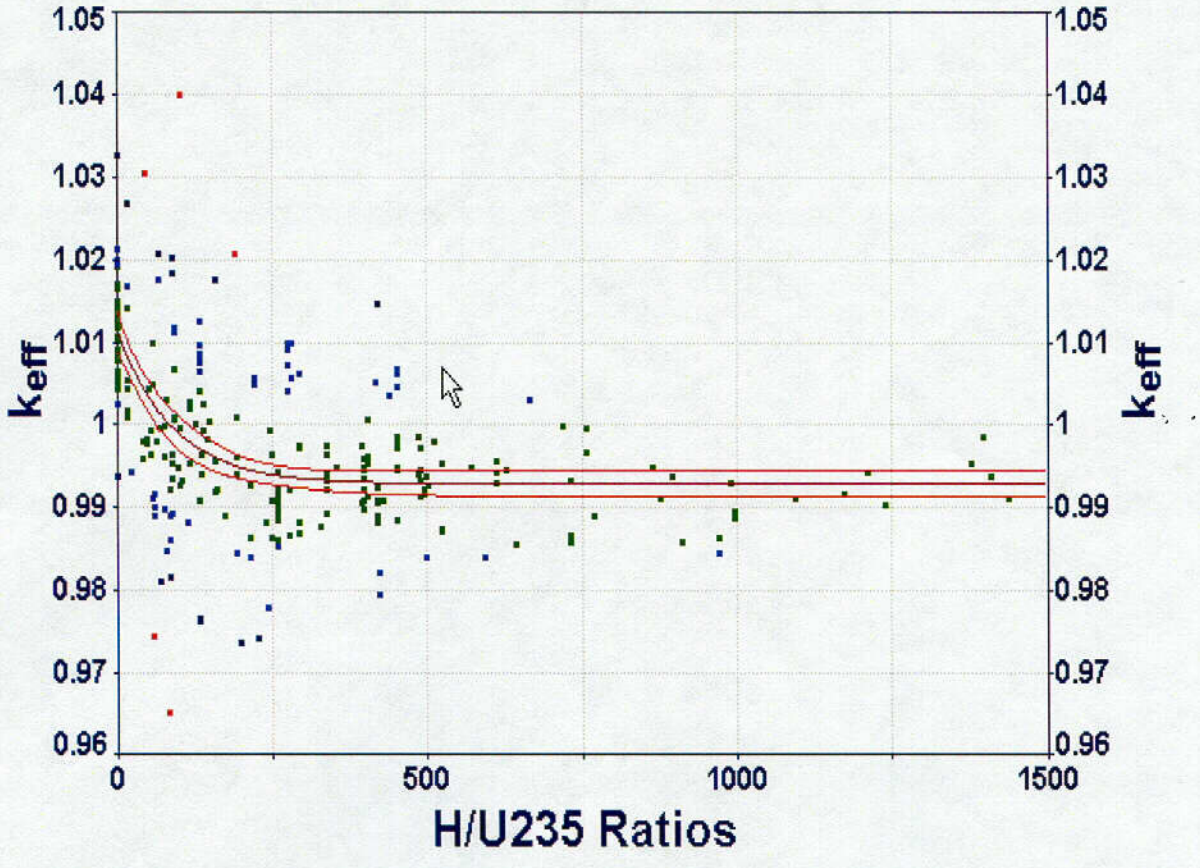

The dark red (center) curve in Figure 6.19 is the least square fit of the data and the bright red curves are the upper and lower 99% confidence intervals for the fit. As indicated, the complete benchmark data consists of the GEMER calculated k_{eff}s of 269 different critical experiments that has been fit with an exponential curve ($y = a + b \bullet \exp(-b/c)$, with $y = k_{eff}$ and x = H/U-235 ratio

C43

and a, b and c as given in the figure). The H/U-235 ratio is the ratio of the average atom densities of hydrogen and U-235 in the fuel region for each of the critical experiments.

For the complete 269-benchmark validation set, the H/U-235 ratios vary between 0.0 and approximately 1450. Optimum moderation is typically in the range of 150 to 500. From Figure 6.19, the maximum bias + bias uncertainty is 0.00868. Here, the "bias + bias uncertainty" is defined to be the value (1.0 – lower 95% confidence interval of the GEMER critical k_{eff} curve). The σ corresponding to the bias uncertainty is in the range of about 0.0006 to 0.0008. The calculated results are consistent with a constant bias over a broad H/U-235 range. This range starts somewhere between an H/U-235 of 250 to 500 and continues out to the maximum ~1450.

For uranium oxides only, bias for GEMER and the ENDF/B-IV library has been established to be no greater than 0.009 $(\Delta k_u - \beta)$ at a 99% confidence level. The area of applicability for the benchmark calculations is enrichment ranges from 1.29 to 9.83 weight percent U-235 and H/U-235 ratio 41 to 866. For uranium nitrate compounds (UN, UNH material forms), bias for GEMER and the ENDF/B-IV library has been established to be 0.0125 $(\Delta k_u - \beta)$ at a 99% confidence level. The area of applicability for the UN, UNH benchmark calculations is enrichment ranges from 9.97 to 94.42 weight percent U-235 and H/U-235 ratio 45 to 1437.

6.8.2 GEMER CADMIUM BIAS

The above documents 269 critical experiments used to establish the bias for the GEMER code for a variety of applications involving enriched uranium. Since most of these experiments do not contain cadmium, the effect of cadmium on the bias is significantly diluted by the non-cadmium experiments. Hence, it was considered prudent to quantify any "bias adjustment" required to allow for the presence of cadmium poison in the NPC package.

A total of sixteen (16) benchmark experiments for UO_2 systems containing cadmium have been analyzed and used to derive the cadmium bias in the GEMER computer code. Of these 16, ten were performed by Sid Bierman et. al., and involved clusters of 4.31% enriched UO_2 rods in water with cadmium plates of varying thickness' placed in between the clusters. Of the remaining six experiments, five were also performed by Bierman et. al., and involved 2.35% enriched UO_2 rod clusters in water also with cadmium plates. The last experiment performed by Handley and Hopper involved 4.98% enriched UO_2F_2 solution inside a steel/cadmium/water reflected cylinder. Table 6.10 provides a description of the names of each experiment as described in ICSBEP Vol. IV and Reference 2 for cross-reference comparison purposes.

Table 6.10 - Bierman Experiments with Cadmium Used in GEMER Validation

No.	ICSBEP Vol. IV Identification	ICSBEP Table #	ICSBEP Experiment #	Reference 4 ID
1	LEU-COMP-THERM-009	4	019	BIER-31
2	LEU-COMP-THERM-009	4	020	BIER-32
3	LEU-COMP-THERM-009	5	021	BIER-33
4	LEU-COMP-THERM-009	5	022	BIER-34
5	LEU-COMP-THERM-009	5	023	BIER-35
6	LEU-COMP-THERM-009	5	024	BIER-36
7	LEU-COMP-THERM-009	5	025	BIER-37
8	LEU-COMP-THERM-009	5	026	BIER-38
9	LEU-COMP-THERM-009	5	027	BIER-39
10	LEU-COMP-THERM-009	5	028	BIER-40
11	LEU-COMP-THERM-016	5	036	RSIC-14
12	LEU-COMP-THERM-016	5	037	RSIC-15
13	LEU-COMP-THERM-016	5	050	RSIC-24
14	LEU-COMP-THERM-016	5	052	RSIC-25
15	LEU-COMP-THERM-016	5	054	RSIC-26
16	-	-	-	HH-33

Figure 6.20a provides a diagram of the arrangement of the pin clusters and the absorber plates used for ten of the experiments involving cadmium. This figure is based on data taken from Volume IV (LEU-COMP-THERM-009) of the International Criticality Safety Benchmark Evaluation Project (ICSBEP) handbook (Ref. 7).

Figure 6.20b shows the arrangement of the 2.35% enriched UO_2 fuel pin clusters and the relative locations of the absorber plates for experiments with cadmium plates. Of these seven, five are used for validation of the GEMER code with cadmium. This figure is based on data taken from Volume IV (LEU-COMP-THERM-016) of the International Criticality Safety Benchmark Evaluation Project (ICSBEP) handbook (Ref. 7).

Figure 6.20a – Typical Arrangement of Fuel Pin Clusters and Absorber Plates for 4.31% Enriched Experiments

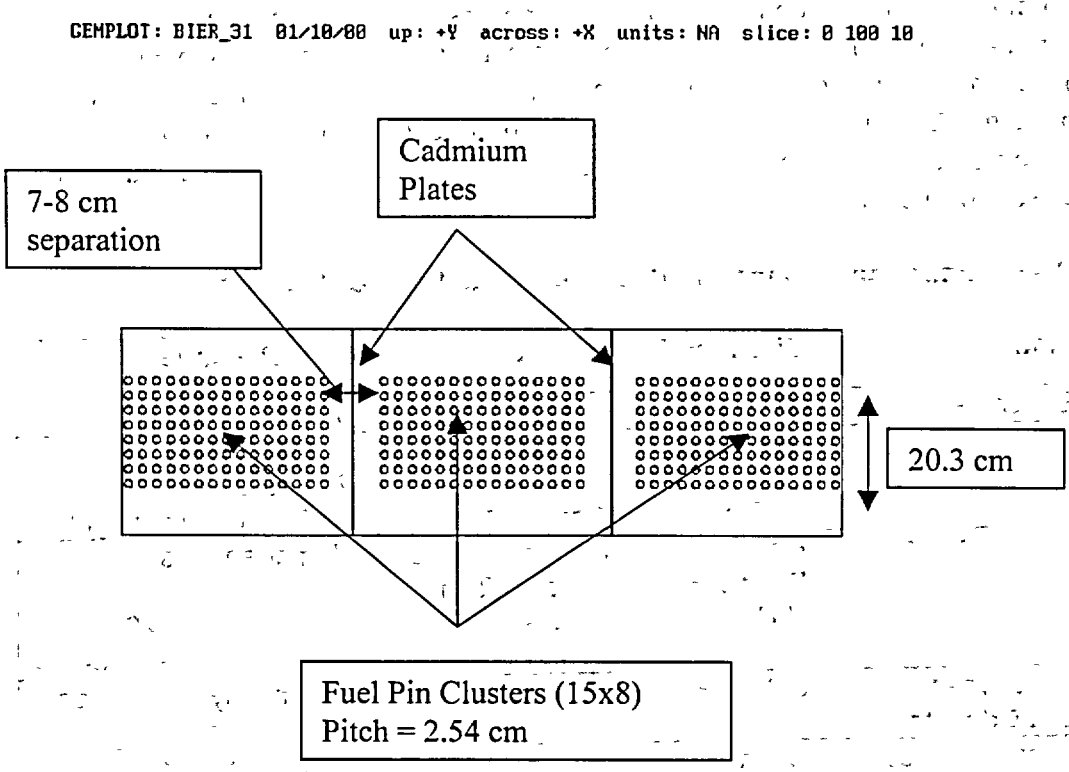

Figure 6.20b - Arrangement of Fuel Pin Clusters and Absorber Plates for 2.35% Enriched Experiments

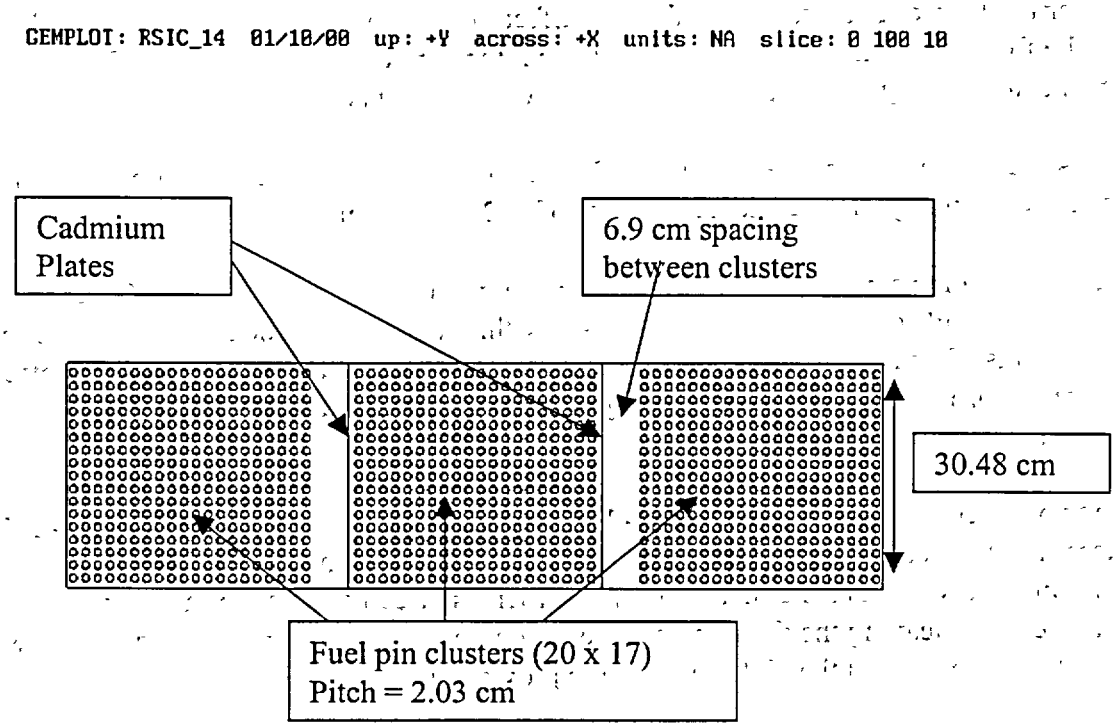

In order to make a determination of the applicability of the existing 16 benchmark experiments with cadmium to the NPC shipping container, a comparison of important neutron physics properties in made in Table 6.11. This table provides a comparison of enrichment, size, uranium moderation, cadmium plate dimensions, and moderation between uranium units and cadmium for the NPC package. A total of 15 Bierman fuel rod experiments are used as a basis for the benchmark comparison data, while the limiting damaged single package and damaged array results are used for the NPC data.

Table 6.11 - Comparison of Benchmark Experiments to NPC Package

Characteristic	Bierman Experiments	NPC Package
Uranium Enrichment	2.35% – 4.31%	5.00%
Geometry	UO_2 fuel lattice clusters 20.32cm x 38.1 cm x 91.44 cm 32.5 cm x 40.64 cm x 91.44 cm	3x3 cylinder array 21.628 cm dia. 80.01 cm max. height
Moderation of Uranium	Heterogeneous fuel pins in water Pin dia. ~1 cm, pitch ~ 2 cm H/U-235 range: 260 – 488	Homogeneous UO_2 + H_2O wtfr. water ~ 0.29 H/U-235 range: 236-254
Moderation between Uranium and Cd plates	3-6 cm H_2O	~3 cm polyethylene and ~5 cm foam
Absorber Plate thickness	Cadmium plates Thks. 0.30 mm – 2.0 mm	Cadmium wrap Thks. 0.381 mm

By comparing the properties that most directly affect the neutron physics behavior of each system, the following conclusions are reached about the applicability of these benchmark experiments to deriving a GEMER bias for the NPC shipping package.

- Both systems are low enriched, and therefore resonance absorption effects present with systems containing relatively large amounts of U-238 are similar.

- The overall dimensions of the two systems are similar (e.g., fuel regions are ~3 feet in length). The NPC cadmium wrap thickness is within the range of thickness of the Bierman experiments. This is expected since very thin regions of cadmium provide the same effective neutron absorption properties as thick regions (i.e., large resonance self-shielding absorption).

- The two systems have very similar H/U-235 ratios over the fissile volume. The H/U-235 ratio determines the neutron energy spectrum inside the fissile region. The effectiveness of the cadmium plates to act as thermal neutron absorbers is directly related to the energy spectrum of the neutrons leaving the fissile assemblies. Sample neutron spectra comparisons between critical experiment and the NPC package are provided in Figures 6.21a-6.21d.

- The overall qualitative effect of the hydrogen and carbon in both the polyethylene and foam regions of the NPC package provide some reasonable degree of thermal neutron moderation between ICCAs. Consequently, the effectiveness of the cadmium to act as a thermal neutron absorber in both systems is roughly equivalent (refer also to spectra comparisons).

Based on these observations, the neutron physics properties of the experiments and the NPC package compare favorably. The GEMER cadmium bias resulting from these benchmark experiments can therefore be successfully applied to criticality calculations involving uranium compounds for the NPC shipping package.

Figure 6.21a - Neutron Energy Spectra for BIER-35 (4.31%)

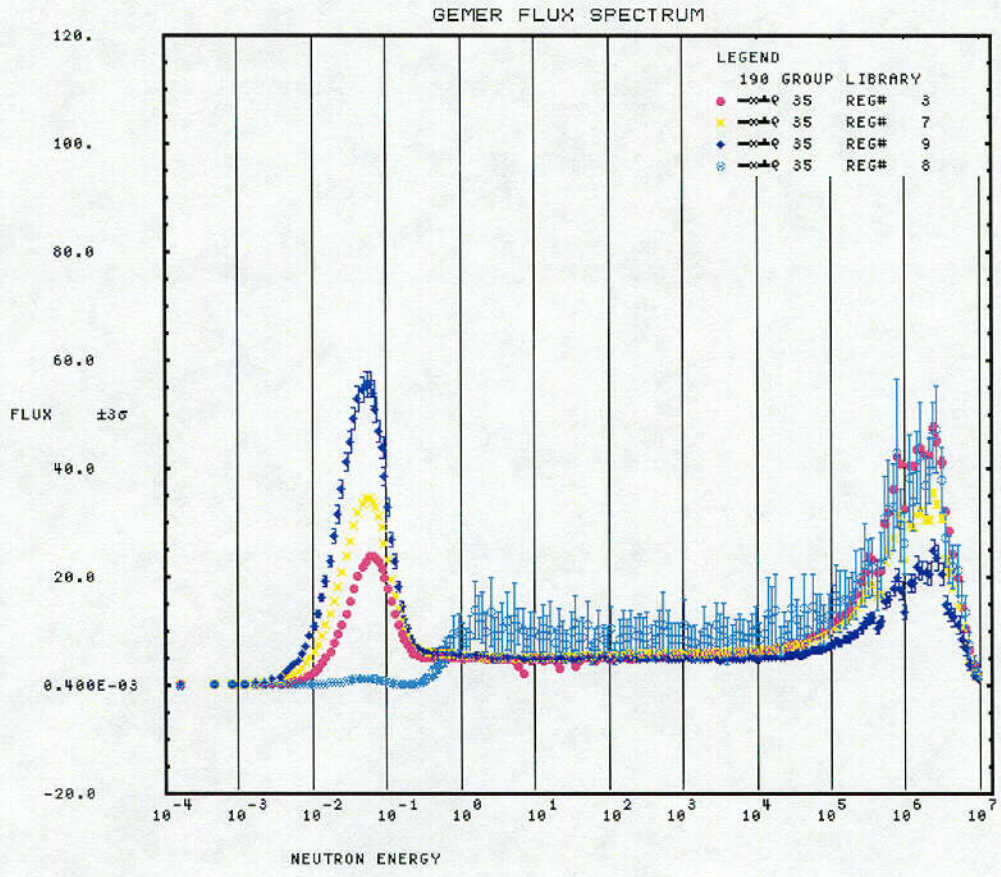

Legend:

Region 3 – Fuel pins
Region 7 – Moderator surrounding fuel pins
Region 8 – Cadmium plates (2.006 mm)
Region 9 – Moderator between fuel bundles and cadmium plates

C44

Figure 6.21b - Neutron Energy Spectra for BIER-38 (4.31%)

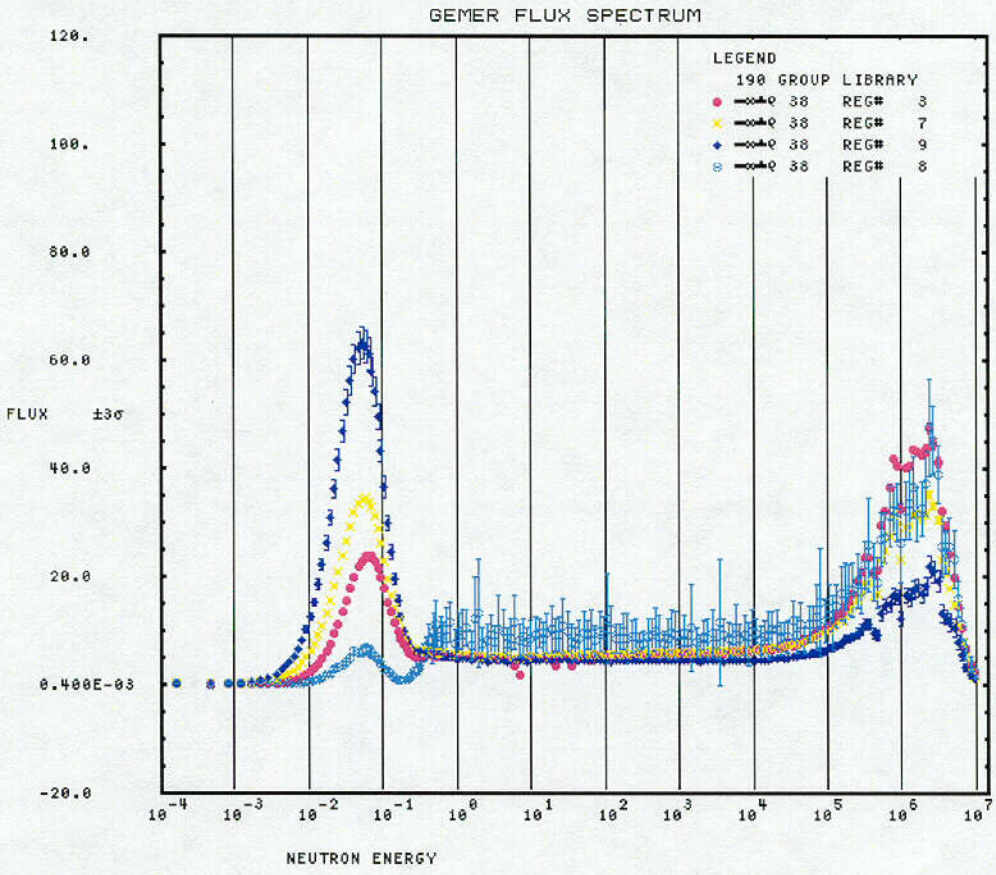

Legend:

Region 3 – Fuel pins
Region 7 – Moderator surrounding fuel pins
Region 8 – Cadmium plates (0.291 mm)
Region 9 – Moderator between fuel bundles and cadmium plates

C45

Figure 6.21c - Neutron Energy Spectra for NPC – Damaged Single Package

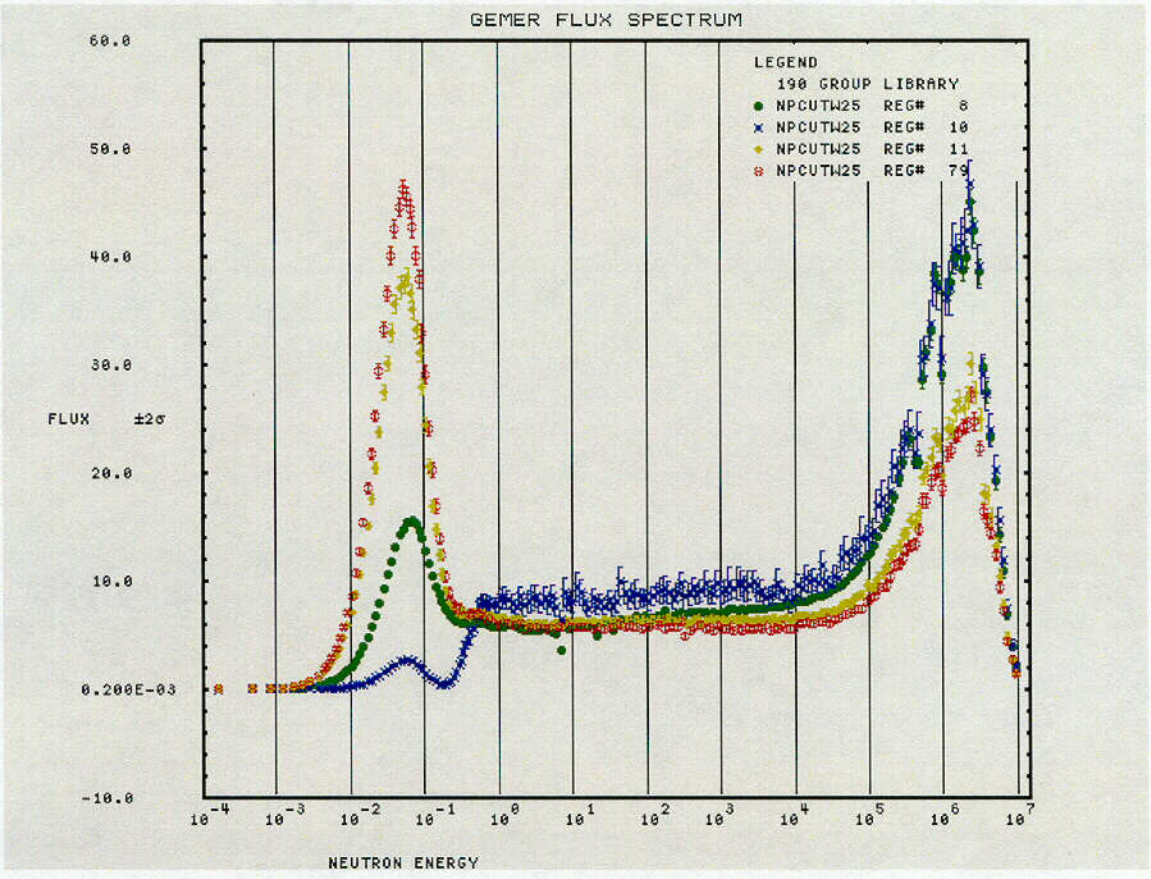

Legend:

Region 8 – ICCA Fuel Region
Region 10 – Cadmium wrap (0.381 mm)
Region 11 – Poly Region between ICCAs
Region 79 – Foam Region between ICCAs

C46

Figure 6.21d - Neutron Energy Spectra for NPC – Damaged Package Array

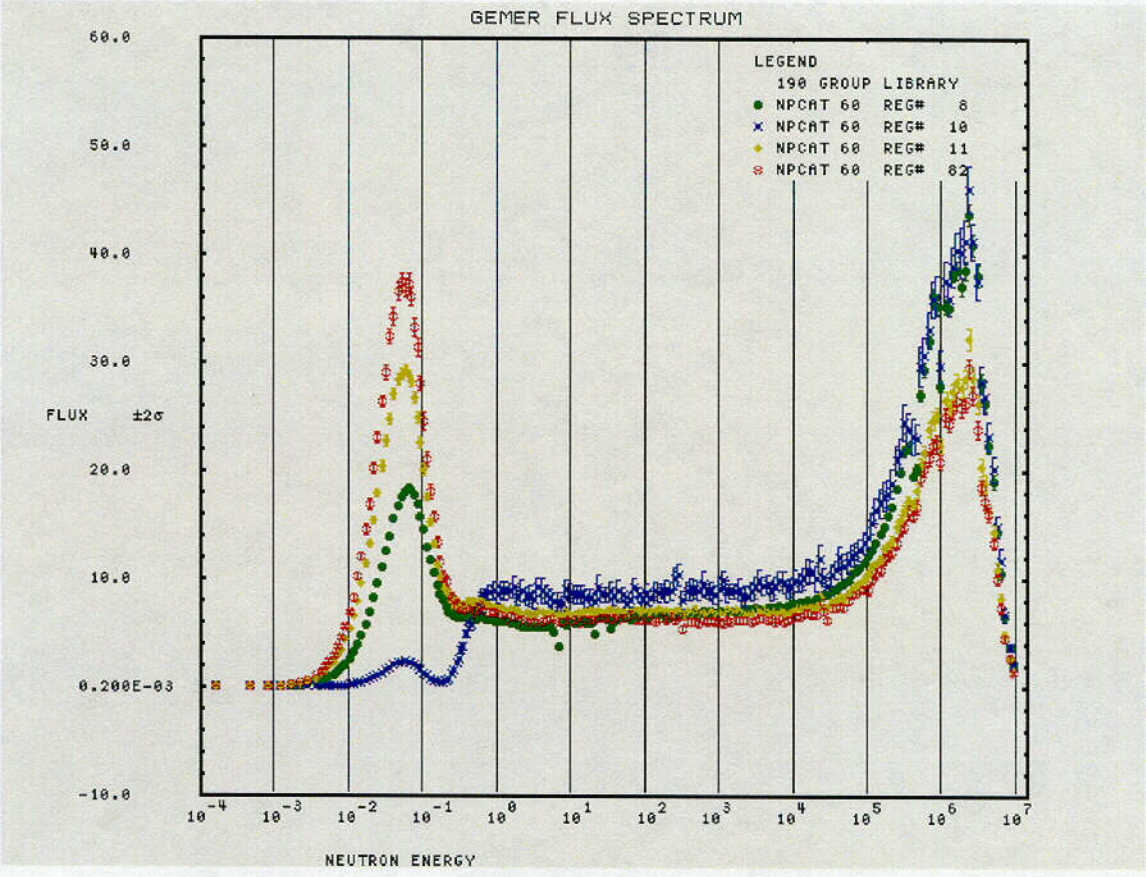

Legend:

Region 8 – ICCA Fuel Region
Region 10 – Cadmium wrap (0.381 mm)
Region 11 – Poly Region between ICCAs
Region 82 – Foam Region between ICCAs

C47